Spine: 4.5 mm

Volume 74 • Issue 4 • October-December 2025

Journal of The Anatomical Society of India • Volume 74 • Issue 4 • October-December 2025 • Pages 289-376

ISSN : 0003-2778

Scopus Indexed

JOURNAL OF THE ANATOMICAL SOCIETY OF INDIA

JASI

An International Journal

An Official Publication of Anatomical Society of India

Full text online at **https://journals.lww.com/joai**
Submit articles online at **https://review.jow.medknow.com/jasi**

Wolters Kluwer

Medknow

Journal of the Anatomical Society of India

Print ISSN: 0003-2778

GENERAL INFORMATION

About the Journal

Journal of the Anatomical Society of India (ISSN: Print 0003-2778) is peer-reviewed journal. The journal is owned and run by Anatomical Society of India. The journal publishes research articles related to all aspects of Anatomy and allied medical/surgical sciences. Pre-Publication Peer Review and Post-Publication Peer Review Online Manuscript Submission System Selection of articles on the basis of MRS system Eminent academicians across the globe as the Editorial board members Electronic Table of Contents alerts Available in both online and print form. The journal is published quarterly in the months of January, April, July and October.

Scope of the Journal

The aim of the *Journal of the Anatomical Society of India* is to enhance and upgrade the research work in the field of anatomy and allied clinical subjects. It provides an integrative forum for anatomists across the globe to exchange their knowledge and views. It also helps to promote communication among fellow academicians and researchers worldwide. The Journal is devoted to publish recent original research work and recent advances in the field of Anatomical Sciences and allied clinical subjects. It provides an opportunity to academicians to disseminate their knowledge that is directly relevant to all domains of health sciences.

The Editorial Board comprises of academicians across the globe.

JASI is indexed in Scopus, available in Science Direct.

Abstracting and Indexing Information

The journal is registered with the following abstracting partners:

Baidu Scholar, CNKI (China National Knowledge Infrastructure), EBSCO Publishing's Electronic Databases, Ex Libris – Primo Central, Google Scholar, Hinari, Infotrieve, Netherlands ISSN center, ProQuest, TdNet, Wanfang Data

The journal is indexed with, or included in, the following:

SCOPUS, Science Citation Index Expanded, IndMed, MedInd, Scimago Journal Ranking, Emerging Sources Citation Index.

Impact Factor® as reported in the 2024 Journal Citation Reports® (Clarivate Analytics, 2025): 0.2

Information for Authors

Article processing and publication charges will be communicated by the editorial office. All manuscripts must be submitted online at https://review.jow.medknow.com/jasi.

Subscription Information

A subscription to JASI comprises 4 issues. Prices include postage. Annual Subscription Rate for non-members-		
Annual Subscription Rate for non-members		
	India	**Outside India**
Institutional	INR 15000	USD 1200
Individual	INR 7,500	USD 800
The Journal of Anatomical Society of India (ISSN: 0003-2778) is published quarterly **Subscriptions** are accepted on a prepaid basis only and are entered on a calendar year basis. Issues are sent by standard mail Priority rates are available upon request.		

Information to Members/Subscribers

All members and existing subscribers of the Anatomical Society of India are requested to send their membership/existing subscription fee for the current year to the Treasurer of the Society on the following address: Prof (Dr.) Punit Manik, Treasurer, ASI, Department of Anatomy, KGMU, Lucknow - 226003. Email: punitamanik@yahoo.co.in. All payments should be made through an account payee bank draft drawn in favor of the **Treasurer, Anatomical Society of India,** payable at **Lucknow** only, preferably for **Allahabad Bank, Medical College Branch, Lucknow.** Outstation cheques/drafts must include INR 70 extra as bank collection charges.

All complaints regarding non-receipt of journal issues should be addressed to the Editor-in-Chief, JASI at editorjasi@gmail.com. The new subscribers may, please contact wkhlrpmedknow_subscriptions@wolterskluwer.com.

Requests of any general information like travel concession forms, venue of next annual conference, etc. should be addressed to the General Secretary of the Anatomical Society of India.

For mode of payment and other details, please visit www.medknow.com/subscribe.asp

Claims for missing issues will be serviced at no charge if received within 60 days of the cover date for domestic subscribers, and 3 months for subscribers outside India. Duplicate copies cannot be sent to replace issues not delivered because of failure to notify publisher of change of address. The journal is published and distributed by Wolters Kluwer India Pvt. Ltd. Copies are sent to subscribers directly from the publisher's address. It is illegal to acquire copies from any other source. If a copy is received for personal use as a member of the association/society, one cannot resale or give-away the copy for commercial or library use.

The copies of the journal to the subscribers are sent by ordinary post. The editorial board, association or publisher will not be responsible for non receipt of copies. If any subscriber wishes to receive the copies by registered post or courier, kindly contact the publisher's office. If a copy returns due to incomplete, incorrect or changed address of a subscriber on two consecutive occasions, the names of such subscribers will be deleted from the mailing list of the journal. Providing complete, correct and up-to-date address is the responsibility of the subscriber.

Nonmembers: Please send change of address information to subscriptions@medknow.com.

Advertising Policies

The journal accepts display and classified advertising. Frequency discounts and special positions are available. Inquiries about advertising should be sent to Wolters Kluwer India Pvt. Ltd, advertise@medknow. com.

The journal reserves the right to reject any advertisement considered unsuitable according to the set policies of the journal.

The appearance of advertising or product information in the various sections in the journal does not constitute an endorsement or approval by the journal and/or its publisher of the quality or value of the said product or of claims made for it by its manufacturer.

Addresses

Editorial Office

Dr. Vishram Singh, Editor-in-Chief, JASI
B5/3 Hahnemann Enclave, Plot No. 40, Sector 6, Dwarka Phase – 2,
New Delhi - 110 075, India.
Email: editorjasi@gmail.com

Published by

Wolters Kluwer India Pvt. Ltd.,
Fourth Floor, East Wing, Marisoft III, Marisoft Premises,
Part of Software Technology Park, S. No. 15, Vadgaon Sheri,
Kalyani Nagar, Pune – 411 014, Maharashtra, India.
Website: www.medknow.com

Printed at

Nikeda Art Printers Pvt. Ltd.,
Building No. C/3 - 14,15,16, Shree Balaji Complex, Vehele Road,
Village Bhatale, Taluka Bhiwandi, District Thane - 421302, India.

Journal of the Anatomical Society of India

Print ISSN: 0003-2778

EDITORIAL BOARD

Journal of the Anatomical Society of India

Volume 74 | Issue 4 | October-December 2025

CONTENTS

Journal of the Anatomical Society of India on Web

https://review.jow.medknow.com/jasi

The Journal of the Anatomical Society of India now accepts articles electronically. It is easy, convenient and fast. Check following steps:

1 Registration

- Register from https://review.jow.medknow.com/jasi as a new author (Signup as author)
- Two-step self-explanatory process

2 New article submission

- Read instructions on the journal website or download the same from manuscript management site
- Prepare your files (Article file, First page file and Images, Copyright form & Other forms, if any)
- Login as an author
- Click on 'Submit new article' under 'Submissions'
- Follow the steps (guidelines provided while submitting the article)
- On successful submission you will receive an acknowledgement quoting the manuscript ID

3 Tracking the progress

- Login as an author
- The report on the main page gives status of the articles and its due date to move to next phase
- More details can be obtained by clicking on the ManuscriptID
- Comments sent by the editor and reviewer will be available from these pages

4 Submitting a revised article

- Login as an author
- On the main page click on 'Articles for Revision'
- Click on the link "Click here to revise your article" against the required manuscript ID
- Follow the steps (guidelines provided while revising the article)
- Include the reviewers' comments along with the point to point clarifications at the beginning of the revised article file.
- Do not include authors' name in the article file.
- Upload the revised article file against New Article File - Browse, choose your file and then click "Upload" OR Click "Finish"
- On completion of revision process you will be able to check the latest file uploaded from Article Cycle (In Review Articles-> Click on manuscript id -> Latest file will have a number with 'R', for example XXXX_100_15R3.docx)

Facilities

- Submission of new articles with images
- Submission of revised articles
- Checking of proofs
- Track the progress of article until published

Advantages

- Any-time, any-where access
- Faster review
- Cost saving on postage
- No need for hard-copy submission
- Ability to track the progress
- Ease of contacting the journal

Requirements for usage

- Computer and internet connection
- Web-browser (Latest versions - IE, Chrome, Safari, FireFox, Opera)
- Cookies and javascript to be enabled in web-browser

Online submission checklist

- First Page File (rtf/doc/docx file) with title page, covering letter, acknowledgement, etc.
- Article File (rtf/doc/docx file) - text of the article, beginning from Title, Abstract till References (including tables). File size limit 4 MB. Do not include images in this file.
- Images (jpg/jpeg/png/gif/tif/tiff): Submit good quality colour images. Each image should be less than 10 MB) in size
- Upload copyright form in .doc / .docx / .pdf / .jpg / .png / .gif format, duly signed by all authors, during the time mentioned in the instructions.

Help

- Check Frequently Asked Questions (FAQs) on the site
- In case of any difficulty contact the editor

Split Cord Malformation: An Overview

Introduction

- Split cord malformation (SCM) is a type of occult spinal dysraphism, characterized by a longitudinal split in the spinal cord into two hemicords occurring during primary neurulation. It is a complex developmental disorder that, in most cases, leads to tethered cord syndrome and the development of neurological and orthopedic symptoms, which include anomalies of the spinal cord, meninges, and bony structures[1]
- The split cord malformation is the most common form of congenital myelodysplasia.

Split cord malformation (SCM) is of two types:[2]

(1) Type I SCM (Diastematomyelia)[3]
  - In this, two hemicords lie within separate dural sacs
  - These sacs are separated by a rigid bony or cartilaginous septum
  - This septum is derived from totipotent cells of the primitive steak.

(2) Type II SCM (Diplomyelia)[4]
  - In this, two hemicords lie within a single dural sac
  - The dural sac, in turn, is divided into two halves by a soft, nonrigid fibrous septum
  - It is generally less severe than Type I.

Three variants of Type II SCM exist as follows:
- Presence of an intervening fibrous septum
- Absence of a septum
- Partial cord splitting within a single dural tube housing both hemicords
- Further, diastematomyelia involves the division of one cord, while diplomyelia involves the duplication of the cord into two
- These can be identified by axial and coronal T2-weighted images as a thin hypointense strip interposed between the two hemicords
- SCM is often associated with other clinical conditions, namely spina bifida, vertebral anomalies such as hemivertebrae, butterfly vertebrae, and other neural tube defects.[5]

Embryological Basis[6]

The embryological processes involved in SCM are as follows:
- Nonobliteration of the neurenteric canal
- Notochord splitting
- Bifurcation of the neural plate
- Development of two hemicords
- Septum formation.

The details are as follows:[6]
- The notochord secretes signaling molecules, namely Shh (Sonic hedgehog protein)[7]
- This is essential for the proper differentiation of the floor plate of the neural tube and the proper formation of adjacent vertebrae. This is facilitated by the transient canal phase
- Normally, the notochord forms a solid rod and separates from the endoderm (23–25 days)
- Normally, a single neurenteric canal exists during the 3rd week of gestation to provide a transient communication between the amniotic cavity and yolk sac in the region of Hensen's node. Usually, it closes within 48 h
- If the process is disrupted, due to persistent adhesion between the ectoderm and endoderm, the developing notochord is prevented from separating completely from the endoderm. Rather, it splits into two heminotochords
- The overlying neural plate also splits into two hemineural plates, which go on to form two separate hemicords – a characteristic of SCM
- Nonclosure of the transient neurenteric canal during notochord formation leads to the formation of two hemineural chords. The paired notochordal processes are separated by primitive streak cells
- The resulting malformation depends upon the nature of the development of totipotent cells of the primitive streak, because being totipotent, these cells can differentiate into ectodermal, mesodermal, and endodermal lineages. For example, if these cells differentiate into cartilage or bone, the two hemicords contained within individual dural sacs will be separated by an osteocartilaginous bar/spur
- The septum is formed between hemicords derived from endomesenchymal tissue in the region that incorporates primitive meningeal tissue
- The neurenteric canal is a part of developmental process of notochordal process.
- The differences between notochondral canal and neurentric canal are as follows:[8]

The notochordal canal and neurocentric canal are related but different embryonic structures. The notochordal canal is a lumen that forms within the notochordal process, while the neurocentric canal is a temporary opening between the amniotic cavity and yolk sac, which develops when the notochordal process fuses with the ectoderm.

The notochordal canal is a part of the process of formation of the notochord. The neurenteric canal equalizes pressure between the amniotic cavity and the yolk sac. Its persistence can lead to split cord malformation.[8]

Congenital Anomalies Associated with SCM[9]

These are as follows:
- Other neural tube defects, namely spina bifida

- Tethered spinal cord syndrome, as well as various spinal and orthopedic deformities (such as scoliosis or kyphoscoliosis and abnormal vertebral bodies)
- In addition, SCM can be accompanied by Chiari malformations, syringohydromyelia, and intraspinal lipomas.[9]

Clinical Presentation of Split Cord Malformation (SCM)

Clinical signs and symptoms of SCM are not distinct and typically occur during infancy or adolescence, mostly between the ages of 6 months and 15 years.

SCM can present clinically with scoliosis and tethered cord syndrome. A hairy tuft on the back of the patient may be seen in these patients.

The common signs and symptoms include the following:

- Back and leg pain, weakness, or sensory loss in the lower limb and bladder or bowel dysfunction
- Other signs may include orthopedic deformities such as scoliosis and cutaneous stigmata such as a tuft of hair or birthmarks over the spine. Lower limb deformities, namely clubfoot and high arched/flat feet etc
- Children are more likely to have neurological defects, while in adults, pain is the most common symptom.[10]

Treatment of SCM[11]

The treatment of SCM is primarily surgical. It involves the following steps:

- Detethering of the spinal cord: Here, the spinal cord is released from its abnormal attachment to the spinal canal to reduce the tension. Further, the filum terminale is also cut to completely untether the spinal cord from the bottom
- Removal of the septum (bony or fibrous) dividing the two hemicords
- Removal of associated lesions at the same time, namely lipomas, dermoid cysts, or epidermoid cysts.[11]

Vishram Singh, Rashi Singh[1], Gaurav Singh[2]

Department of Anatomy, Kasturba Medical College, Manglore, Manipal Academy of Higher Education, Karnataka, [1]Department of Pediatric and Preventive Dentistry, Santosh Dental College and Hospital, Ghaziabad, [2]Clinical Editor, British Medical Journal, Noida, Uttar Pradesh, India

Address for correspondence: *Dr. Vishram Singh, B5/3 Hahnemann Enclave, Plot No. 40, Sector 6, Dwarka Phase - 2, New Delhi - 110 075, India.*
E-mail: drvishramsingh@gmail.com

References

1. Pang D, Dias MS, Ahab-Barmada M. Split cord malformation: Part I: A unified theory of embryogenesis for double spinal cord malformations. Neurosurgery 1992;31:451-80.
2. Dias MS, Pang D. Split cord malformations. Neurosurg Clin N Am 1995;6:339-58.
3. Tortori-Donati P, Rossi A, Cama A. Spinal dysraphism: A review of neuroradiological features with embryological correlations. Childs Nerv Syst 2000;16:675-97.
4. Barkovich AJ. Pediatric Neuroimaging. 5th ed. Philadelphia: Lippincott Williams and Wilkins; 2012.
5. McLone DG, Naidich TP. Spinal dysraphism: Experimental and clinical aspects. Clin Neurosurg 1986;33:359-70.
6. Rossi A, Biancheri R, Cama A, Piatelli G, Ravegnani M, Tortori-Donati P. Imaging in spinal dysraphism. Childs Nerv Syst 2004;20:470-84.
7. Pang D, Zovickian J, Oviedo A. Split cord malformation: Part II. Clinical syndrome. Neurosurgery 2010;67:658-75.
8. Naidich TP, editor. Imaging of the Spine and Spinal Cord. Philadelphia: Saunders; 2010.
9. Reigel DH. Tethered cord syndrome: Pathophysiology and clinical manifestations. Semin Pediatr Neurol 1997;4:139-45.
10. Oakes WJ. The tethered spinal cord. In: Youmans JR, editor. Neurological Surgery. 4th ed. Philadelphia: WB Saunders; 1996.
11. Mahapatra AK, Gupta DK. Split cord malformations: A clinical study of 48 cases. Pediatr Neurosurg 2005;41:57-63.

Article Info

Received: 28 November 2025
Accepted: 01 December 2025
Available online: 31 December 2025

Access this article online

Quick Response Code:

Website: https://journals.lww.com/joai

DOI: 10.4103/jasi.jasi_187_25

How to cite this article: Singh V, Singh R, Singh G. Split cord malformation: An overview. J Anat Soc India 2025;74:289-90.

Original Article

CD68+ Microglial Landscape in Optic Pathway of Donated Cadavers: Correlation with Demographics and Comorbidities

Chetana Sharma, Anita Rani[1], Archana Rani[1], Shalini Bhalla[2], Yatendra Parashar[3], Arvind Kumar Pankaj[1], Rakesh Kumar Dewan[1], Ram Kumar Sha[4]

Department of Anatomy, Gautam Buddha Chikitsa Mahavidyalaya, [4]Department of Neonatology, Graphic Era Hospital, Dehradun, Uttarakhand, Departments of [1]Anatomy and [2]Pathology, King George's Medical University, Lucknow, [3]Department of Hematology Oncology and BMT, Max Super Speciality Hospital, Noida, Uttar Pradesh, India

Abstract

Introduction: Microglia, is the resident immune cell of the central nervous system (CNS), playing a key role in maintaining homeostasis and responding to injury. This study investigates the spatial distribution of CD68+ microglia within the human optic pathway, examining the influence of age, gender, laterality, and co-morbidities (e.g., hypertension, diabetes) on microglial density across white and grey matter. Understanding distribution patterns is crucial for insights into neurodegenerative diseases affecting the optic pathway. **Methods:** Fifteen cadaveric brains (11 males, 4 females) were analysed. Tissue blocks from the optic nerve, optic chiasma, optic tract, and lateral geniculate body (LGB) were stained using CD68 immunohistochemistry to identify activated microglia. Counts were performed under 400X magnification across five non-overlapping fields per sample. **Results:** Microglial density was significantly higher in grey matter compared to white matter regions of the optic pathway, with a mean of 45.5 ± 24.4 cells in the LGB versus 33.1 ± 26.7 in white matter (p = 0.011). Age-related trends showed higher microglial counts in individuals above 60 years. Gender differences were also observed with females showing higher median counts in age-matched samples. Donors with co-morbidities (hypertension, diabetes) exhibited a notable increase in CD68+ microglia, especially in gray matter regions. **Conclusion:** This study reveals distinct microglial distribution patterns within the optic pathway, affected by age, gender, and chronic health conditions. The findings underscore the potential role of microglia in neuroinflammatory and neurodegenerative processes associated with the optic pathway, supporting further research on microglial contributions to CNS health and disease.

Keywords: *Aging, CD68+ microglia, immunohistochemistry, optic pathway, neurodegeneration, neuroinflammation*

Introduction

The visual pathway, a functional syncytium, includes neurons and synapses that transmit visual information from the environment to the brain, passing through structures such as the retina, optic nerve (ON), optic chiasma (OC), optic tract (OT), lateral geniculate nucleus (LGN), and optic radiation, terminating at the primary visual cortex.[1] Among the nonneural components, the optic pathway houses microglia. Resident macrophages of the central nervous system (CNS) were first described by Pio del Rio-Hortega in 1932. These cells contribute significantly in mediating immune response.[2]

Microglia are primarily recruited for surveillance, maintaining homeostasis within the central CNS. However, they alter their morphology and increase in number in response to acute neuroinflammation. Upon activation, microglia release signals that attract other immune cells, such as macrophages, lymphocytes, and monocytes, from outside the brain to assist in managing inflammation. When inflammation persists, microglia may become dysfunctional, producing reactive oxygen species and nitric oxide (NO), which can exacerbate neuronal damage. In aging, senescent microglia show reduced phagocytic and chemotactic abilities but an increased release of pro-inflammatory cytokines, further contributing to neuroinflammation.[3]

Although most of the optic pathway lies outside the cerebrum, it is not exempt from neurodegenerative disorders. In fact, it is particularly vulnerable to damage due to constant exposure to ultraviolet light through the retina. Drugs that can inhibit abnormal activation of microglia can be game changer in several neuroinflammatory and neurodegenerative disorders.[3] While the microglial function has been well

How to cite this article: Sharma C, Rani A, Rani A, Bhalla S, Parashar Y, Pankaj AK, *et al.* CD68+ microglial landscape in optic pathway of donated cadavers: Correlation with demographics and comorbidities. J Anat Soc India 2025;74:291-6.

Article Info

Received: 24 March 2025
Revised: 13 October 2025
Accepted: 23 November 2025
Available online: 31 December 2025

Address for correspondence:
Dr. Shalini Bhalla, Department of Pathology, King George's Medical University, Lucknow - 226 003, Uttar Pradesh, India.
E-mail: shalinibhalla@kgmcindia.edu

Access this article online

Website: https://journals.lww.com/joai

DOI: 10.4103/jasi.jasi_59_25

Quick Response Code:

studied in rodent models, research on their distribution in human optic pathways, particularly in white and gray matter, remains very limited. Understanding microglial distribution in these regions is crucial for insights into the pathogenesis of neurodegenerative diseases affecting the optic pathway.[4-14]

Minocycline can inhibit the activation of microglia in retinal neurodegenerative disease by suppressing the production of NO and inflammatory cytokines.[4] Another drug known as cannabinoids has anti-inflammatory properties and is considered a potential therapeutic agent as minocycline.[5]

Given the optic pathway's susceptibility to neurodegenerative processes, this study aims to quantify and compare the distribution of CD68+ microglia in the white and gray matter of the human optic pathway using immunohistochemistry. In addition, an effort has been made to correlate the microglial population with factors such as age, gender, laterality, and comorbidities to better understand their role in neuroinflammatory conditions.

Methods

Fifteen cadaveric human brains (11 males and 4 females) were procured to assess the site-specific distribution of CD68-positive microglia in the optic pathway. All donated bodies received within 36 h after death were embalmed in the department of anatomy. The bodies were kept in the preservative for a minimum of 1 week before dissection. The donors gave consent to use their carapace for research and educational purposes during registration. Ethical clearance for the study was obtained from the institutional ethical committee.

Demographic profile, history of trauma, history of eye diseases, comorbidities (hypertension [HT] an diabetes), drug history, and cause of death were collected in a standardized questionnaire. Out of 19 cadavers embalmed, 1 was excluded due to a positive history of glaucoma, and 3 brains were discarded due to inadequate preservation of areas of interest. Whole brains were removed from the cranium by following standard dissection steps.[15] Brains were kept in labeled containers containing the solution of 10% formaldehyde for at least 24 h before grossing. Small sections (5 mm × 5 mm) of the right and left side ON, OC, OT, and lateral geniculate body (LGB) were taken for tissue processing [Figure 1].

The fixed tissue specimens were processed for paraffin block formation. One hundred and twenty paraffin blocks were made. 3–5 µm thick sections were cut and fixed on saline-coated slide at 60°C, and immunohistochemistry was done using the CD68 antibody. Primary antibody used was – RTU Mouse Monoclonal CD68 Macrophage clone: PG-M1, PDM065 prediluted (Diagnostic BioSystems).

Observations were done under ×40 on the Olympus BX 41 microscope. Five nonoverlapping field images were taken from each slide. Brown-colored amoeboid-shaped microglia were counted manually, carefully from each field and noted down [Figure 2].

The statistical analysis was done using SPSS (version 24 IBM Corp., Armonk, NY, USA). Nonparametric tests, namely Mann–Whitney *U*-test and Kruskal–Wallis test were applied to calculate the significance of differences.

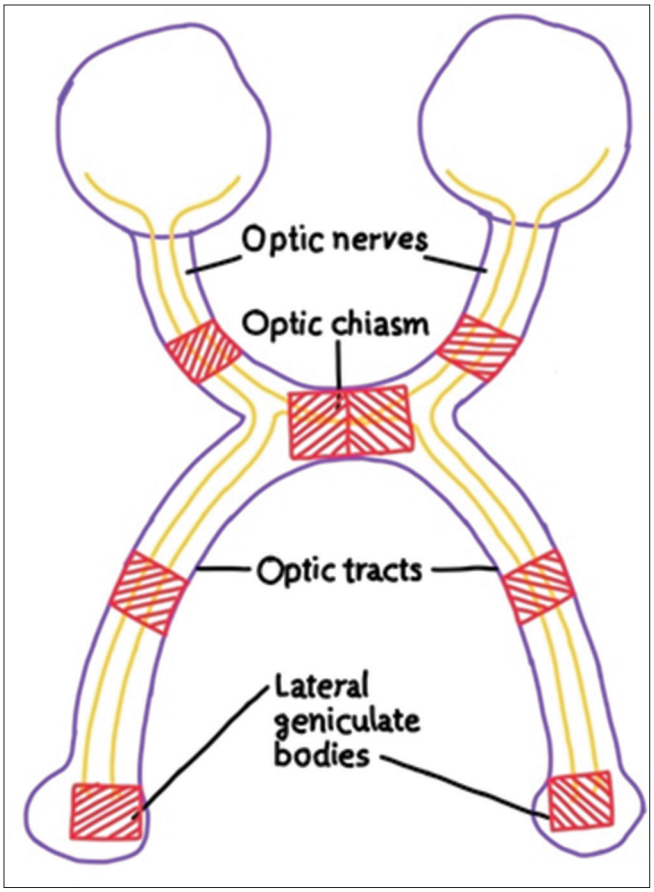

Figure 1: Parts of the optic pathway showing different sites from which tissues were retrieved

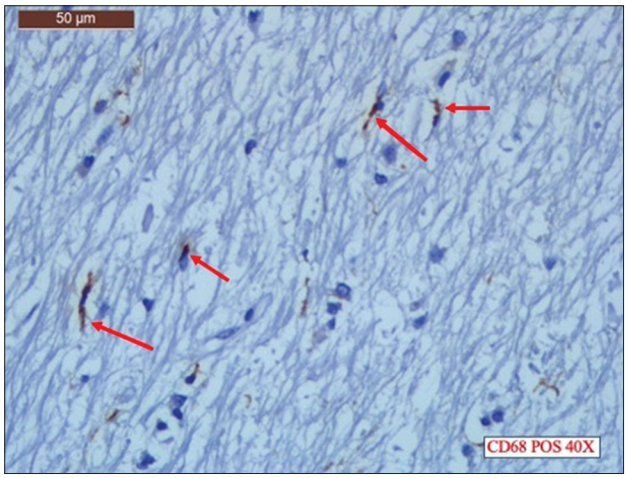

Figure 2: Photomicrograph showing brown colored microglia in a field under microscope at ×400

Results

Demographic and comorbidity profile of donors

The age of male and female cadavers ranged between 18 and 96 years. The heterogeneous sample of optic pathway areas comprised approximately 80% (n = 12) population above 60 years. Out of 15 brain samples, one-third (33.33%) had a history of diabetes, whereas more than half (53.33%) had a history of HT, and 53.33% of the samples had a positive history of both diseases. 46.66% of donors were operated for cataract, whereas 26.64% of cases were wearing correcting glasses for myopia. None of the selected donors (n = 15) had a history of stroke, trauma (head injury), tumor, Parkinson's disease, multiple sclerosis, Alzheimer's disease, glaucoma, any type of visual impairment, or any noticeable psychiatric illnesses. In all cases, the cause of death was mentioned as cardiorespiratory arrest.

Overall distribution of CD68+ microglia along the selected regions of the optic pathway

Number of microglia ranged between 5–93, 8–88, and 4–93, with median numbers of 15, 28, and 22 in the ON, OC, and OT, respectively. Whereas, in LGB, CD68+ microglia count ranged from 17 to 94 with a median of 37. The minimum number in the white matter areas was less than that observed in gray matter (4, 17). A high standard deviation in the mean value of counts was observed for all regions of the optic pathway (24.4 and 29.7), suggesting a high variation in the number of microglia in individuals [Table 1]. The quantity of microglia in all white matter regions (33.1 ± 26.7, median = 22) was significantly lower than in gray matter (45.5 ± 24.4, median = 37.5) (P value 0.011).

Table 1: Site-specific distribution of CD68+ microglia

Region (n=number of samples)	CD68+ microglia count		
	Range	Mean±SD	Median
ON (n=22)	5–93	31.3±29.7	15
OC (n=19)	8–88	36.4±24.4	28
OT (n=17)	4–93	31.6±26.4	22
LGB (n=22)	17–94	45.5±24.4	37

SD: Standard deviation, LGB: Lateral geniculate body, ON: Optic nerve, OC: Optic chiasma, OT: Optic tract

Age-wise distribution of CD68+ microglia along white and gray matter areas of the optic pathway

Upon classifying the available samples according to age decades, the maximum number of samples belonged to the ninth decade (n = 5), followed by the eighth decade (n = 4). Samples of the first, fourth, and sixth decades were not available. Due to improper processing, the LGB block from the second-decade donor could not be stained. Across all the age groups, gray matter generally exhibited a higher and more consistent distribution of CD68+ microglia compared to white matter. There was noticeable variability in microglial distribution with age, particularly in white matter. This variability was less pronounced in gray matter [Table 2 and Figure 3]. On calculating the mean values of those above (12 samples) and those below 60 years (68 samples), the higher number of microglia was a consistent finding.

Comparison of microglial count in male and female donors along the optic pathway

Total count in females along the optic pathway varied between 5 and 93, with a mean value of 34.3 ± 24.6 and 39.9 ± 29.1, respectively, on the right and left side of the tract. In males, the count ranged from a minimum of 4 to a maximum of 94, with mean values of 41.6 ± 27.3 and 30.2 ± 25.8 on the right and left sides, respectively. The differences were insignificant (0.342, Kruskal–Wallis test).

Comparison of CD68+ microglia distribution between genders of age-matched samples along the white and gray matter areas of the optic pathway

Only samples from the ninth decade had donors from both genders. Therefore, gender differences were analyzed only for this decade. Both white and gray matter areas of the optic pathway showed higher counts in female subjects as compared to male counterparts. The difference in the gray matter was remarkably high [Table 3 and Figure 4].

Comparison of right/left dominance of CD68+ microglia along the white and gray matter areas of the optic pathway

No consistent pattern of distribution or predominant side was observed. In ON samples, a higher count was observed

Table 2: Age decade-wise distribution of CD68+ microglia across white and gray matter areas of optic pathways

Decade and sample size	White matter			Gray matter		
	Range	Mean±SD	Median	Range	Mean±SD	Median
10–20 (n=1)	12–22	18.3±5.5	21	25–33	29±5.65	29
21–30 (n=1)	5–17	10.4±4.92	8	*	*	*
41–50 (n=1)	11	11	11	24–29	26.5±3.53	26.5
61–70 (n=2)	5–93	31.5±30.53	18.5	44–51	46.3±4.04	44
71–80 (n=4)	4–88	49.25±30.08	53	25–94	54.75±29.62	50
81–90 (n=5)	6–56	26.16±15.98	20.5	17–86	45.33±29.4	38
91–100 (n=1)	10–93	53.75±33.98	56	42	42	42

SD: Standard deviation

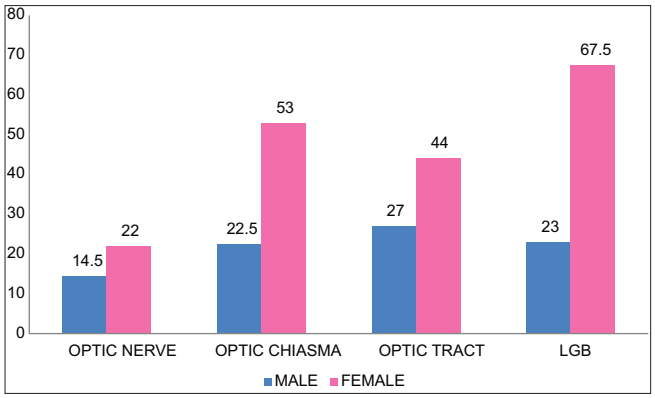

Figure 3: Bar diagram showing comparative distribution (median value) of CD68+ microglia between white and gray matter areas of extracerebral parts of optic pathway according to age decades in donated cadavers

Table 3: Gender-wise comparison of the microglial population between age-matched samples of white and gray matter areas of optic pathways (81–90 years) age group

	Male (*n*=3)	Female (*n*=2)	Mann–Whitney test (*P*)
ON			
Mean	15.25±2.6	18±10.6	0.629
Median	14.5	22	
OC			
Mean	28.25±19.5	39.3±25.4	0.999
Median	22.5	53	
OT			
Mean	27±8	44	NA
Median	27	44	
LGB			
Mean	34.25±26.8	67.5±26.1	0.533
Median	23	67.5	

LGB: Lateral geniculate body, NA: Not available, OC: Optic chiasma, OT: Optic tract, ON: Optic nerve

in more than 60% of cases on the right side in both genders. However, in the OC, the number was higher on the left side in males (75%), whereas in females, it showed equal distribution on both the sides. In all the samples of male OT, right-sided predominance was observed in contrast to a single female with left-sided predominance. In LGB, again males showed a higher number on the right side in more than 60% of cases in contrast to left-sided dominance in both female samples [Table 4].

Comparison of CD68+ microglial count in the optic pathway of donors with positive and negative history for hypertension/diabetes/both

The history of diabetes and HT was collected from the relatives of the donors. Those with a negative history for both diseases served as the control population. A lesser count of microglia was observed in both white and gray matter of the optic pathway of control subjects as compared to samples with the above comorbidity, except for one value, with both comorbidities in white matter. A consistent rise in counting was observed in LGB [Table 5 and Figure 5].

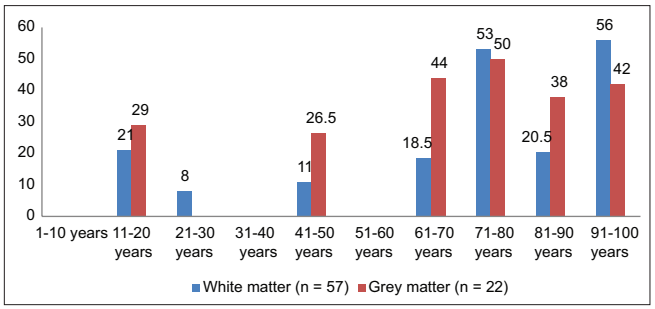

Figure 4: Bar diagram to compare the median between males and females of 81–90-year age group

Discussion

The optic pathway is a particularly vulnerable part of the CNS, showing a decline in ON fibers with age, likely due to retinal ganglion cell damage.[13,16] This study, based on 92 extracerebral optic pathway samples, revealed a broad range of CD68+ microglia (4-93) without a linear aging correlation, though a marked shift was observed between individuals above and below 60 years.[17]

Microglial density varies with the CNS environment. Derived from yolk sac macrophages, microglia migrate to the brain in the second trimester, with adult population maintained through local proliferation rather than monocyte differentiation.[18,19] CD68 serves as an inflammatory activation marker for these cells. Regionally, microglia are more abundant in gray matter areas like the hippocampus and substantia nigra, while white matter areas exhibit lower densities. The systematic distribution highlights microglial sensitivity to their environment.[20,21]

Microglial aging brings morphological and functional changes, leading to a chronic inflammatory state. As cytokines from dying neurons recruit microglia, they release neurotoxic substances (e.g., tumor necrosis factor), exacerbating neurodegeneration instead of providing neuroprotection.[22-25] Gender-related differences in microglia were observed, with higher median counts in females in this study, possibly influenced by immune-related gene expression and estradiol.[26-28]

Microglial lateralization studies suggest a higher count in the right ON in both sexes, although males exhibited right-sided dominance and females left-sided dominance in specific regions. Physiological conditions or coexisting pathologies seem to impact distribution more significantly than gender or side.[29]

Coexisting chronic diseases, such as HT and diabetes mellitus (DM), were linked to increased microglial activation, particularly in the LGB and OT. HT-related neuroinflammation and early microglial activation in

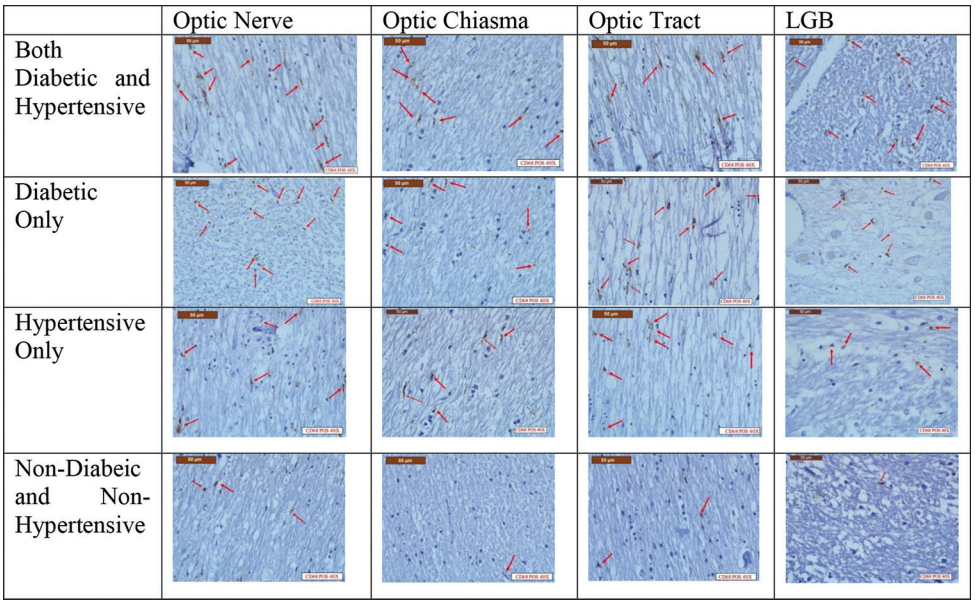

Figure 5: Photomicrographs of optic pathway regions showing distribution of CD68+ microglia (red arrows) in donors with and without a history of hypertension/diabetes/both

Table 4: Sidewise distribution of CD68+ microglial population in white and gray matter areas in optic pathway

Site	ON		OC		OT		LGB	
	Male	Female	Male	Female	Male	Female	Male	Female
Number of B/L observation	5	3	4	2	3	1	8	2
Percentage of sample showing increase/decrease in microglial number	Right ↑ (60) Left ↑ (40)	Right ↑ (67) Right=left (33)	Right ↑ (25) Left ↑ (75)	Right ↑ (50) Left ↑ (50)	Right ↑ (100)	Right ↓ (100)	Right ↑ (62.5) Left ↓ (37.5)	Right ↓ (100)

OC: Optic chiasma, ON: Optic nerve, OT: Optic tract, LGB: Lateral geniculate body

Table 5: Comparison of CD68+ microglial count in white and gray matter regions of the optic pathway of donors with positive and negative history for hypertension/diabetes/both

	Diabetic only (*n*=5; 33.33%) of sample	Hypertensive only (*n*=8; 53.33%) of sample	Diabetic and hypertensive (*n*=3; 20%) of sample	Nondiabetic nonhypertensive (*n*=5; 33.33%) of sample	Kruskal–Wallis test (*P*)
White matter					
Range	4–88	5–93	5–88	5–93	0.494
Mean	35.15±31.07	36.21±27.93	34.27±36.54	24.2±24.70	
Median	19	26.5	12	14	
Gray matter					
Range	25–94	17–94	44–94	24–42	0.042
Mean	62.22±26.09	49.92±26.69	72±22.77	30.6±7.30	
Median	67	44	85	29	

diabetic retinas further substantiate the link between systemic disease and CNS degeneration.[30] This study observed a trifold increase of activated microglia in patients with both HT and DM in gray matter compared to controls.

Limitations

This study is limited by its small sample size and manual counting method, which may affect accuracy. In addition, CD68 marks lysosomal activity, representing both parenchymal microglia and perivascular macrophages, complicating morphotype-specific analysis.

Conclusion

This study highlights the differential distribution of CD68+ microglia across various regions of the optic pathway, showing a significantly higher presence of gray matter, particularly within the LGB, compared to white matter areas such as the ON, chiasma, and tract. Age-related

and comorbid factors, including HT and diabetes, influence microglial density, with females exhibiting higher median counts than males in age-matched samples. The findings suggest that microglial density in the optic pathway correlates with site, age, and health conditions, which could offer insights into the pathogenesis and progression of neurodegenerative diseases affecting the optic pathway. Further research with larger samples and automated counting is recommended to validate these preliminary findings.

Financial support and sponsorship

Nil.

Conflicts of interest

Both Dr. Chetana and Dr. Anita have contributed equally to the article and hence should be considered as first coauthors.

References

1. Standring S. Gray's Anatomy. The Anatomical Basis of Clinical Practice. 41st ed. Edinburgh: Elsevier Limited; 2016.
2. Cho KH, Cheong JS, Kim JH, Abe H, Murakami G, Cho BH. Site-specific distribution of CD68-positive microglial cells in the brains of human midterm fetuses: A topographical relationship with growing axons. Biomed Res Int 2013;2013:762303.
3. Rashid K, Akhtar-Schaefer I, Langmann T. Microglia in retinal degeneration. Front Immunol 2019;10:1975.
4. Wang AL, Yu AC, Lau LT, Lee C, Wu le M, Zhu X, *et al*. Minocycline inhibits LPS-induced retinal microglia activation. Neurochem Int 2005;47:152-8.
5. Stella N. Endocannabinoid signaling in microglial cells. Neuropharmacology 2009;56 Suppl 1:244-53.
6. Garcia-Miralles M, Yusof NA, Tan JY, Radulescu CI, Sidik H, Tan LJ, *et al*. Laquinimod treatment improves myelination deficits at the transcriptional and ultrastructural levels in the YAC128 mouse model of huntington disease. Mol Neurobiol 2019;56:4464-78.
7. Evanson NK, Guilhaume-Correa F, Herman JP, Goodman MD. Optic tract injury after closed head traumatic brain injury in mice: A model of indirect traumatic optic neuropathy. PLoS One 2018;13:e0197346.
8. Hart AD, Wyttenbach A, Perry VH, Teeling JL. Age related changes in microglial phenotype vary between CNS regions: Grey versus white matter differences. Brain Behav Immun 2012;26:754-65.
9. Ekdahl CT, Claasen JH, Bonde S, Kokaia Z, Lindvall O. Inflammation is detrimental for neurogenesis in adult brain. Proc Natl Acad Sci U S A 2003;100:13632-7.
10. Krady JK, Basu A, Allen CM, Xu Y, LaNoue KF, Gardner TW, *et al*. Minocycline reduces proinflammatory cytokine expression, microglial activation, and caspase-3 activation in a rodent model of diabetic retinopathy. Diabetes 2005;54:1559-65.
11. El-Sayyad HI, Khalifa SA, El-Sayyad FI, Al-Gebaly AS, El-Mansy AA, Mohammed EA. Aging-related changes of optic nerve of Wistar albino rats. Age (Dordr) 2014;36:519-32.
12. Park YG, Lee JY, Kim C, Park YH. Early microglial changes associated with diabetic retinopathy in rats with streptozotocin-induced diabetes. J Diabetes Res 2021;2021:4920937.
13. Yassa HD. Age-related changes in the optic nerve of Sprague-Dawley rats: An ultrastructural and immunohistochemical study. Acta Histochem 2014;116:1085-95.
14. Cavallotti C, Pacella E, Pescosolido N, Tranquilli-Leali FM, Feher J. Age-related changes in the human optic nerve. Can J Ophthalmol 2002;37:389-94.
15. Singh V, Pal GP, Gangane SD. Thiemes Dissector for Head, Neck and Brain. India: Thieme Medical and Scientific Publisher's Private Limited.; 2016.
16. Sandell JH, Peters A. Effects of age on the glial cells in the rhesus monkey optic nerve. J Comp Neurol 2002;445:13-28.
17. Fatoba O, Itokazu T, Yamashita T. Microglia as therapeutic target in central nervous system disorders. J Pharmacol Sci 2020;144:102-18.
18. Casano AM, Albert M, Peri F. Developmental apoptosis mediates entry and positioning of microglia in the zebrafish brain. Cell Rep 2016;16:897-906.
19. Vela JM, Dalmau I, González B, Castellano B. Morphology and distribution of microglial cells in the young and adult mouse cerebellum. J Comp Neurol 1995;361:602-16.
20. Carson MJ, Doose JM, Melchior B, Schmid CD, Ploix CC. CNS immune privilege: Hiding in plain sight. Immunol Rev 2006;213:48-65.
21. Lawson LJ, Perry VH, Dri P, Gordon S. Heterogeneity in the distribution and morphology of microglia in the normal adult mouse brain. Neuroscience 1990;39:151-70.
22. Raivich G, Banati R. Brain microglia and blood-derived macrophages: Molecular profiles and functional roles in multiple sclerosis and animal models of autoimmune demyelinating disease. Brain Res Brain Res Rev 2004;46:261-81.
23. Kreutzberg GW. Microglia: A sensor for pathological events in the CNS. Trends Neurosci 1996;19:312-8.
24. Chao CC, Hu S, Molitor TW, Shaskan EG, Peterson PK. Activated microglia mediate neuronal cell injury via a nitric oxide mechanism. J Immunol 1992;149:2736-41.
25. Nissen JC. Microglial function across the spectrum of age and gender. Int J Mol Sci 2017;18:561.
26. Xu Y, Jin MZ, Yang ZY, Jin WL. Microglia in neurodegenerative diseases. Neural Regen Res 2021;16:270-80.
27. Thion MS, Low D, Silvin A, Chen J, Grisel P, Schulte-Schrepping J, *et al.* Microbiome influences prenatal and adult microglia in a sex-specific manner. Cell 2018;172:500-16. e16.
28. Villa A, Gelosa P, Castiglioni L, Cimino M, Rizzi N, Pepe G, *et al*. Sex-specific features of microglia from adult mice. Cell Rep 2018;23:3501-11.
29. Steiner J, Mawrin C, Ziegeler A, Bielau H, Ullrich O, Bernstein HG, *et al*. Distribution of HLA-DR-positive microglia in schizophrenia reflects impaired cerebral lateralization. Acta Neuropathol 2006;112:305-16.
30. Shen XZ, Li Y, Li L, Shah KH, Bernstein KE, Lyden P, *et al*. Microglia participate in neurogenic regulation of hypertension. Hypertension 2015;66:309-16.

Original Article

Giant Nutrient Foramina and Their Distribution Patterns in Acetabular Fossa

Sinan Bakirci, Gonca Ay Keselik

Department of Anatomy, Faculty of Medicine, Izmir Katip Celebi University, Izmir, Turkey

Abstract

Background: The distribution of nutrient foramina sheds light on the branching pattern of arteries supplying flat and irregular bones. In this study, it was aimed to reveal the distribution pattern of the big nutrient foramina in the acetabular fossa. **Materials and Methods:** Our study was performed on 46 dry coxae. It was first divided into two regions, anterior and posterior, by a line descending perpendicularly from the acetabular fossa to the acetabular notch. Afterwards, the anterior and posterior regions were divided into two with an angle of 45°, and the fossa was divided into four equal regions in total. The distribution pattern of the nutrient foramina in the acetabular fossa was examined and typified. In addition, the coxal bones were photographed from the lateral and the morphometric parameters of the acetabulum and acetabular fossa were measured with the Image-J program. **Results:** Very big (up to 7 mm in diameter) nutrient foramina were detected in the acetabular fossa. Classification was performed according to the number and localization of these large nutrient foramina, and a total of six different types of distribution patterns were determined. Their incidence rates were Type I 13%, Type II 16%, Type III 18%, Type IV 2%, Type V 2%, and Type VI 2%. No correlation was found between the acetabular fossa morphometric values and distribution pattern types. **Conclusion:** The presence and localization information of giant nutrient foramina can be benefit orthopedists performing hip joint surgery.

Keywords: *Acetabular fossa, acetabulum, hip bone, nutrient foramen, obturator artery*

Introduction

The localization, number and size of the nutrient foramina in the bones may be important for anatomists in terms of revealing the differences between the morphometric properties of the bone, and for orthopedic surgeons in terms of bone fracture repair and replacement. Due to fractures, it is possible that the nutrient artery is damaged along with the nutrient foramen. It is possible to find enough studies in the literature regarding nutrient foramina in long bones.[1-3] In the body part of long bones, there is usually a single nutrient foramen. The number of foramens located in the proximal and distal parts of the bone is more, and their distribution varies regionally. Mei *et al*. divided the femoral neck into three different zones, examined the nutrient foramina in these zones and revealed the differences between the zones.[4]

There are many study reports in the literature on acetabulum morphometry. It can be accepted that the width of the acetabulum is approximately 5.5 cm and its depth is 3 cm.[5] The shape features of the anterior edge of the acetabulum are important for total hip replacement surgeries. The anterior margin of the acetabulum can be of four different types, and the percentage values of these types are available in the literature. For the anterior edge of the acetabulum, four different types are defined as curved, irregular, angular and straight. The most common type is the curved type. Then, respectively, straight, angular and irregular types.[5,6]

In clinical terms, arterial nutrition of the acetabulum is important both for the successful implementation of surgical procedures and for minimizing postoperative complications. The acetabulum is supplied by branches originating from different arteries. Three important branches, the superior gluteal artery, inferior gluteal artery, and obturator artery, that branch off from the internal iliac artery, are responsible for supplying the acetabular region. Superior and inferior gluteal arteries supply the borders of the

How to cite this article: Bakirci S, Keselik GA. Giant nutrient foramina and their distribution patterns in acetabular fossa. J Anat Soc India 2025;74:297-301.

Article Info

Received: 28 May 2024
Revised: 10 September 2025
Accepted: 21 November 2025
Available online: 31 December 2025

Address for correspondence:
Dr. Sinan Bakirci, Department of Anatomy, Faculty of Medicine, Izmir Katip Celebi University, Izmir, Turkey. E-mail: sinan.bakirci@ikcu.edu.tr

Access this article online

Website: https://journals.lww.com/joai

DOI: 10.4103/jasi.jasi_70_24

Quick Response Code:

acetabulum. The obturator artery supplies the interior of the acetabulum. It extends from anterior to posterior along the upper edge of the obturator foramen and gives off the acetabular branch at the level of the acetabular notch. The acetabular branch passes under the transverse ligament here and enters the fat layer that fills the acetabuli, where it divides into many branches. Branches from the medial femoral circumflex artery also join the structure of the arterial ring formed at the lower edge of the acetabulum.[7,8]

Although there are many studies on acetabular morphometry in the literature, there is no classification study for the distribution pattern of arterial branches in the acetabular fossa. Also, there is not enough discussion about the very big nutrient foramina in the acetabular fossa. In our study, the distribution of very big nutrient foramina in the acetabular fossa was typified in order to draw attention to the branching pattern of the acetabular artery.

Materials and Methods

These are the bones belonging to our university collection, obtained from the Aegean Region of our country in accordance with the legal regulations. 46 coxae bones, 15 right (8M,7F), 31 left (16M, 15F) belonging to different individuals were used in the study. The gender of the bones is unclear. However, according to the Bruzek method, gender was determined as 24 males and 22 females.[9] Gender differences were not included in the analyses.

The acetabular fossa was first divided into two regions, anterior and posterior, by a line descending perpendicular to the acetabular notch. Afterwards, the anterior and posterior regions were divided into two with an angle of 45°, and the fossa was divided into four equal regions in total [Figure 1]. The distribution pattern of the nutrient foramen in the acetabular fossa was examined and typified. In addition, the coxal bones were photographed laterally and the morphometric parameters of the acetabulum and acetabular fossa were measured with the Image-J program.

Statistics

Statistical analysis was performed with IBM SPSS Statistics 25.0 (IBM Corp., Armonk, New York, USA). Descriptive statistical analysis (median, minimum, maximum, standard deviation, standard deviation, and mean value) was determined. The distribution pattern of the obtained data (normality) was determined by the Shapiro–Wilk test. Right and left side differences were compared with the Mann–Whitney *U*-test.

Ethics

Study approval was obtained from the Local-Non-Interventional Clinical Research Ethics Committee with the decision numbered 26.05.2022-0231.

Results

In the acetabular fossa, nutrient foramen were detected in some areas, reaching very big sizes (up to 7 mm in diameter) (in 57% of all coxa) [Figure 2]. Classification was performed according to the number and localization of these very big nutrient foramens, and a total of 6 different types of distribution patterns were determined. Their incidence is Type 1 13%, Type 2 16%, Type 3 18%, Type 4 2%, Type 5 2%, Type 6 2% [Figure 3]. No correlation was found between the acetabular fossa morphometric values and the distribution pattern types. Morphometric mean values (in cm) were 4.28 ± 0.38 for acetabular height, 4.14 ± 0.34 for acetabulum width, 2.43 ± 0.33 for acetabular fossa length, 2.41 ± 0.29 for acetabular fossa width, and 1.98 ± 0.37 for acetabular notch width [Table 1]. The numerical values obtained showed a normal distribution. There was no significant difference between the right and left sides [Table 2].

Discussion

The acetabular branch of the obturator artery, after passing through the acetabular notch, gives a thin (sometimes 2) branch into the ligamentum capitis femoris and then enters itself into the acetabular fat pad. It is difficult to find

Table 1: Descriptive values

	n	Minimum	Maximum	Mean±SD
Acetabulum hight	46	3.55	4.93	4.28±0.38
Acetabulum width	46	3.21	4.82	4.15±0.34
Acetabular fossa length	46	1.74	3.18	2.43±0.33
Acetabular fossa width	46	1.78	3.21	2.41±0.29
Acetabular notch width	46	1.21	2.97	1.98±0.37

Average of morphometric values of the acetabulum, acetabular fossa, and acetabular notch. SD: Standard deviation

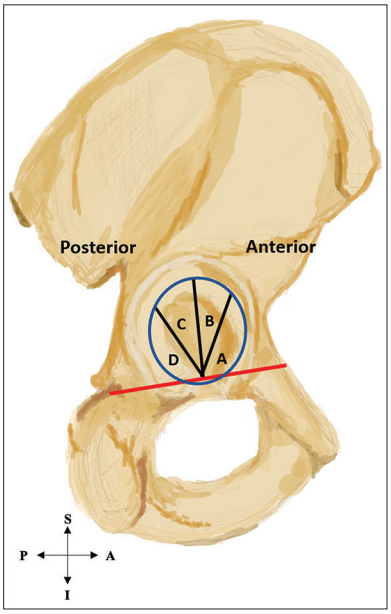

Figure 1: Division of the acetabular fossa into four regions

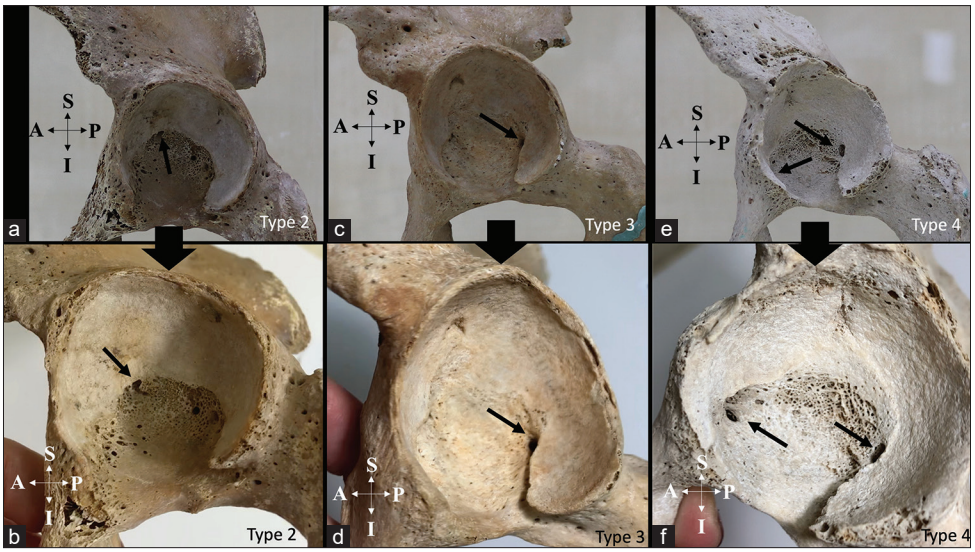

Figure 2: A few examples of giant foramens, (a) Single giant nutrient foramen on the second quadrant from the anterior, (b) Zoomed version of Figure 2a, (c) Single giant nutrient foramen in the posterior quadrant, (d) Zoomed version of Figure 2c), (e) Two giant nutrient foramens, one in the posterior and one in the anterior quadrant, (f) Zoomed version of figure 2e). (All examples in the picture are on the left). Black arrows indicate the locations of the giant nutrient foramina

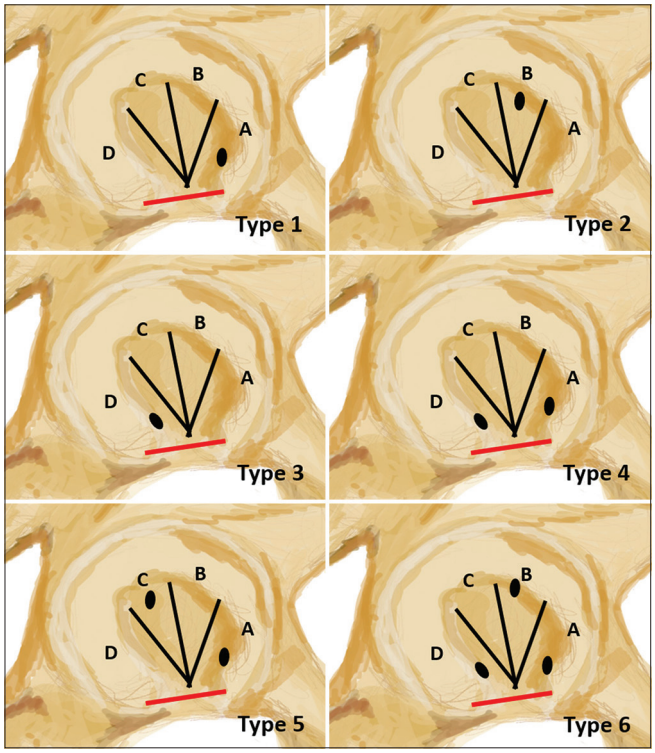

Figure 3: Giant nutrient foramina and their typing according to their localization. Type 1: Single giant nutrient foramen in the anterior quadrant only (schematized drawing on the right coxae). Type 2: Single giant nutrient foramen in the second anterior quadrant only. Type 3: Single giant nutrient foramen in the most posterior quadrant only. Type 4: A total of two giant nutrient foramen in the anterior and posterior quadrants. Type 5: A total of two giant nutrient foramen in the anterior quadrant and the second posterior quadrant. Type 6: A total of three giant nutrient foramen in the two anterior quadrants and the posterior quadrant

detailed information about the branching pattern of this artery, which is distributed in the acetabular fossa, both in classical anatomy and surgery books and in the literature. In our study, it was determined that apart from many small nutrient foramina in the acetabular fossa, there are nutrient foramina with very big dimensions (reaching 7 mm in diameter). Considering that these giant foramens may be of clinical importance, we performed a classification study according to the localization of these giant foramina. We created a representative figure showing the arterial distribution pattern according to the locations of these giant nutrient foramina in the acetabular fossa [Figure 4]. There were 3 fixed significant localizations in this typing. We believe that the knowledge of these localizations and the existence of giant nutrient foramen should be taken into account by orthopedists. It is possible to come across many dry bone studies in the literature suggesting that the shape features of the anterior edge of the acetabulum are important for total hip replacement surgeries.[5,6] We want to add a different perspective to this topic. The presence of a giant nutrient foramen (probably representing a giant arterial nutrition) at the anterior initiation of lunate facies, as in Type 1, which is especially common among the typings we have made, can be important in terms of complications that may occur during and after total hip replacement surgeries.

In periacetabular osteotomies, the acetabulum is freed by cutting from the anterior, posterior and upper sides and rotated to eliminate the acetabulum incompatibility of the femoral head.[10] The arterial supplying pattern of the acetabulum should also be considered in terms of the direction, inclination and angular value of the surgical screws to be placed. The presence of a giant nutrient foramens in the 11 and 1 o'clock directions, especially in Types 2, 5, and 6, which we detected in our study, may cause the surgeon to make a different decision about the location and direction of the screw to be inserted during surgery. The distribution pattern of arteries causing giant nutrient foramen may explain why some of the unexpected

Table 2: Comparison between right and left sides

	Independent samples test								
	F	Significant	*t*	df	Significant (two-tailed)	Mean difference	SE difference	95% CID	
								Lower	Upper
Acetabulum hight	0.673	0.416	0.284	44	0.778	0.03387	0.11924	−0.20644	0.27418
Acetabulum width	0.598	0.443	0.181	44	0.857	0.01971	0.10875	−0.19946	0.23889
Acetabular fossa length	0.023	0.881	1.705	44	0.095	0.17452	0.10237	−0.03180	0.38084
Acetabular fossa width	0.865	0.357	0.613	44	0.543	0.05636	0.09190	−0.12885	0.24157
Acetabular notch width	1.161	0.287	0.119	44	0.906	0.01404	0.11761	−0.22298	0.25106

There is no significant difference between the right and left sides of the hip bones in terms of the average morphometric values of acetabulum, acetabular fossa and acetabular notch $P>0.05$. SE: Standard error, CID: Confidence interval for the difference

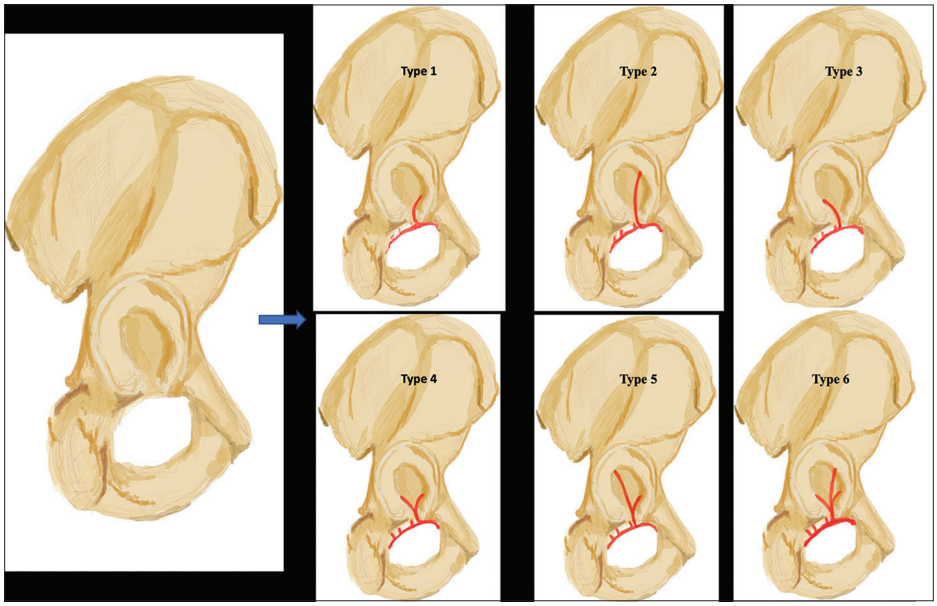

Figure 4: Schematizing the possible arterial distribution pattern. Possible branching types of the acetabular branch branching off from the obturator artery (schematic drawing on the right coxae), drawn as an estimate, taking into account the localization of the giant nutrient foramens (prepared with the application called "Procreate" Typing was performed according to the distribution pattern of the giant nutrient foramina shown in Figure 3)

complications after surgery or possible delays in the patient's recovery process.

It is difficult to decide whether surgical or palliative treatment is the treatment for acetabulum fractures. Surgical treatment is applied for displaced fractures larger than 3 mm. In a study, it was shown that after acetabular fracture surgical treatment, approximately 15% of patients had avascular necrosis in the later period (between 6 and 52 months). Of the patients with complications, 6 were operated for posterior wall fractures, 3 for transverse fractures, and 4 for both column fractures. Different surgical techniques (Kochen Langenberk, modified trochanteric, triradiate, ilioinguinal) were applied in 10 cases with A vascular necrosis.[11] We believe that the distribution of nutrient foramina representing the arterial distribution pattern of the acetabular fossa, which we revealed in our study, and especially the location and positional status of the giant nutrient foramina may be related to the occurrence of avascular necrosis complication after surgery of acetabular fractures. The arterial distribution pattern of the acetabular fossa also seems to affect the time of occurrence of complications. Therefore, differences in the arterial pattern in the supplying of the acetabular fossa may be among the reasons affecting the prognosis of the patients.

If we consider a different clinical issue, in clinical cases such as femoral acetabular impingement, cartilage and bone tissue should be removed by hip arthroscopy. Complications due to bone tissue removal may be due to regional vascular distribution differences. During these processes, it can be usefully to remember the detailed information about the issues that we drew attention to in our study.

Conclusion

Our study focused on drawing the attention of orthopedists to the issue of how the pattern of big nutriant foramina distribution in the acetabular fossa might be. There is a need for more detailed cadaver and angiographic studies on this subject.

Acknowledgements

We would like to thank, the head of the anatomy department of our university, for his support during the studies.

Financial support and sponsorship

Nil.

Conflicts of interest

There are no conflicts of interest.

References

1. Kizilkanat E, Boyan N, Ozsahin ET, Soames R, Oguz O. Location, number and clinical significance of nutrient foramina in human long bones. Ann Anat 2007;189:87-95.
2. Sendemir E, Cimen A. Nutrient foramina in the shafts of lower limb long bones: Situation and number. Surg Radiol Anat 1991;13:105-8.
3. Gümüsburun E, Yücel F, Ozkan Y, Akgün Z. A study of the nutrient foramina of lower limb long bones. Surg Radiol Anat 1994;16:409-12.
4. Mei J, Ni M, Wang G, Jia G, Liu S, Cui X, *et al*. Number and distribution of nutrient foramina within the femoral neck and their relationship to the retinacula of Weitbrecht: An anatomical study. Anat Sci Int 2017;92:91-7.
5. Aksu FT, Ceri NG, Arman C, Tetik S. Morphology and morphometry of the acetabulum. Dokuz Eylul Univ Med Fac J 2006;20:143-8.
6. Maruyama M, Feinberg JR, Capello WN, D'Antonio JA. Morphologic features of the acetabulum and femur: Anteversion angle and implant positioning. Clin Orthop Related Res 2001;393:52-65.
7. Beck M, Leunig M, Ellis T, Sledge JB, Ganz R. The acetabular blood supply: Implications for periacetabular osteotomies. Surg Radiol Anat 2003;25:361-7.
8. Howe WW Jr., Lacey T, Schwartz RP. A study of the gross anatomy of the arteries supplying the proximal portion of the femur and the acetabulum. J Bone Joint Surg Am 1950;32 A: 856-66.
9. Bruzek J. A method for visual determination of sex, using the human hip bone. Am J Phys Anthropol 2002;117:157-68.
10. Ganz R, Klaue KA, Vınh TS, Mast JW. A new periacetabular osteotomy for the treatment of hip dysplasias technique and preliminary results. Clin Orthop Related Res 1988;232:26-36.
11. Bilekdemir U, Civan O, Cavit A, Özdemir H. Acetabular fractures treated surgically: Which of the parameters affect prognosis. Turk J Trauma Emerg Surg 2020;26:265-73.

Original Article

Anatomical Features and Clinical Importance of Cubital Fossa

Aysen Calikusu, Hulya Ucerler

Department of Anatomy, Faculty of Medicine, Ege University, Izmir, Türkiye

Abstract

Objective: Healthcare professionals in healthcare practice frequently use the cubital fossa. Any problem occurring in this area can affect the patient's quality of life and cause severe financial and moral penalties for healthcare professionals. While previous studies often examine structures unilaterally, we aimed to examine this area with a holistic approach. **Materials and Methods:** Dissection of the upper extremities of 30 adult male cadavers was performed by fixing them with 10% formalin. Upper extremity superficial vein course types, median nerve (MN), and brachial artery courses and branches were checked and measured. **Results:** Positive correlations have been identified between the arm, forearm, midline, and biceps aponeurosis in cadaver upper extremities. It was observed that four atypical vein courses, the MN root junctions were in the arm, the musculocutaneous nerve branched into the MN, the proximal branch of the MN was above the midline, the Struthers' ligament was present, the MN did not pass through the head of the pronator teres (PT), the MN passed under the ulnar head of the PT muscle, which appeared as a fibrous band after piercing the head of the humerus, and the brachioradial artery (radial artery with high origin) was present. **Conclusions:** This study distinguishes itself from previous research by presenting a comprehensive compilation of measurement results and anatomical variations. We believe that the data provided are crucial for optimizing surgical approaches and diagnosing issues related to the structures within this region.

Keywords: *Brachial artery, cubital fossa, median nerve, superficial veins*

Introduction

The cubital fossa is a triangular depression where the main neurovascular structures pass into the forearm.[1,2] The structures in the cubital fossa are often preferred for intravenous injections, venous blood sampling, blood transfusions,[1,3] cardiac catheterization and coronary angiography,[1,4] interventional radiology,[5] and peripheral nerve blocks.[6] After interventions in this area, accumulation of blood, medication, etc., between the tissues, sensitivity and pain in the surrounding tissues, and spasms in the flexor muscles may be observed.[4,5,7] Complex regional pain syndrome (CRPS) may develop.[7-9] This study aims to reveal the close relationships of the structures in the region as a whole and to describe their variations.

Materials and Methods

Thirty upper limbs from 10% formalin-fixed adult male cadavers (16 right and 14 left upper limbs). They were dissected from superficial to deep, and their measurements were recorded. The study conforms to the provisions of the Helsinki Declaration of 1964 and all subsequent revisions.

The cubital fossa region of the forearm was dissected in 30 cadaver upper extremities. These were superficial veins (basic vein, median cubital vein [MCuV], cephalic vein [CV]), and the bicipital aponeurosis, which is the extension of the biceps brachii (BB) just below and deeper, the brachial artery (BA), and median nerve (MN) were dissected by following their course. Morphometric measurements were made according to the reference points. Since the superficial veins of 7 upper extremities were removed in previous dissections, superficial vein measurements of 23 upper extremities were made. Measurements of other parameters were made in 30 upper extremities.

Measurements

All measurements were taken with a digital caliper to the nearest 0.01 mm (mm) and expressed in mm.

- Arm length measurement: A pin was placed over the greater tubercle and

How to cite this article: Calikusu A, Ucerler H. Anatomical features and clinical importance of cubital fossa. J Anat Soc India 2025;74:302-12.

Article Info

Received: 19 March 2025
Accepted: 23 November 2025
Available online: 31 December 2025

Address for correspondence:
Dr. Aysen Calikusu, Department of Anatomy, Faculty of Medicine, Ege University, Izmir, Türkiye.
E-mail: aysencalikusu01@gmail.com

Access this article online

Website: https://journals.lww.com/joai

DOI: 10.4103/jasi.jasi_54_25

Quick Response Code:

lateral epicondyle (LE). A thread was stretched between the pins. The thread length was measured

- Forearm length measurement: A pin was placed over the LE and styloid process, and the thread length between the pins was measured
- The length between the medial epicondyle (ME) and LE measurement: A pin was placed over the ME and LE. The thread length between the pins was measured. For clarity, this line will be referred to as the "midline."
- The superficial vein measurements:
  - The presence of the MCuV was assessed. If present, the distance from the point where it joins the basilic vein (BV) to the midline was measured (a), and the distance from this point on the midline to ME (A) and LE (B) was measured [Figure 1.1]
  - Similarly, the distance from the point where the MCuV joins the CV to the midline was measured (b), and the distance from this point on the midline to ME (A) and LE (B) was measured [Figure 1.1]
  - The presence of the median BV (MBV) was assessed. If present, the distance from the point where it joins the BV to the midline was measured (a). The distance from this point on the midline to ME (A) and LE (B) was measured [Figure 1.2]
  - The presence of the median CV was assessed. If present, the distance from the point where the CV joins to the midline was measured (b). The distance from this point on the midline to ME (A) and LE (B) was measured [Figure 1.2]
  - The presence of the median antebrachial vein was assessed. If present, the distance from the bifurcation point to the midline was measured (c). The distance from this point on the midline to ME (A) and LE (B) was measured [Figure 1.2].
- The bicipital aponeurosis measurement: A straight line was drawn from the BB muscle (A) to the brachioradialis muscle (B) to determine the long side of the bicipital aponeurosis. The midpoint of the long side was marked (C). From here, a perpendicular line was drawn laterally (D). Thus, its width was determined [Figure 1.3]
- The bifurcation of BA measurement: The distance from the point where the BA bifurcates (A) into the radial artery and the ulnar artery to the midline was measured. In addition, the distance from this point on the midline to ME (A) and LE (B) was measured [Figure 1.4]. In addition, it was assessed whether the BA passed beneath the bicipital aponeurosis.

Variant status assessment

It was assessed whether the MN passed under the bicipital aponeurosis and between the two heads of the pronator teres muscle (PT) and whether it pierced the two heads of the PT. The passage of the BA beneath the bicipital aponeurosis and its bifurcation into terminal branches were assessed. The courses and anastomoses of the superficial veins were examined. Frequently, common vein courses were named Type 1 and Type 2 [Figure 2]. The groups exhibiting atypical vein courses were classified as Type 3, Type 4, Type 5, and Type 6, with corresponding illustrative images presented using Microsoft Paint [Figure 2]. Furthermore, all variations were documented in the form of case reports.

Statistical method

Variations were excluded from statistical analysis because they would affect the analysis and were reported under headings. Measurements were obtained from 23 of the 30 upper extremity cadavers with superficial vein routes. Five of the 23 superficial vein courses were categorized as an atypical group, excluded from the statistical analysis, and reported separately. Type 1 and Type 2 superficial vein course measurements detected in the remaining 18 upper extremities were analyzed. In three of the 30 cadavers, a radial artery branching from the top (brachioradial artery) was observed. These cases were excluded from the statistical analysis and reported separately. BA measurements in the remaining 27 upper extremities were analyzed.

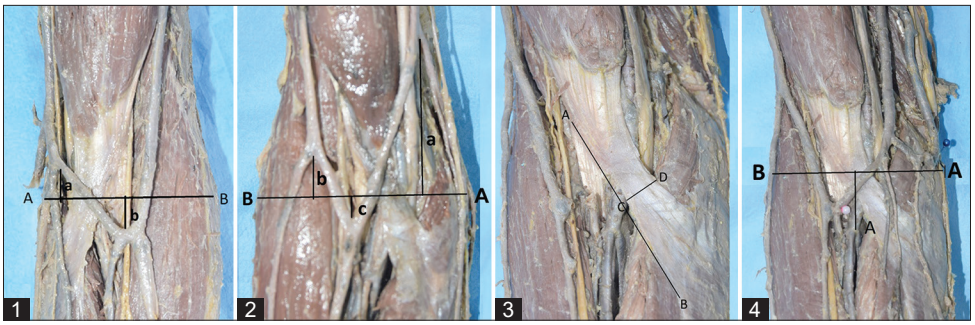

Figure 1: Demonstrating reference points of measurements. (1) Measurement of Type 1 A: Medial epicondyle, B: Lateral epicondyle, a: Distance of basilic vein to the midline, b: Distance of cephalic vein to the midline. This photo shows the left arm of a cadaver. (2) Measurement of Type 2 A: medial epicondyle, B: Lateral epicondyle, a: Distance of basilic vein to the midline, b: Distance of cephalic vein to the midline, c: Median cubital vein bifurcation point to the midline. This photo shows the right arm of a cadaver. (3) Measurement of the bicipital aponeurosis; A: The biceps brachii muscle, B: The brachioradial muscle, C: Bicipital aponeurosis, D: The end of perpendicular line. This photo shows the right arm of a cadaver. (4) Measurement of bifurcation of the brachial artery; A: The distance between the point where the brachial artery divides into the radial artery and the ulnar artery. This photo shows the right arm of a cadaver

The data obtained from the measurements were statistically analyzed using Statistical software (IBM SPSS software, version 25.0, SPSS Inc. Chicago, IL, USA). Data conforming to a normal distribution were analyzed using the *t*-test. In addition, the Mann–Whitney *U*-test analyzed data that did not conform to normal distribution. In addition, Pearson correlation analysis was performed to investigate the relationship between arm length, forearm length, midline, and bicipital aponeurosis width.

Results

Measurement results

- All measurements of arm length, forearm length, midline length, and bicipital aponeurosis width are presented in Table 1. No significant difference was found in the right and left upper extremity values in any measured parameter ($P > 0.05$)
- It was determined that there was a positive correlation between arm length and both bicipital aponeurosis width and midline length ($P < 0.05$) [Figure 3a and b]. Similarly, a positive correlation was found between forearm length, both bicipital aponeurosis width and midline length (seriatim; $P < 0.05$, $P < 0.01$) [Figure 3c and d]. In addition, a positive correlation was found between bicipital aponeurosis width and midline length ($P < 0.01$) [Figure 3e]. Pearson correlation analysis values are presented in the graphs
- In all cadavers where both right and left upper extremities were examined, it was observed that the BA passed under the bicipital aponeurosis (100%). In 3 upper extremities, the radial artery was found to have a high origin and was excluded from statistical analysis. This variation in the anatomical structure was explained in detail in the section on arterial variations. When the right and left upper extremities were compared in the remaining 27 upper extremities, no significant difference was found in the length measurements of the BA bifurcation ($P > 0.05$) [Table 2]. BA bifurcation was less common above the midline in both the right and the left upper extremities (right 6.3%, left 14.3%) [Figure 4]. No significant difference was found when comparing the right and left upper extremities ($P > 0.05$)
- In all upper extremities of 30 upper extremity cadavers examined, it was seen that the MN passed under the bicipital aponeurosis (100%). In addition, it was determined that the MN did not pass between the two heads of the PT in 1 right upper extremity and 1 left upper extremity (6.6%). This variation in the anatomical structure was explained in detail in the section on MN variations
- The superficial vein course types and data in the right upper extremities and left upper extremities are presented in Figure 5
- Measurements were obtained from 23 of the 30 upper extremity cadavers exhibiting superficial vein courses. Type-1 and Type-2 vein courses, which are generally accepted as courses, are included in the statistics. Five superficial vein courses (1 right upper extremity and 4 left upper extremities) were

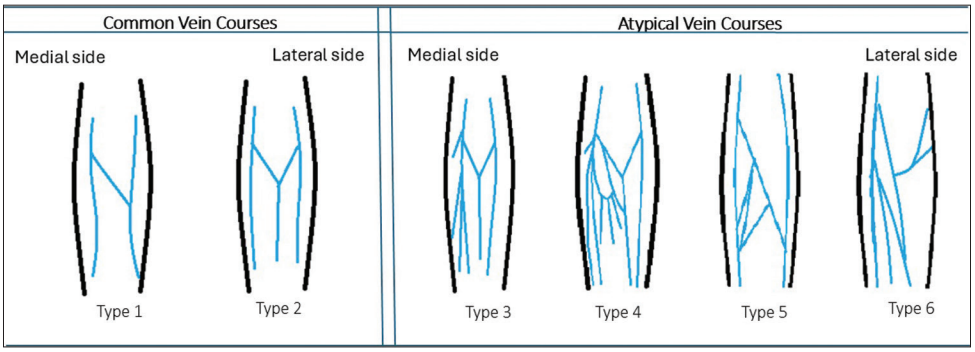

Figure 2: Illustrating the different types of vein courses

Table 1: Measurements of arm length, forearm length, midline length, and bicipital aponeurosis width

	Direction	*n*	*Mean±SD	*Minimum–maximum	*P*
Arm length	Left	14	281.4±16.2	253.6–300.7	0.969[a]
	Right	16	282.2±14.8	252.6–305.6	
Forearm length	Left	14	252.92±13.23	229.9–275.2	0.944[a]
	Right	16	256.14±13.37	225.3–274.7	
Straight line length between ME and LE, "midline"	Left	14	64.9±4.1	59.3–76.1	0.208[a]
	Right	16	67.6±4.7	57.7–75.6	
Bicipital aponeurosis width	Left	14	11.6±1.7	8.3–14.4	0.769[a]
	Right	16	11.5±1.8	7.9–14.3	

*The measurements above are expressed in "mm." Statistical analysis was done with the *t*-test. ME: Medial epicondyle, LE: Lateral epicondyle, SD: Standard deviation

found to have atypical vein courses. This variation in the anatomical structure was explained in detail in the section on vein course variations. Out of 23, 18 upper extremities were included in the statistics. The results of the measurement of the MCuV joining the CV on the right and left upper extremities, and the analysis of whether it joins above or below the midline are presented in Table 3. It was seen that MCuV bifurcated in 9 of 18 upper extremities, excluding atypical groups. This bifurcation was below the midline in all samples (100%).

Variation Results

Vein course variations

- It was determined that 5 vein courses of 23 upper extremities were in the atypical group (1 in the right upper extremity and 4 in the left upper extremity). Of these, Type 3 vein courses were found in 2 left upper extremities (16.6%) [Figure 6.1], Type 4 vein courses in 1 left upper extremity (8.3%), Type 5 vein courses in 1 left upper extremity (8.3%), Type 6 vein courses in 1 right upper extremity (8.3%)

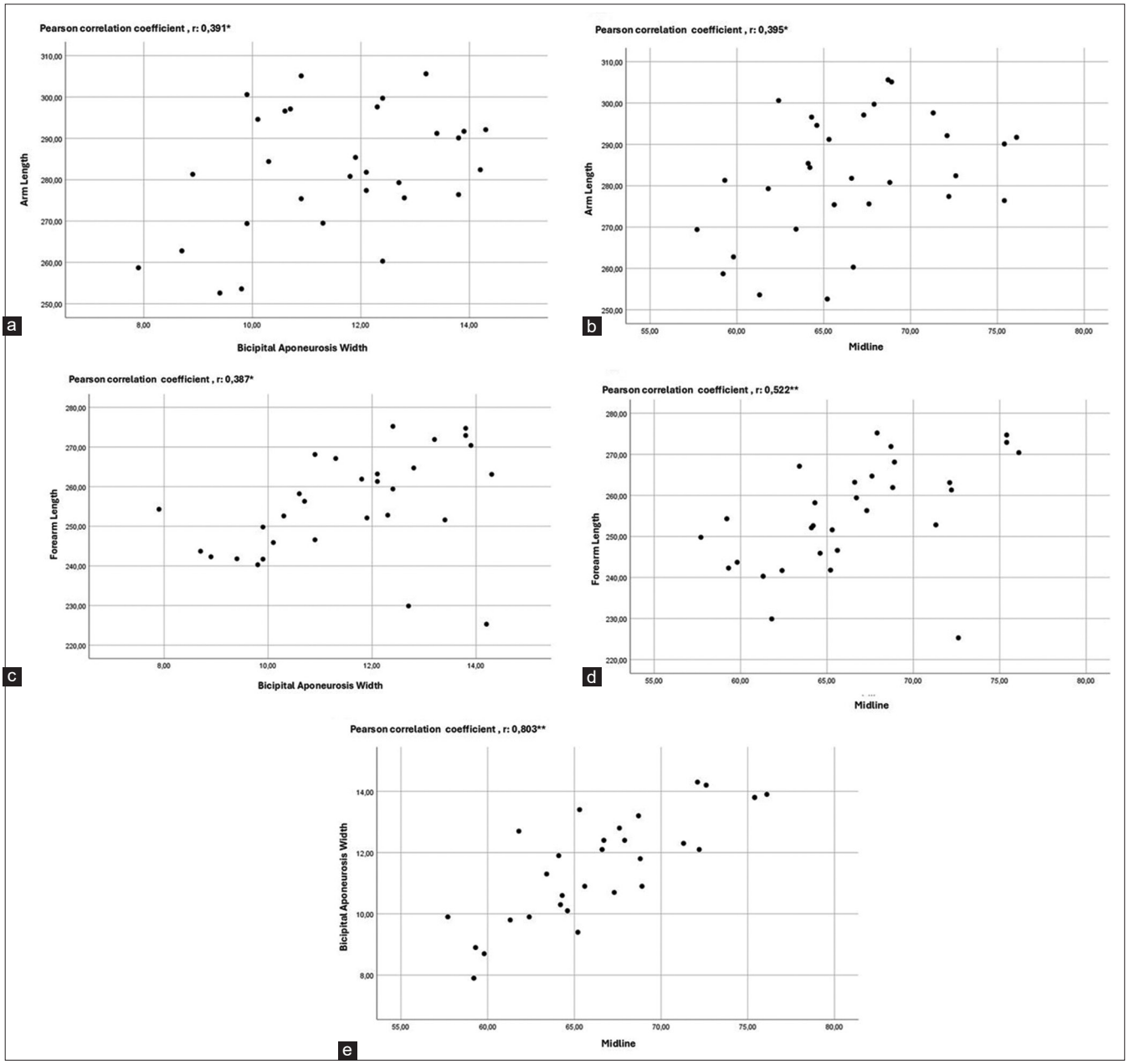

Figure 3: Correlation graphs of the arm length, the forearm length, the midline length and the bicipital aponeurosis width. Pearson correlation analysis was used. *<0.05, **<0.01. (a) Correlation of the arm length with the midline length, (b) Correlation of the arm length with the midline length, (c) Correlation of the forearm length with the bicipital aponeurosis width, (d) Correlation of the forearm length with the midline length, (e) Correlation of the bicipital aponeurosis width with the midline length

- In a cadaver upper extremity sample in the atypical group Type 3 vein course, it was seen that it bifurcated 10.1 mm below the midline and divided into 2 more branches, one of these branches joined the CV 0.2 mm above the midline, and the other joined the BV 37.2 mm above the midline. It was determined that the unnamed a and c branches joined the BV (b), which continues from distal to proximal, 0.3 mm below the midline, and in addition, the unnamed d branch joined 45.2 mm above the midline [Figure 6.1]. In the other sample, it was seen that it bifurcated 15.1 mm below the midline and divided into 2 more branches; one of these branches joins the CV 32.3 mm above the midline, and the other joins the BV 17.8 mm above the midline. It was determined that the unnamed branch joined the BV (b), which continues from distal to proximal, 1.6 mm above the midline, and in addition, the unnamed and d branches joined 22.6 mm above the midline
- In the Type 4 vein course sample, it was seen that it bifurcated 3.6 mm above the midline and divided into 2 more branches; one of these branches joined the CV 28.2 mm above the midline, and the other joined the BV 32.4 mm above the midline. In this sample, it was noticed that 4 unnamed branches (a, b, c, d) formed an arch 22.1 mm below the midline. The B branch of the arch continued and joined an unnamed (A) branch 27.3 mm above the midline. This branch (X) joined the BV 32.4 mm above the midline, and the other branch of the arch, unnamed (C), joined the BV 32.2 mm above the midline [Figure 6.2]. It was also observed that the MN gave off a high proximal branch 31.9 mm above the midline [Figure 6.2]
- In the Type 5 vein course sample, it was noticed that MCuV joined CV 106.8 mm below the midline and joined BV 99.1 mm above the midline. In addition, anastomosis of unnamed branches (a, b, and c) was seen between MCuV and BV [Figure 6.3] (in this case, the MN also pierced the PTh, and a Type 5 vein course and the high origin of the radial artery were detected)
- In the Type 6 vein course sample, CV was seen to course from the wrist to the cubital fossa in the midline. MCuV was located just to the left. MCuV joined CV 105.7 mm below the midline. It anastomosed again 85.8 mm below as an additional. It joined BV 0.3 mm above the midline.

Table 2: Brachial artery measurements

	Direction	*n*	*Mean±SD	*Minimum–maximum	*P*
The distance from the bifurcation point of the BA to the midline	Left	12	28.63±7.1	20.8–41.3	0.885[a]
	Right	15	28.27±5.7	19.4–41.8	
The distance from the projection of the bifurcation point of the BA in the midline to the ME	Left	12	31.23±4.7	21.6–39.4	0.222[a]
	Right	15	33.66±5.2	24.9–44.1	
The distance from the projection of the bifurcation point of the BA in the midline to the LE	Left	12	34.91±4.3	25.8–40.8	0.659[a]
	Right	15	35.94±7.5	23.4–48.1	

*The measurements above are expressed in "mm." [a]Independent samples t-test. BA: Brachial artery, ME: Medial epicondyle, LE: Lateral epicondyle, SD: Standard deviation

Table 3: Measurement results of the median cubital veins in the right and left upper extremities

	Direction	*n*	*Mean±SD	*Minimum–maximum	*P*
The distance from the point of joining of the MCuV to the BV to the midline	Left	7	38.3±17.3	10.4–59.6	0.225[a]
	Right	11	21.0±11.3	5.2–40.9	
The distance of the projection of the point of joining of the MCuV to the BV in the midline to the ME	Left	7	16.1±4.1	8.8–20.9	0.741[a]
	Right	11	16.8±4.7	11.2–25.5	
The distance of the projection of the point of joining of the MCuV to the BV in the midline to the LE	Left	7	49.10±5.3	43.7–56.4	0.307[a]
	Right	11	52.4±7.0	42.1–61.2	
The distance from the point of joining the MCuV to the CV to the midline	Left	7	29.8±22.9	7.80–78.4	0.179[a]
	Right	11	18.3±18.1	1.3–60.6	
The distance of the projection of the point of joining of the MCuV to the CV in the midline to the ME	Left	7	44.5±6.8	32.9–51.5	0.430[a]
	Right	11	47.1±6.6	35.9–59.5	
The distance of the projection of the point of joining of the MCuV to the CV in the midline to the LE	Left	7	21.3±8.6	10.9–32.3	0.948[a]
	Right	11	21.5±7.2	13.2–35.4	
The distance of the bifurcation point of the MCuV to the midline	Left	4	16.7±8.3	6.3–24.0	0.692[a]
	Right	5	14.4±8.6	3.8–25.4	
The distance of the projection of the MCuV bifurcation point on the midline to the ME	Left	4	32.6±0.9	31.4–33.5	0.064[a]
	Right	5	36.9±3.9	31.7–41.4	
The distance of the projection of the MCuV bifurcation point on the midline to the LE	Left	4	30.1±2.7	28.2–33.9	0.463[a]
	Right	5	32.4±5.4	26.2–38.3	

*The measurements above are expressed in "mm." [a]Independent samples t-test. MCuV: Median cubital vein, BV: Basilic vein, ME: Medial epicondyle, LE: Lateral epicondyle, CV: Cephalic vein, SD: Standard deviation

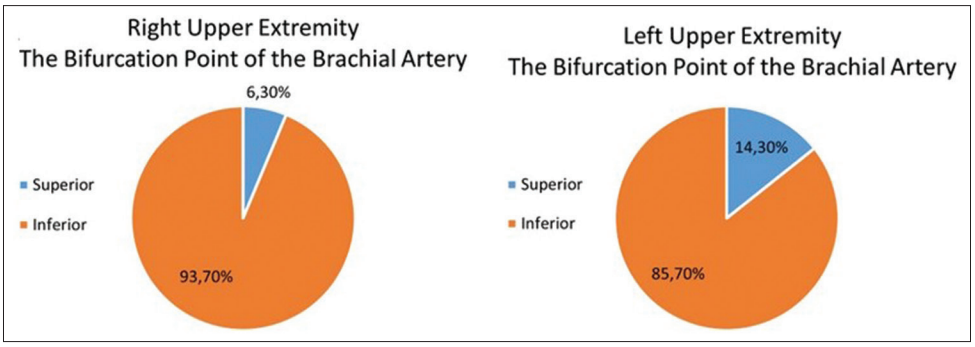

Figure 4: Brachial artery bifurcation is superior or inferior to the midline in the right and left upper extremities

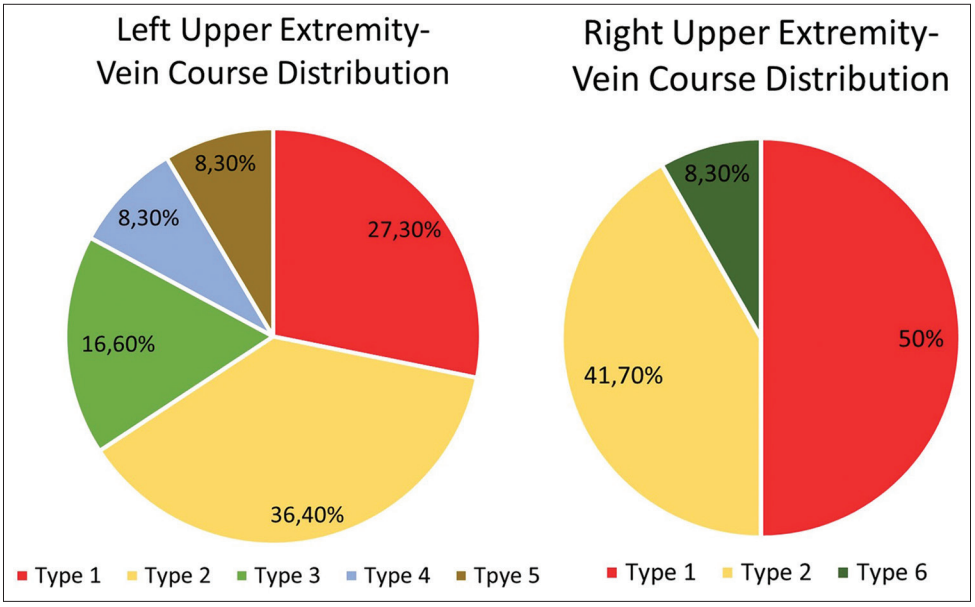

Figure 5: Comparative analysis of superficial vein course types of right and left upper extremities. Type 6 was not found in the left extremity. Type 3, Type 4, and Type 5 were not found in the right extremity

Figure 6: Atypical group superficial vein, (1) Type 3 vein course, CV: Cephalic vein, MCuV: median cubital vein, BV: basilic vein, b: basilic vein on the forearm, and a, c, d: unnamed branches. This photo shows the left arm of a cadaver. (2) Type 5 vein course. CV: Cephalic vein, MCuV: Median cubital vein, BV: Basilic vein and a, b, c: Unnamed branches. This photo shows the left arm of a cadaver. (3) Type 4 course, CV: cephalic vein, MCuV: median cubital vein, BV: Basilic vein and A, B, X, a, b, c, d: unnamed branches. *arcus formed by branches of unnamed veins, MN: median nerve, ++: Early branch of the median nerve. This photo shows the left arm of a cadaver. (4) Type 6 course image. CV: cephalic vein, MCuV: median cubital vein, BV: Basilic vein, A, B, C: Unnamed branches. This photo shows the right arm of a cadaver.

Unnamed branches (A, B, and C) were seen to join MCuV just before joining BV. CV gave one branch on the cubital fossa, then turned lateral and continued its normal course in the arm. Its branch (*) joined BV 136.2 mm above the midline [Figure 6.4] (In this case, the MN was seen to give a proximal branch 8.6 mm above the midline).

Median nerve variations

- In 30 upper extremity cadavers, it was observed that the roots forming the MN in 2 upper extremities (1 right and 1 left) were united distally, that is, in the arm (6.7%). In the right upper extremity case, the lateral root pierced the coracobrachialis muscle (CM). It converged with the medial root 138.8 mm above the midline of the arm and continued as the MN (in this case, the MN was seen to give a proximal branch 16.9 mm above the midline) [Figure 7.1]. In the left upper extremity, the lateral root and the medial root were seen to converge 200.8 mm above the midline of the arm and continued as the MN [Figure 7.2] (In this case, the musculocutaneous nerve (MCN) variation was also seen)
- In 1 right upper extremity of 30 upper extremity cadavers, it was determined that the MCN first

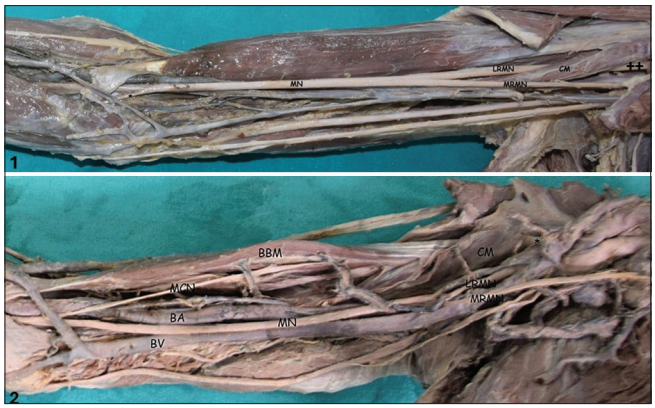

Figure 7: Median nerve roots arm junction and median nerve high proximal branch. (1) This photo shows the right arm of a cadaver. CM: Ccoracobrachialis muscle, LRMN: The lateral root of the median nerve, MRMN: the medial root of the median nerve, MN: median nerve, ++: Upper part of the lateral root, *: Early branch of the median nerve. (2) This photo shows the right arm of a cadaver. CM: Coracobrachialis muscle, MCN: Musculocutaneous nerve, LRMN: The lateral root of the median nerve, MRMN: the medial root of the median nerve, MN: median nerve, BBM: biceps brachii muscle, BV: Basilic vein and BA: Brachial artery, *: Passage of the musculocutaneous nerve by piercing the coracobrachialis muscle

Figure 8: Median nerve variations. (1) The MN did not pass between the two heads of the PT, MN: median nerve, PTu: Ulnar head of the pronator teres muscle. This photo shows the right arm of a cadaver. (2) Median nerve high proximal branch. MN: median nerve, *: Early branch of the median nerve. This photo shows the right arm of a cadaver. (3) The bicipital aponeurosis was elevated with forceps and the Struthers' ligament was shown. MN: Median nerve, *: Struthers' ligament. This photo shows the right arm of a cadaver

pierced the CM and then gave a branch to the MN 18.1 mm (3.3%) above the midline [Figure 7.2]

- It was determined that the MN did not pass between the two heads of the PT in 2 upper extremities (1 right and 1 left) of 30 upper extremity cadavers (6.7%) [Figure 8.1]
- In 30 upper extremity cadavers, the MN was found to give a proximal branch before the cubital fossa in 5 upper extremities (4 right and 1 left), (16.6%). It was determined that it gave a proximal branch 31.9 mm above the midline (in this case, Type 4 vein course was seen) [Figure 6.2]; 36.1 mm above, 15.7 mm above [Figure 8.2]; 16.9 mm above (in this case, there was also a MN formation variation) [Figure 7.1] and 8.6 mm above (in this case, Type 6 vein course and the high origin of the radial artery variation were seen)
- Struthers ligament was detected in 1 right upper extremity of 30 upper extremity cadavers (3.3%). Fibrous fibers extending from EM to PT surrounded the BA, brachial veins, and MN under the bicipital aponeurosis [Figure 8.3]
- It was determined that the MN pierced the humeral head of the PT (PTh) and then passed under a fibrous band extending from the ulnar head (PTu) in 1 right upper extremity of 30 upper extremity cadavers (3.3%) (in this case, Type 6 vein course and the high origin of the radial artery were also seen) [Figures 9.1 and 9.2].

Arter variations

In 30 upper extremity cadavers, the high origin of the radial artery was detected in 3 upper extremities (1 right and 2 left). In 30 upper extremity cadavers, the high origin of the radial artery was detected in 3 upper extremities (1 right and 2 left). In one of the left upper extremities, the radial artery was divided 198.3 mm above the midline (in this case, the convergence of the MN roots in the arm was also seen). In the other left upper extremity, the high origin of the radial artery was detected 152.8 mm above the midline (in this case, the MN also pierced the PTh, and a Type 5 vein course was detected) [Figure 10]. The high origin of the radial artery in the right upper extremity was found 150.4 mm above the midline (in this case, the proximal branch of the MN, and the course of the Type 6 vein were also seen).

Discussion

This study systematically investigated the anatomical structures within the cubital fossa of adult male cadavers. It is known that the course of superficial veins in the upper extremity is quite variable and has been the subject of numerous studies. Researchers have sought to categorize superficial vein courses by designating them with alphanumeric labels, such as Type M, Type N, or Type 1, Type 2, to enhance clarity and comprehension. These classifications are often derived from cadaveric studies, which are frequently employed for this purpose. One study classified superficial vein courses as Type N-M-Y and Type I, with Type M and Type Y being the common types,[10] whereas another study identified Types M, N, and H.[11] Subsequently, another study suggested that a Type M vein course could also be called a Type H vein course.[12] In another review, which included a substantial sample size of 9,924 upper extremity superficial vein courses across 27 studies, a total of eight types of vein courses were identified to establish a classical definition. These included Type M, Type N (or Type H), Type I, Type O, and Types 4 through 8.[13] However, this has led to ambiguity and inconsistency in the literature. The frequency of superficial vein courses, which are complicated to name, also varies among populations. The most common types are reported to be Type N (Type 1) vein course and Type M (Type 2) vein course.[4,5,10,14,15] In this study, when the total values were

analyzed without regard to the right or left sides, Types 1 and 2 were observed to be more prevalent, consistent with the literature. However, the Type Y vein course, as reported in previous studies, was not observed. In addition, four distinct types were identified as atypical vein courses.

The MN passes between the two heads of the PT muscle during its course and is reported to be between 70% and 90% in the researcher's sample.[16-22] In this study, it was observed that the MN passed between the two heads of the PT in 90% of the cases, a result that aligns with existing literature.

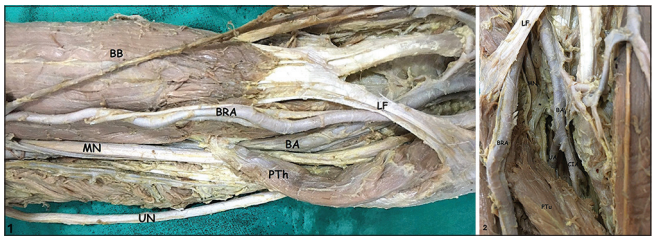

Figure 9: (1) It is seen that the median nerve continues distally by piercing the humeral head of pronator teres. MN: Median nerve, BB: Biceps brachii muscle, UN: Ulnar nerve, BA: Brachial artery, PTh: Humeral head of pronator teres, BRA: brachioradial artery (or high origin of the radial artery), LF: Lacertus fibrosus (also known as bicipital aponeurosis) (2). In front view of the cubital fossa in the left upper extremity. The median nerve passes under the fibrous band extending from the ulnar head of the pronator teres muscle. LF: lacertus fibrosus (also known as bicipital aponeurosis), MN: Median nerve, BA: brachial artery, UA: Ulnar artery, CIA: common interosseous artery, PTu: Ulnar head of the pronator teres, BRA: Brachioradial artery (or high origin of the radial artery), *: Fibrous band. This photo shows the left arm of a cadaver

However, this rate was lower in the left extremity (78.6%) and higher in the right upper extremity (100%). Due to the anatomical course of MN, it is adjacent to many structures. Therefore, it is associated with entrapment neuropathies due to variations. The absence of the ulnar head of PT was reported in 8%,[21] 8.7%,[17] 8.75%,[16] 13%,[19] and 14%.[20,22] n addition, it has been shown in studies that during MN, PT penetrates the ulnar head in 11%,[20] and 2%.[19] It has been shown in previous studies that the PTu has a fibromuscular structure, that is, the PTu adheres to the ulna in the form of a fibrous band, sometimes even in the form of two fibrous bands.[21] It was reported that the PTu (PT ulnar head) was underdeveloped in 28.3%[20] and 17%[22] of cases, with the ulnar head being attached to the ulna as a fibrous structure. However, PTu has been reported to appear as a fibrous band not associated with the muscle in 6.7%[20] and 9%[19] of cases. Another variation is that the MN pierces PTh. MN penetrating the humeral head of the PT has been reported in 3%,[22] 2.5%,[16] 2%,[19] and 2%.[17] In this study, no case was detected without the PTu. It was observed that MN pierced the PTh in 3.3% of cases and passed under the ulnar head, which extended as a fibrous band. No previous studies were found showing that variation. To the best of our knowledge, this is the first time this phenomenon has been demonstrated.

Another trapping point of MN is the presence of Struthers' ligament, a fibrous band. This ligament generally starts from the supracondylar humeral process. The ligament of Struthers has been reported in case reports on MRI studies

Figure 10: (1) The left upper extremity showing multiple variations is shown. In the left upper extremity, a high origin of the radial artery (2), MN also punctured the PTh (3), and Type 5 vein course (4) were detected. Close-ups are presented in images 2, 3, and 4, (2) The branching site of the brachioradial artery (or high origin of the radial artery) and its course through the upper extremity BRA: Brachioradial artery (or high origin of the radial artery), BA: brachial artery, MN: Median nerve, BB: Biceps brachii muscle, UN: ulnar nerve, LRMN: The lateral root of the median nerve, MRMN: The medial root of the median nerve, PTh: Humeral head of pronator teres, LF: Lacertus fibrosus (also known as bicipital aponeurosis), UA: Ulnar artery, CIA: Common interosseous artery, *: Fibrous band. This photo shows the left arm of a cadaver, (3) It is seen that the median nerve continues distally by piercing the humeral head of pronator teres. MN: Median nerve, BB: Biceps brachii muscle, UN: Ulnar nerve, BA: Brachial artery, PTh: Humeral head of pronator teres, BRA: brachioradial artery (or high origin of the radial artery), LF: Lacertus fibrosus (also known as bicipital aponeurosis) (4) In front view of the cubital fossa in the left upper extremity. The median nerve passes under the fibrous band extending from the ulnar head of the pronator teres muscle. LF: lacertus fibrosus (also known as bicipital aponeurosis), MN: Median nerve, BA: brachial artery, UA: Ulnar artery, CIA: common interosseous artery, PTu: Ulnar head of the pronator teres, BRA: Brachioradial artery (or high origin of the radial artery), *: Fibrous band. This photo shows the left arm of a cadaver

or cadaver dissections.[23-25] Struthers' ligament may also be present in the absence of the supracondylar humeral process.[18,20,26,27] However, this is a scarce condition occurring in 0.7% of the population.[26,28] This study detected Struthers' ligament in 3.3%.

The branches of the MN to innervate the PT generally emerge after passing the epicondylar line. In rare cases, it is stated that this branch originates from the proximal part of the EL.[29] The proximal branch of the MN, 1.31 ± 0.58 cm,[30] 4.9 cm,[31] 2.8 cm–3.5 cm,[20] and 10 cm[32] were stated to be proximal to the EL. In this study, it was observed that the proximal branch of the MN was identified in 10% of the cases. The highest proximal of these branches measured 3.6 cm, while the most distal measured 1.6 cm.

Variations of the MCN are quite common.[18] There are cases where the MCN is absent, pierces the coracobrachialis (CB), joins the MN, or passes behind the BB.[18,33-37] It has been reported that the MCN originates from the lateral root, then pierces the CB and joins the MN as the third root in 1.7%.[36] Another study reported that the MCN gives off a branch that joins the MN 2.5 cm above the midline after piercing the CB.[37] MCN perforation is frequently reported in the CB. The upper part of the CB was detected in 56%[38] and 43%;[39] the middle part was detected in 24%[40] and 37%;[41] and the distal part was detected in 20%[40] and 17%.[41] In this study, all cases had MCN (100%). It was found that MCN pierced the CB and sent branches to the MN in 3.3%. When the root unions of the MN were examined, it was reported that the lateral root of the MN pierced the CB in 1.8% of the cases[33] or the medial and lateral roots of the MN united in the arm and formed the MN in 17.3% of the cases.[42] In this study, it was noted that the medial and lateral roots of the MN united in the arm region in 6.7% of the cases.

The BA typically bifurcates into two arteries near the radial head: the ulnar artery and the radial artery. However, in some instances, the radial artery has been observed to separate from the BA in the arm region or directly from the axillary artery.[38,43-45] Some studies use different terminology for the separated radial artery.[39] Established nomenclature guidelines to address issues such as the topographic analysis of the separation point, determination of the region, and whether the separated vessel follows a superficial course. The brachioradial artery is the superior division of the radial artery arising from the BA. When the arm was examined in three sections, it was reported that there was no significant difference between the origin of the radial artery from the axillary artery or any part of the BA. In both cases, it can be identified as the brachioradial artery. The brachioradial artery is the most common variation among arteries.[39] In this study, the radial artery can be defined as the brachioradial artery when its course is considered, and the radial artery arises from the upper part of the BA. Rates of the brachioradial artery have been reported as 13.8%,[39] 9.2%,[44] 8%,[46] 0.47%,[47] and 0.25%.[38] After branching off, the brachioradial artery exhibits variations in its distal course. In the cubital fossa, research has shown that it travels over the bicipital aponeurosis in 36%,[39] and 0.47%.[47] It has been documented to pass under the bicipital aponeurosis in 64%,[39] 0.47%,[47] and 0.25%.[38]

Radial artery or BA may be preferred for arterial catheterization in newborns and children.[48] A comprehensive retrospective study found that of 62,626 arterial lines examined in 57,787 patients, radial artery catheterization was associated with the lowest risk of complications, while femoral artery catheterization was the most dangerous.[49] For coronary artery bypass graft surgery, it is considered safer to remove the radial artery than the ulnar artery.[50] The radial artery is the preferred site for coronary interventions over femoral artery catheterization due to its lower relative risk of complications, easier access, and improved patient comfort. It is also a preferred site for dialysis. However, it requires caution during interventions due to its proximity to the CV. Variations in the radial artery can pose risks for interventional procedures.[46] In addition, the presence of the brachioradial artery and its tortuous course can negatively impact processes such as cannulation and surgical procedures.[51]

CRPS is a condition in which neuropathic pain persists despite apparent tissue healing.[8] CRPS can occur as a result of simple venipuncture,[7,8] IV injection and vaccination,[52] risk of arterial puncture of the BA,[53] fractures or surgical interventions in the forearm[9] or in the case of the cubital tunnel in the forearm.[8] It can be most painful for patients and affects their quality of life. In some cases, it can cause a loss of work capacity. However, it can lead to large compensation decisions for healthcare professionals and authorities to pay CRPS patients.[7,9] For these reasons, rather than examining the structures passing over or through the cubital fossa individually, a more holistic approach seems to be a better option.

Conclusions

A comprehensive understanding of the anatomy of the cubital fossa and its associated neurovascular structures is essential to minimizing complications in both surgical and radiological interventions in this region. Preoperative imaging, particularly ultrasonography, plays a critical role in ensuring a safe and precise surgical approach, thereby preserving the integrity of the nerve and surrounding anatomical structures.

Financial support and sponsorship

Nil.

Conflicts of interest

There are no conflicts of interest.

References

1. Moore KL, Dalley AF, Agur AM, editors. Clinically Oriented Anatomy. 7th ed. Baltimore: Lippincott Williams and Wilkins; 2014. p. 670-820.
2. Snell RS. Clinical Anatomy. 9th ed. Baltimore: Lippincott Williams and Wilkins: 2012. p. 334-435.
3. Mikuni Y, Chiba S, Tonosaki Y. Topographical anatomy of superficial veins, cutaneous nerves, and arteries at venipuncture sites in the cubital fossa. Anat Sci Int 2013;88:46-57.
4. Singh JD. Patterns of superficial veins of the cubital fossa in Nigerian subjects. Acta Anat (Basel) 1982;112:217-9.
5. Lee H, Lee SH, Kim SJ, Choi WI, Lee JH, Choi IJ. Variations of the cubital superficial vein investigated by using the intravenous illuminator. Anat Cell Biol 2015;48:62-5.
6. Ellis H. The antecubital fossa. Surgery (Oxford) 2010;28:e1-9.
7. Yamada K, Yamada K, Katsuda I, Hida T. Cubital fossa venipuncture sites based on anatomical variations and relationships of cutaneous veins and nerves. Clin Anat 2008;21:307-13.
8. Oaklander AL, Horowitz SH. The complex regional pain syndrome. Handb Clin Neurol 2015;131:481-503.
9. Petersen PB, Mikkelsen KL, Lauritzen JB, Krogsgaard MR. Risk factors for post-treatment Complex Regional Pain Syndrome (CRPS): An analysis of 647 cases of CRPS from the Danish patient compensation association. Pain Pract 2018;18:341-9.
10. Jasiński R, Poradnik E. Superficial venous anastomosis in the human upper extremity – A post-mortem study. Folia Morphol (Warsz) 2003;62:191-9.
11. Ukoha UU, Oranusi CK, Okafor JI, Ogugua PC, Obiaduo AO. Patterns of superficial venous arrangement in the cubital fossa of adult Nigerians. Niger J Clin Pract 2013;16:104-9.
12. Singh V. Textbook of Anatomy: Upper Limb and Thorax. Haryana: Reed Elsevier India Private Limited.; 2014.
13. Yammine K, Erić M. Patterns of the superficial veins of the cubital fossa: A meta-analysis. Phlebology 2017;32:403-14.
14. Dharap AS, Shaharuddin MY. Patterns of superficial veins of the cubital fossa in Malays. Med J Malaysia 1994;49:239-41.
15. Vasudha TK. A study on superficial veins of the upper limb. Natl J Clin Anat 2013:2:204-8.
16. Beaton LE, Anson BJ. The relation of the median nerve to the pronator teres muscle. Anat Rec 1939;75:23-6.
17. Jamieson RW, Anson BJ. The relation of the median nerve to the heads of origin of the pronator teres muscle, a study of 300 specimens. Q Bull Northwest Univ Med Sch 1952;26:34-5.
18. Tubbs RS, Riz E, Shoja MM, Loukas M, Barbaro N, Spinner RJ. Nerves and Nerve Injuries: History, Embryology, Anatomy, Imaging, and Diagnosis. 1st ed., Vol 1. London: Elsevier; 2015.
19. Stabille SR, Duarte E, Carvalho VC. Pronator teres muscle: Anatomical variations and predisposition for the compression of the median nerve. Acta Sci Biol Sci 2002;24:631-7.
20. Caetano EB, Vieira LÂ, Sprovieri FA, Petta GC, Nakasone MT, Serafim BL. Anatomical variations of pronator teres muscle: Predispositional role for nerve entrapment. Rev Bras Ortop 2017;52:169-75.
21. Gurses IA, Altinel L, Gayretli O, Akgul T, Uzun I, Dikici F. Morphology and morphometry of the ulnar head of the pronator teres muscle in relation to median nerve compression at the proximal forearm. Orthop Traumatol Surg Res 2016;102:1005-8.
22. Nebot-Cegarra J, Perez-Berruezo J, Reina de la Torre F. Variations of the pronator teres muscle: Predispositional role to median nerve entrapment. Arch Anat Histol Embryol 1991;74:35-45.
23. Camerlinck M, Vanhoenacker FM, Kiekens G. Ultrasound demonstration of Struthers' ligament. J Clin Ultrasound 2010;38:499-502.
24. Mizia E, Zarzecki MP, Pekala JR, Baginski A, Kaythampillai LN, Golebiowska M, *et al*. An anatomical investigation of rare upper limb neuropathies due to the Struthers' ligament or arcade: A meta-analysis. Folia Morphol (Warsz) 2021;80:255-66.
25. Pećina M, Borić I, Anticević D. Intraoperatively proven anomalous Struthers' ligament diagnosed by MRI. Skeletal Radiol 2002;31:532-5.
26. Nucchi AB, Desai SD, Karjagi SB, Bulaguda RS. Variant origin of pronater teres from Struthers' ligament with higher bifurcation of brachial artery. J Pharm Sci Res 2012;4:1986-8.
27. Suranyi L. Median nerve compression by Struthers ligament. J Neurol Neurosurg Psychiatry 1983;46:1047-9.
28. Allieu Y, Mackinnon SE. Nerve Compression Syndromes of the Upper Limb. London, Martin Dunitz: Elsevier Limited.; 2002.
29. Tetro AM, Pichora DR. High median nerve entrapments. An obscure cause of upper-extremity pain. Hand Clin 1996;12:691-703.
30. Bindurani MK, Lokesh HM, Nanjundappa BN. Study of muscular branch of median nerve to the pronator teres. Natl J Clin Anat 2013;2:67-70.
31. Alves N, Cândido PL, Frazão R. Innervation of The pronator teres muscle. Int J Morphol 2004;22:237-40.
32. Gunther SF, DiPasquale D, Martin R. The internal anatomy of the median nerve in the region of the elbow. J Hand Surg Am 1992;17:648-56.
33. Guerri-Guttenberg RA, Ingolotti M. Classifying musculocutaneous nerve variations. Clin Anat 2009;22:671-83.
34. Barone R, D'Amico AG, Di Lorenzo N, Di Grado GL, Matranga E, Spinoso, G, *et al*. Anastomosis between median and musculocutaneous nerve: Presentation of a very rare anatomical variation in comparison to classical divisions. Anatomia 2022;1:68-74.
35. Nascimento SR, Ruiz CR, Pereira E, Andrades L, de Souza CC. Rare anatomical variation of the musculocutaneous nerve – Case report. Rev Bras Ortop 2016;51:366-9.
36. Rawlani S, Rawlani S, Meshram S. Anatomical variations between median and musculocutaneous nerve. J Datta Meghe Inst Med Sci Univ 2011;6:200-3.
37. Gelmi CA, Pedrini FA, Fermi M, Mariani GA, Cocco LI, *et al*. Communication between median and musculocutaneous nerve at the level of cubital fossa-a case report. Transl Res Anat 2018;11:1-4.
38. Zhan D, Zhao Y, Sun J, Ling EA, Yip GW. High origin of radial arteries: A report of two rare cases. ScientificWorldJournal 2010;10:1999-2002.
39. Rodríguez-Niedenführ M, Vázquez T, Nearn L, Ferreira B, Parkin I, Sañudo JR. Variations of the arterial pattern in the upper limb revisited: A morphological and statistical study, with a review of the literature. J Anat 2001;199:547-66.
40. Ertürk H, Seyaz M, Öztürk K, Dursun A, Kastamoni Y. Anatomical variations of the musculocutaneous nerve in the human fetus. World Neurosurg 2023;179:e458-66.
41. Uysal II, Karabulut AK, Büyükmumcu M, Unver Dogan N, Salbacak A. The course and variations of the branches of the musculocutaneous nerve in human fetuses. Clin Anat 2009;22:337-45.
42. Budhiraja V, Rastogi R, Asthana AK. Anatomical variations of median nerve formation: Embryological and clinical correlation. J Morphol Sci 2011:28:283-6.
43. Bundi BN, Mutua V, Cheruiyot I, Munguti J, von Csefalvay C,

Nurani KM, *et al*. The unusual high origin radial artery in a black Kenyan population: A cadaveric study. Ethiop J Health Sci 2022;32:445-52.
44. Haładaj R, Wysiadecki G, Dudkiewicz Z, Polguj M, Topol M. The high origin of the radial artery (Brachioradial Artery): Its anatomical variations, clinical significance, and contribution to the blood supply of the hand. Biomed Res Int 2018;2018:1-11.
45. Konarik M, Knize J, Baca V, Kachlik D. Superficial brachioradial artery (radial artery originating from the axillary artery): A case-report and its embryological background. Folia Morphol (Warsz) 2009;68:174-8.
46. Nasr AY. The radial artery and its variations: Anatomical study and clinical implications. Folia Morphol (Warsz) 2012;71:252-62.
47. Konarik M, Kachlik D, Baca V. A coincidental variation of the axillary artery: The brachioradial artery and the aberrant posterior humeral circumflex artery passing under the tendon of the latissimus dorsi muscle. Bosn J Basic Med Sci 2014;14:239-43.
48. Schindler E, Kowald B, Suess H, Niehaus-Borquez B, Tausch B, Brecher A. Catheterization of the radial or brachial artery in neonates and infants. Paediatr Anaesth 2005;15:677-82.
49. Nuttall G, Burckhardt J, Hadley A, Kane S, Kor D, Marienau MS, *et al*. Surgical and patient risk factors for severe arterial line complications in adults. Anesthesiology 2016;124:590-7.
50. Brzezinski M, Luisetti T, London MJ. Radial artery cannulation: A comprehensive review of recent anatomic and physiologic investigations. Anesth Analg 2009;109:1763-81.
51. Clarke E, Skrzat J, Tubbs RS, Iwanaga J, Mazurek A, Wysiadecki G. Rare origin of the brachioradial artery – A case found on a historical specimen prepared by Ludwik Karol Teichmann. Transl Res Anat 2021;23:100-9.
52. Babineau R, Alweis R. Intramuscular injection and complex regional pain syndrome development after "Harmless" procedures. Cureus 2020;12:e9393.
53. Vaz A, Costa A, Pinto A, Silva AI, Figueiredo P, Sarmento A, *et al*. Complex regional pain syndrome after severe COVID-19 – A case report. Heliyon 2021;7:e08462.

Original Article

Fetal Type Posterior Cerebral Artery in the Tribal and Nontribal Populations of Assam

Farheen Atia Karim, Raihan Uddin Ahmed[1]

Departments of Anatomy and [1]Forensic Medicine, Assam Medical College and Hospital, Dibrugarh, Assam, India

Abstract

Background: Fetal type posterior cerebral artery (FTP) is a variant of the circle of Willis in which the distal posterior cerebral artery is perfused by a branch of internal carotid artery. **Objectives:** Estimation of different types of posterior cerebral artery configurations in the tribal, nontribal and total populations of Assam. **Subjects and Methods:** The circle of Willis of 109 human brains belonging to both tribal and nontribal populations of Assam were dissected and observed under the dissecting microscope. External diameters of both sided precommunicating and postcommunicating segments of posterior cerebral arteries close to their origins and that of the posterior communicating artery at the midpoint were measured using Vernier calipers. The circle of Willis was classified as having adult configuration, transitional configuration, and fetal or embryonic configuration using the specific criteria. **Results and Observations:** Right transitional configuration was observed in 10.53% tribals, 6.67% nontribals, and 7.34% of total population. Left transitional configuration was observed in 5.56% nontribals and 4.59% of otal population. Right fetal configuration was observed in 10.53% tribals, 21.11% nontribals, and 19.27% of total population. Left fetal configuration was observed in 10.53% tribals, 15.56% nontribals, and 14.68% of total population. Bilateral fetal configuration was observed in 3.3% nontribals and 2.75% of total population. **Conclusion:** A study of this nature is potentially useful to vascular surgeons, neurosurgeons performing surgeries in the tribal and nontribal populations of Assam.

Keywords: *Adult configuration, circle of Willis, fetal configuration, fetal type posterior cerebral artery, transitional configuration, tribal and nontribal populations of Assam*

Introduction

The cerebral arteries of opposite sides are intimately connected together at the base of the brain by anastomosing channels, an arrangement which provides for the continuation of a regular blood supply if one or more of the main trunks should be obstructed.

These vessels form the so-called circulus arteriosus, described by Willis (1664) and long known as the "Circle of Willis.' It is situated at the base of the brain in the interpeduncular cistern and is irregularly polygonal in outline. It is formed by the termination of basilar and the two posterior cerebral arteries, the posterior communicating arteries and the internal carotids, the anterior cerebral arteries, and the anterior communicating artery. A comprehensive account of the circle is that by Alpers, Berry, and Paddison (1959). It is subject to many variations, the most common being an enlargement of one (or both) posterior communicating artery so that a greater portion (or all) of the blood in the posterior cerebral artery is derived from the internal carotid artery.[1]

Fetal type posterior (FTP) cerebral artery is a common anatomic variation observed in the circle of Willis and defined as a posterior cerebral artery that originates from the internal carotid artery with or without a small connection with the basilar artery.[2] In this condition instead of the basilar artery, the internal carotid artery supplies blood to the posterior cerebral artery.[3]

The posterior cerebral artery is divided into two parts by the posterior communicating artery, the proximal part is named as precommunicating part (P1) and the distal part the post communicating part (P2), three basic configurations of the posterior communicating artery has been described;[4] adult, transitional and fetal. In the Fetal configuration: The diameter of

How to cite this article: Karim FA, Ahmed RU. Fetal type posterior cerebral artery in the tribal and nontribal populations of Assam. J Anat Soc India 2025;74:313-9.

Article Info

Received: 23 February 2025
Revised: 23 March 2025
Accepted: 08 November 2025
Available online: 31 December 2025

Address for correspondence:
Dr. Farheen Atia Karim, House No. 18, Hemgiri Path, South Sarania, Ulubari, Guwahati - 781 007, Assam, India.
E-mail: farheenak75@gmail.com

Access this article online

Website: https://journals.lww.com/joai

DOI: 10.4103/jasi.jasi_37_25

Quick Response Code:

ipsilateral pre communicating (P1) segment is less than the diameter of posterior communicating artery, so that the blood supply to the occipital lobe is mainly via the internal carotid arteries. In transitional configuration, the posterior communicating artery is equal in diameter to the P1 segment of posterior cerebral artery; here both P1 and posterior communicating artery make an approximately equal contribution to posterior cerebral artery distal to circle of Willis. In the adult configuration P1 has a diameter larger than the posterior communicating artery so that the blood supply to the occipital lobe is mainly via vertebrobasilar system. Such anatomical variations as in fetal configuration may have clinical significance as it makes it possible for thrombotic material arising in atherosclerotic lesions in the internal carotid artery to be dislodged into the posterior cerebral artery via the larger diameter posterior communicating artery.[5]

Two definitions of fetal posterior cerebral artery exist in the literature: complete fetal cerebral artery and partial fetal cerebral artery. Complete fetal cerebral artery is defined as posterior cerebral artery that completely originates from internal carotid artery with no connection with the basilar artery. Partial fetal cerebral artery is defined as posterior cerebral artery originating from internal carotid artery with a small, or atretic, connection with the basilar artery.

An important consequence of the fetal variant of the circle of Willis could be an increased stroke risk in patients with obstructive arterial disease, as has been described in postmortem studies.[6]

Anomalies found in a pattern of the posterior part of circle of Willis result due to persistence of vessels that normally disappear or disappearance of normal vessels.[7]

Different distributions of variations of the circle of Willis may partially explain the different incidence of some cerebrovascular diseases in different ethnic or racial groups.[8,9] The incidence of ischemic stroke is different among different populations, especially negroes and Hispanics compared with Whites.[10]

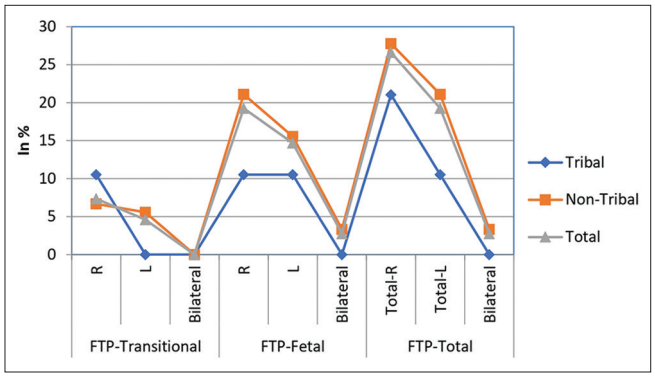

Figure 1: Line diagram depicting transitional, fetal and total fetal type posterior circulation in the tribal, nontribal, and the total population in the right and left sides and bilaterally. FTP: Fetal type posterior, T: Tribal, NT: Nontribal, Total: Total population, R: Right, L: Left, B/L: Bilaterally

Assamese population can be divided broadly into tribals and nontribals (the majority). In Assam, there are as many as 23 tribal communities which constitute 12.82% of the total population of the state [Figure 1].[11]

Aim of the study

The aim of the study is to estimate the prevalence of various configurations of the posterior circulation of the circle of Willis such as, adult configuration, transitional configuration, and fetal or embryonic configuration in the population of Assam and their differences in the constituent ethnic groups of the population of Assam the "Tribal" and "Non-Tribal."

Subjects and Methods

The study had been carried out in an apex government hospital in Assam located at Guwahati. It is a referral hospital and dead bodies from all over Assam are brought here, hence, they are considered to represent the population of Assam. Brain specimens were randomly collected from the autopsies done in the department of forensic medicine.

Selection of brain specimens

Inclusion criteria

- Brains were collected from cadavers of both sexes of ages ranging from ages 14–72 years
- Brains were collected from autopsies done within 3 h following death.[12]

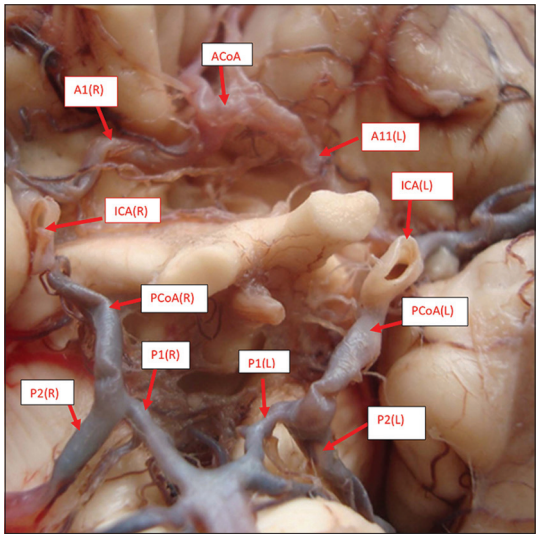

Figure 2: Bilateral fetal configuration of posterior cerebral artery. Red Arrow directed towards the point of interest. ACoA: Anterior communicating artery, A1(R): Precommunicating part of anterior cerebral artery (right), A1(L): Precommunicating part of anterior cerebral artery (left), ICA (R): Internal carotid artery (right), ICA (L): Internal carotid artery (left), PCoA (R): Posterior communicating artery (right), PCoA (L): Posterior communicating artery (left), P1(R): Precommunicating part of posterior cerebral artery (right), P1(L): Precommunicating part of posterior cerebral artery (left), P2(R): Postcommunicating part of posterior cerebral artery (right), P2(L): Postcommunicating part of posterior cerebral artery (left)

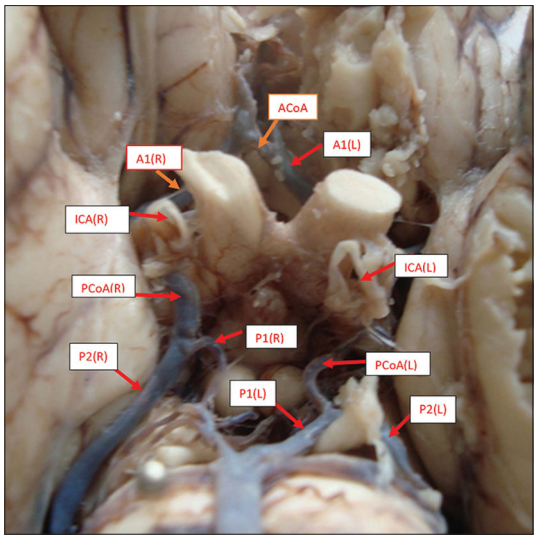

Figure 3: Right-sided fetal configuration of posterior cerebral artery. Red Arrow directed towards the point of interest. ACoA: Anterior communicating artery, A1(R): Precommunicating part of anterior cerebral artery (right), A1(L): Precommunicating part of anterior cerebral artery (left), ICA (R): Internal carotid artery (right), ICA (L): Internal carotid artery (left), PCoA (R): Posterior communicating artery (right), PCoA (L): Posterior communicating artery (left), P1(R): Precommunicating part of posterior cerebral artery (right), P1(L): Precommunicating part of posterior cerebral artery (left), P2(R): Postcommunicating part of posterior cerebral artery (right), P2(L): Postcommunicating part of posterior cerebral artery (left)

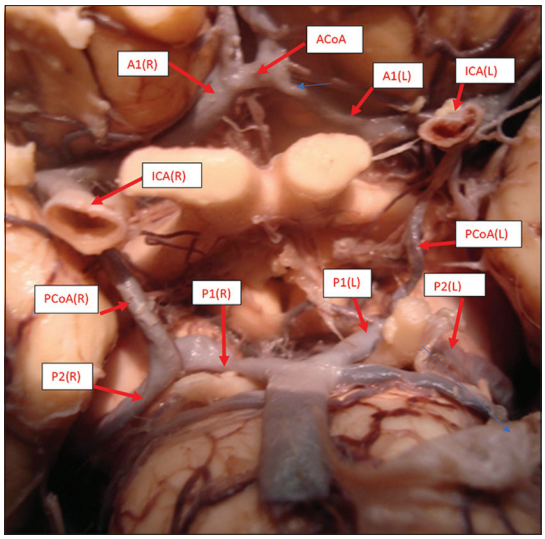

Figure 4: Right-sided transitional configuration of posterior cerebral artery. Red Arrow directed towards the point of interest. ACoA: Anterior communicating artery, A1(R): Precommunicating part of anterior cerebral artery (right), A1(L): Precommunicating part of anterior cerebral artery (left), ICA (R): Internal carotid artery (right), ICA (L): Internal carotid artery (left), PCoA (R): Posterior communicating artery (right), PCoA (L): Posterior communicating artery (left), P1(R): Precommunicating part of posterior cerebral artery (right), P1(L): Precommunicating part of posterior cerebral artery (left), P2(R): Postcommunicating part of posterior cerebral artery (right), P2(L): Postcommunicating part of posterior cerebral artery (left)

Exclusion criteria

- Brains belonging to decomposed bodies
- Brains with remarkable alterations in brain arteries or evidence of gross pathological lesions (such as crush injuries, macroscopically identified cortical tumors, severe hemorrhage, or infections).[12]

Sample size

A total of 109 brain specimens belonging to the population of Assam were collected randomly which included the number of brain belonging to the tribal group to be 19 and those belonging to the nontribal group to be 90.

Data collection procedure

The approval of institutional ethics committee was taken for the present study. Brains were serially numbered. Relevant data concerning the age and ethnicity (tribal or nontribal) were disclosed in the consent form and in the pro forma by the guardian of the deceased. Fine dissection of the circle of Willis at the base of the brain which was formaldehyde preserved was done under the dissecting microscope. Vernier calipers graduated to measure up to 0.1 mm were used to measure the external diameters at the following specific reference points:

- Right and left precommunicating and postcommunicating part of posterior cerebral arteries, (P1) and (P2), respectively, close to their origin
- Right and left posterior communicating arteries at their middle point.[13]

The measurements were taken twice. The calculated average was taken as the value for each artery. Photographs of each dissected circle of Willis were taken using the Sony digital camera.

Three configurations of the posterior bifurcation of posterior communicating artery can be distinguished as shown in Figures 2-4.

1. The adult configuration: This configuration is designated as the normal posterior part of the circle of Willis in which the P1 has a diameter larger than the posterior communicating artery which is not hypoplastic[4]
2. A transitional configuration: Here the posterior communicating artery and P1 have the same diameter and make an approximately equal contribution to the posterior cerebral artery distal to the circle of Willis[14,15]
3. A fetal or embryonic configuration: The diameter of the P1 is smaller than the diameter of the posterior communicating artery and the blood supply to the occipital lobes is mainly from the internal carotid artery.[5]

Since in transitional configuration and fetal configuration, there is a contribution of blood from internal carotid artery through ipsilateral posterior communicating artery to posterior cerebral artery, they are both considered as fetal type posterior circulation (FTP). Transitional configuration and fetal configuration of posterior circulation of circle of Willis together has been described as "Total FTP" in this present study.

Table 1: Transitional configuration, fetal type posterior circulation and total fetal type posterior circulation in the tribal, nontribal and the total population in the right and left sides and bilaterally

PCA	Tribal (%)	NT (%)	TP (%)	*t*	df	*P*
Transitional configuration (right)	2 (10.53)	6 (6.67)	8 (7.34)	0.178	6	0.864
Transitional configuration (left)	0	5 (5.56)	5 (4.59)			
Transitional configuration (bilaterally)	0	0	0			
Fetal configuration (right)	2 (10.53)	19 (21.11)	21 (19.27)	0.355	19	0.726
Fetal configuration (left)	2 (10.53)	14 (15.56)	16 (14.68)	0.187	14	0.855
Fetal configuration (bilaterally)	0	3 (3.3)	3 (2.75)			
Total FTP (right)	4 (21.05)	25 (27.78)	29 (26.61)	0.282	27	0.780
Total FTP (left)	2 (10.53)	19 (21.11)	21 (19.27)	0.355	19	0.726
Total FTP (bilaterally)	0	3 (3.33)	3 (2.75)			

P-value: Level of statistical significance, *t*: Student's *t*-test value, df: Degree of freedom. FTP: Fetal type posterior, TP: Total population, NT: Nontribal, PCA: Posterior cerebral artery

Table 2: Transitional, fetal and total; fetal type posterior circulation in the total population in the right and left sides and bilaterally

PCA	TP (%)	*t*	df	*P*
Transitional configuration (right)	8 (7.34)	0.199	11	0.8460
Transitional configuration (left)	5 (4.59)			
Transitional configuration (bilaterally)	0			
Fetal configuration (right)	21 (19.27)	0.366	35	0.7167
Fetal configuration (left)	16 (14.68)			
Fetal configuration (bilaterally)	3 (2.75)			
Total FTP (right)	29 (26.61)	0.164	28	0.8711
Total FTP (left)	21 (19.27)			

P-value: Level of statistical significance, *t*: Student's *t*-test value, df: Degree of freedom. FTP: Fetal type posterior, TP: Total population, PCA: Posterior cerebral artery

Table 3: Percentage of adult, fetal, and transitional configurations in the total population of Assam and the constituent tribal population and nontribal populations of Assam

	Total Assamese population (%)	Tribal population (%)	NT population (%)
Adult configuration	56 (51.37)	13 (68.42)	41 (45.56)
Transitional configuration	13 (11.93)	2 (10.53)	13 (12.43)
Fetal configuration	40 (36.70)	4 (21.06)	36 (39.97)

NT: Nontribal

The study variables and the relevant data were recorded, arranged, statistically analyzed, and displayed in tabulated forms as those belonging to

a. The "Total population" of Assam
b. The "Tribal" population of Assam
c. The "Non-Tribal" population of Assam.

Data collected were thoroughly cleaned and entered into MS-Excel spread sheet and analysis was carried out. The $P < 0.05$ is considered statistically significant in the present study The data is represented in 3 tables - Tables 1-3.

The authors declare that they have no competing interests.

Results and Observations

Right Transitional configuration was observed in 10.53% Tribals, 6.67% 44 Non-Tribals and 7.34% of Total population. Left Transitional configuration was observed in 5.56% Non45 Tribals and 4.59% of otal population. Right Fetal configuration was observed in 10.53% Tribals, 46 21.11% Non-Tribals, 19.27% of Total population. Left Fetal configuration was observed in 10.53% 47 Tribals, 15.56% Non-Tribals and 14.68% of Total population. Bilateral Fetal configuration was observed 48 in 3.3% Non-Tribals and 2.75% of Total population.

Discussion

In the present study, adult configuration was found in 51.37% in the total population of Assam, whereas it was found in 68.42% and 47.78% of its constituent tribal and nontribal populations, respectively. On an magnetic resonance angiography (MRA) study of 923 healthy volunteers, adult configuration was found in 776 (84.1%).[39] In a study done in Andhra Pradesh, out of 50 adult brains, 80% showed adult configuration, of which bilateral configuration were present in 26 brains, left-sided adult configuration was seen among three brains and right-sided configuration was seen in seven brains.[25] A Sri Lankan study of 225 brains showed adult configuration in 220 (93%); bilaterally in 200 (88.8%); and unilaterally in 20 (8.8%) ten being on the left side and ten on the right side.[27]

In the present study, the tribal population showed transitional configuration in 2 (10.53%) brains on the right side, whereas none on the left side and bilaterally. Nontribal population demonstrated transitional configuration 6 (6.67%) on the right side, 5 (5.56%) on the left side, and none bilaterally. The total population of Assam showed the presence of transitional configuration 8 (7.34%) on the right, 5 (4.59%) on left, and nil bilaterally. According to the literature, transitional configuration was found in 3 out of 50 total brains, i.e., 6% while none on the left side and bilaterally in a study in Andhra Pradesh.[25] Other studies showed transitional configuration in 7%,[33] 8%,[40]

Table 4: Prevalence of various developmental configurations of the circle of Willis in different populations

Author (year)	Population	Method	Sample size	Adult configuration (%)	Fetal configuration (%)	Transitional configuration (%)
Hoang *et al*. (2022)[16]	Vietnam	MSCT64	102	55 (53.92)	25 (24.51)	3 (2.94)
Rangus *et al*. (2022)[17]	Berlin, Germany	TOF MRA	1000	-	33.3	33
Haghighimorad *et al*. (2022)[18]	Iran	MRI and MRA	298	-	63 (21.1)	-
Prefulla *et al*. (2021)[19]	South India	Cadaveric study	44	78.41	Partial FTP: 12.5 Complete FTP: 3.41	5.68
Malamateniou *et al*. (2009)[20]	-	MRA	130 infants	-	36 (27.7)	7 (5.4)
Ravikanth and Philip (2019)[21]	Bengaluru, Karnataka	MRA	200	34 (17)	46 (23) Partial FTP: 37 (18.5) Complete FTP: 9 (4.5)	19 (9.5)
Sawant and Rizvi (2017)[22]	Mumbai, Maharashtra	Cadaveric dissection	40	60	12.5	2.5
Saha *et al*. (2015)[23]	India	Cadaveric dissection	56	32 (57.2)	21 (37.5)	3 (5.4)
Wilson *et al*. (2010)[24]	Puerto Rico	Cadaveric dissection	34	50 (73.52)	Partial FTP: 10 (14.70) Complete fetal: 2 (2.94)	2 (2.94)
Prasanna Veera Kumar and Prasad (2016)[25]	Andhra Pradesh	Cadaveric dissection	50	80	13.3	6.7
Van Overbeeke *et al*. (1991)[26]	Netherlands	Cadaveric dissection	100	84	14	2
De Silva *et al*. (2009)[27]	Sri Lanka	Cadaveric dissection	225	93.30	4.40	2.20
Li *et al*. (2011)[28]	China	CTA	163	85.63	11.87	2.5
Dodevski *et al*. (2014)[29]	Macedonia	CTA	53	70	23	7
Karatas *et al*. (2015)[30]	Turkey	CTA	100	82	17	1
Yeniçeri *et al*. (2017)[31]	Turkey	3D TOF MRI	384	85	13	2
Naveen *et al*. (2015)[32]	Bangalore	MRA	300	51 (17)	69 (23)	29 (9.6)
Riggs and Rupp (1963)[33]	-	-	-	76	17	7
Zeal and Rhoton (1978)[34]	-	-	-	58	40	2
Kamath (1981)[35]		Cadaveric dissection		73.5	25	1.5
Yasargil (1984)[36]				67.5	24.5	8
Saeki and Rhoton (1977)[4]				54	22	
Gunnal *et al*. (2018)[37]		Cadaveric dissection		79.41	16.47	
Eftekhar *et al*. (2006)[38]		Cadaveric dissection			27	
Present study (2014–2017)	TP of Assam	Cadaveric dissection	109	51.37	36.70	11.93
	Tribal population of Assam		19	68.42	21.06	10.53
	NT population of Assam		90	45.56	39.97	12.43

TP: Total population, NT: Nontribal, CTA: Computed tomography angiography, 3D: Three-dimensional, TOF: Time-of flight, MRA: Magnetic resonance angiography, MRI: Magnetic resonance imaging, FTP: Fetal type posterior

and 8.5%. In a previous study in Sri Lanka, transitional configuration was seen in 8 (2.2%), bilaterally in 2 (0.9%), and unilaterally in 6 (2.5%) 2 on the left and 4 on the right.[27] In a time-of flight MRA study of 1000 subjects in Berlin transitional variant was seen in 1.8% on the left side, 1.3% on the right side, and 0.2% on both sides.[17]

In the present study, tribal population of Assam showed fetal configuration 2 (10.53%) on the right side, 2 (10.53) on the left, and none bilaterally. The nontribal population had fetal configuration 19 (21.11%) on the right, 14 (15.56%) on the left, and 3 (3.3%) bilaterally. Total population of Assam showed 21 (19.27%) fetal configuration on the right, 16 (14.68%) on the left, and 3 (2.75%) bilaterally. In comparison in a study 50 brains in Andhra Pradesh demonstrated 1 (2%) fetal configuration on the right, 4 (8%) on the left, and 1 (2%) bilaterally.[25] An MRA study of 923 brains in Lithuania showed left-sided fetal configuration among 58 (6.3%), right-sided fetal configuration in 68 (7.4%), and bilateral fetal configuration in 21 (2.3%).[39] A Sri Lankan study showed fetal configuration in 17 (4.4%), bilaterally in 3 (1.3%), and unilaterally in 14 (6%) 8 on the left and 6 on the right.[27] A German study showed unilateral fetal configuration more common than bilateral fetal configuration (25.6% vs. 7.7%, $P < 0.001$) and fetal configuration was observed significantly more often on the right side than left side (14.9% vs. 10.7%, $P < 0.001$).[17]

On a computed tomography angiography (CTA) study of 53 patients, 2 (3.77%) had bilateral fetal configuration. Right-sided configuration was seen in 6 (11.32%) and 4 (7.54%) were seen on the left.[29] A study of 202 patients who had undergone multi-slice CTA examinations 20 had partial FTP, 9 had right sided, 6 had left sided, and 5 had bilateral partial FTP.[2] Cadaveric study of 102 Iranian males 27% had fetal configuration, of which 26% of cases were on the right side and 28% were on the left side .[38] Data represented in Tables 1-4.

Conclusion

This study comprehensively describes transitional and fetal configurations of the posterior cerebral artery in tribal, nontribal, and total population of Assam and compares the study with similar studies done in different ethnic groups in various other geographical locations. Although the prevalence and unilaterality or bilaterality of different configurations of posterior cerebral artery are different in tribal and nontribal populations; the findings are not statistically significant. Hence, we rule out that different types of posterior cerebral artery configurations are different in different populations.

Financial support and sponsorship

Nil.

Conflicts of interest

There are no conflicts of interest.

References

1. Walls EW. The blood vascular and lymphatic systems. In: Romanes GJ, editor. Cunningham's Textbook of Anatomy. 12th ed. New Delhi: Oxford University Press; 1981. p. 911.
2. Arjal RK, Zhu T, Zhou Y. The study of fetal-type posterior cerebral circulation on multislice CT angiography and its influence on cerebral ischemic strokes. Clin Imaging 2014;38:221-5.
3. Lv X, Li Y, Yang X, Jiang C, Wu Z. Potential proneness of fetal-type posterior cerebral artery to vascular insufficiency in parent vessel occlusion of distal posterior cerebral artery aneurysms. J Neurosurg 2012;117:284-7.
4. Saeki N, Rhoton AL Jr. Microsurgical anatomy of the upper basilar artery and the posterior circle of Willis. J Neurosurg 1977;46:563-78.
5. van der Zwan A, Hillen B, Tulleken CA, Dujovny M, Dragovic L. Variability of the territories of the major cerebral arteries. J Neurosurg 1992;77:927-40.
6. van Raamt AF, Mali WP, van Laar PJ, van der Graaf Y. The fetal variant of the circle of Willis and its influence on the cerebral collateral circulation. Cerebrovasc Dis 2006;22:217-24.
7. Vasović LP. The tenth vascular component in a rare form of the cerebral arterial circle of fetuses. Cells Tissues Organs 2004;178:231-8.
8. Henderson RD, Eliasziw M, Fox AJ, Rothwell PM, Barnett HJ. Angiographically defined collateral circulation and risk of stroke in patients with severe carotid artery stenosis. North American Symptomatic Carotid Endarterectomy Trial (NASCET) Group. Stroke 2000;31:128-32.
9. Hoksbergen AW, Majoie CB, Hulsmans FJ, Legemate DA. Assessment of the collateral function of the circle of Willis: Three-dimensional time-of-flight MR angiography compared with transcranial color-coded duplex sonography. Am J Neuroradiol 2003;24:456-62.
10. White H, Boden-Albala B, Wang C, Elkind MS, Rundek T, Wright CB, *et al*. Ischemic stroke subtype incidence among whites, blacks, and Hispanics: The Northern Manhattan study. Circulation 2005;111:1327-31.
11. Saikia S, Medhi B, Medhi BK. Spatial distribution of tribal population and inter tribal differences in population growth: A critical review on demography and immigration in Assam. J Humanit Soc Sci 2012;3:23-30.
12. Ansari S, Dadmehr M, Eftekhar B, McConnell DJ, Ganji S, Azari H, *et al*. A simple technique for morphological measurement of cerebral arterial circle variations using public domain software (Osiris). Anat Cell Biol 2011;44:324-30.
13. De Silva KR, Silva R, Amaratunga D, Gunasekera WS, Jayesekera RW. Types of the cerebral arterial circle (circle of Willis) in a Sri Lankan population. BMC Neurol 2011;11:5.
14. Padget DH. The circle of Willis. Its embryology and anatomy. In: Dandy WE, editor. Intracranial Arterial Aneurysms. Ithaca, N.Y: Comstock Publishing Co, Inc.; 1947. p. 67-90.
15. Kirgis HD, Llewellyn RC, Peebles EM. Functional trifurcation of the internal carotid artery and its potential clinical significance. J Neurosurg 1960;17:1062-72.
16. Hoang TM, Huynh TV, Ly AV, Pham MV. The variations in the circle of Willis on 64-multislice spiral computed tomography. Trends Med Sci 2022;2:e128729.
17. Rangus I, Milles LS, Galinovic I, Villringer K, Audebert HJ, Fiebach JB, *et al*. Reclassifications of ischemic stroke patterns due to variants of the circle of Willis. Int J Stroke 2022;17:770-6.
18. Haghighimorad M, Bahrami Motlagh H, Salehi E, Radmanesh A. Anatomiocal variations in posterior part of the circle of Willis and their associations with brain infarct in different vascular territories. Egypt J Radiol Nucl Med 2022;53:51.
19. Prefulla PR, Mohanpriya E, Bose E, Keerthi S. Study of variations of posterior communicating artery and types of posterior circulation in human cadaveric brains of South Indian population. J Anat Soc India 2021;70:221-5.
20. Malamateniou C, Adams ME, Srinivasan L, Allsop JM, Counsell SJ, Cowan FM, *et al*. The anatomic variations of the circle of Willis in preterm-at-term and term-born infants: An MR angiography study at 3T. Am J Neuroradiol 2009;30:1955-62.
21. Ravikanth R, Philip B. Magnetic resonance angiography determined variations in the circle of Willis: Analysis of a large series from a single center. Tzu Chi Med J 2019;31:52-9.
22. Sawant SP, Rizvi S. Study of variant posterior cerebral circulation and its clinical relevance. Anat Physiol 2017;7:264.
23. Saha A, Sarkar A, Mandal S. A cadaveric study of bilateral configuration of posterior bifurcation of posterior communicating artery in Indian population. J Clin Diagn Res 2015;9:C01-4.
24. Wilson R, Veras T, Elhert GW. Variation of the posterior cerebral artery and its embryological explanation: A cadaveric study. Bol Asoc Med *P* R 2010;102:55-8.
25. Prasanna Veera Kumar A, Prasad KS. Variation in the origin of posterior cerebral artery in the adult population. Int J Anat Res 2016;4:2440-3.
26. Van Overbeeke JJ, Hillen B, Tulleken CA. A comparative study of the circle of Willis in fetal and adult life. The configuration of the posterior bifurcation of the posterior communicating artery. J Anat 1991;176:45-54.

27. De Silva KR, Silva TR, Gunasekera WS, Jayesekera RW. Variation in the origin of the posterior cerebral artery in adult Sri Lankans. Neurol India 2009;57:46-9.
28. Li Q, Li J, Lv F, Li K, Luo T, Xie P. A multidetector CT angiography study of variations in the circle of Willis in a Chinese population. J Clin Neurosci 2011;18:379-83.
29. Dodevski A, Tosovska Lazarova D, Mitreska N, Aliji V, Stojovska Jovanovska E. Posterior cerebral artery – Variation in the origin and clinical significance. Pril (Makedon Akad Nauk Umet Odd Med Nauki) 2014;35:163-8.
30. Karatas A, Coban G, Cinar C, Oran I, Uz A. Assessment of the circle of Willis with cranial tomography angiography. Med Sci Monit 2015;21:2647-52.
31. Yeniçeri IÖ, Çullu N, Deveer M, Yeniçeri EN. Circle of Willis variations and artery diameter measurements in the Turkish population. Folia Morphol (Warsz) 2017;76:420-5.
32. Naveen SR, Bhat V, Karthik GA. Magnetic resonance angiographic evaluation of circle of Willis: A morphologic study in a tertiary hospital set up. Ann Indian Acad Neurol 2015;18:391-7.
33. Riggs HE, Rupp C. Variation in form of circle of Willis. The relation of the variations to collateral circulation: Anatomic analysis. Arch Neurol 1963;8:8-14.
34. Zeal AA, Rhoton AL Jr. Microsurgical anatomy of the posterior cerebral artery. J Neurosurg 1978;48:534-59.
35. Kamath S. Observations on the length and diameter of vessels forming the circle of Willis. J Anat 1981;133:419-23.
36. Yasargil MG. Microsurgical Anatomy of the Basal Cisterns and Vessels of the Brain. Microneurosurgery I. Stuttarg-New York: George Thieme Verlag; 1984.
37. Gunnal SA, Farooqui MS, Wabale RN. Anatomical variability of the posterior communicating artery. Asian J Neurosurg 2018;13:363-9.
38. Eftekhar B, Dadmehr M, Ansari S, Ghodsi M, Nazparvar B, Ketabchi E. Are the distributions of variations of circle of Willis different in different populations? Results of an anatomical study and review of literature. BMC Neurol 2006;6:22.
39. Gaigalaite V, Dementaviciene J, Vilimas A, Kalibatiene D. Association between the posterior part of the circle of Willis and the vertebral artery hypoplasia. PLoS One 2019;14:e0213226.
40. Mitterwallner FV. Statistical Studies of variations in the basal cere bral vessels. Acta Anat 1955;24:51-88.

Original Article

A Survey on Awareness of Body Donation for Medical Education among a Cross-section of Semi-urban Population in Uttar Pradesh, India

Thummala Naveen Sagar, Rajat Subhra Das, Tarun Prakash Maheshwari

Department of Anatomy, All India Institute of Medical Sciences, Raebareli, Uttar Pradesh, India

Abstract

Introduction: Cadaveric dissection is the best method to teach and learn anatomy. It gives the opportunity to learn basic surgical skills for medical graduates and to master advanced surgical procedures for postgraduates of different specialties. Vertical integration of cadaveric dissection with clinical subjects has a key role in the medical curriculum. **Aims and Objectives:** The aim of this study was to assess the awareness of body donation for medical education among the adult population of Raebareli, Uttar Pradesh. **Materials and Methods:** The survey used a validated questionnaire containing 12 items. The sample size consisted of 1000 individuals. **Results:** A total of 1000 participants took part in the survey. Participants of the study were from different age groups and educational backgrounds. The frequency distribution of individual scores of study participants shows that 237 (23.7%) participants scored between 0 and 3 (poor), 543 (54.3%) participants scored between 4 and 6 (average), 198 (19.8%) participants scored between 7 and 9 (good), and 22 (2.2%) scored between 10 and 12 (excellent). **Conclusion:** We conclude that irrespective of age, sex, and educational qualification, a large-scale awareness program can only improve the knowledge of body donation and will further ensure an adequate supply of cadavers through voluntary body donation for the cause of medical education.

Keywords: *Anatomy, awareness, cadaver, knowledge, medical education*

Introduction

Cadaveric dissection is the best method of teaching anatomy for better clinical foundation and efficient medical and surgical practice.[1,2] In the UK reduction in use of cadavers for teaching in anatomy has raised concern especially for surgical specialty postgraduates.[3,4] In addition, dissection practice helps professional development and teamwork.[5] Cadavers for medical teaching can be obtained through – (1) unclaimed bodies from mortuary, (2) voluntary body donation program, and (3) posthumous body donation by the next of kin or acquaintance.

Due to issues, e.g., religious, social, and faith, the easy availability of the cadavers through voluntary donation program is not satisfactory and awareness regarding this social responsibility for the benefit of medical education needs to be addressed.

The present study is undertaken to assess the awareness of body donation for medical education among the cross-section of the adult population of Raebareli, Uttar Pradesh, India, a semi-urban region.

Materials and Methods

Methodology

This survey was carried out by the department of anatomy at All India Institute of Medical Sciences Raebareli, India over a period of 2 years. The survey was conducted using a validated questionnaire containing 12 items, and the results obtained were statistically analyzed. The sample size was composed of 1000 healthy individuals who were sourced from the community-based places through field visits, colleges or schools, workplaces, and outpatient department services of the hospital. Adult population only (age above 18 years) who can read, write, and understand Hindi and/or English were included in the study. Participants with age <18 years, adults who cannot read or write, and mentally challenged people were excluded. The sample size was determined in two steps – first, the sample size was calculated for infinite population, and

How to cite this article: Sagar TN, Das RS, Maheshwari TP. A survey on awareness of body donation for medical education among a cross-section of semi-urban population in Uttar Pradesh, India. J Anat Soc India 2025;74:320-5.

Article Info

Received: 28 June 2025
Revised: 29 August 2025
Accepted: 28 September 2025
Available online: 31 December 2025

Address for correspondence:
Prof. Rajat Subhra Das, Department of Anatomy, All India Institute of Medical Sciences, Dalmau Road, Munshiganj, Raebareli - 229 405, Uttar Pradesh, India.
E-mail: rajatsubhrad0@gmail.com

Access this article online

Website: https://journals.lww.com/joai

DOI: 10.4103/jasi.jasi_109_25

Quick Response Code:

then, the sample size was adjusted for required population. The formula used for calculating sample size for infinite population was $n = z^2 \times p\ (1 - p)/E^2$, where n is the sample size for infinite population, P is the population proportion assumed to be 50% =0.5, E is the margin of error which is taken as 5% =0.05, and Z is 1.96 for 95% confidence level. The population for infinite population is 384.16.[6] The second step is adjusting the sample size for required population of 277,000 (as per population statistics in 2025, the population of Raebareli city where the study was conducted is approximately 277,000). The formula used for adjusting the sample size to the population under study is $S = n/1+ ([n - 1]/\text{population})$,[6] S = sample size adjusted for population under study, n is sample size for infinite population = 384.16, and population is the total population of the city or region where the study will be conducted = 270,000. The sample size required for the population under study is 383.62. For making the study statistically more significant and to simplify the data analysis easier, the sample size was taken as 1000 adult individuals.

The study was conducted after obtaining clearance of the ethical committee of All India Institute of Medical Sciences Raebareli, Uttar Pradesh. Written consent was obtained from all the study participants.

The following steps were utilized for developing and validating the content of the questionnaire:[7-10]

1. Generate item pool
2. Prepare instrument pattern
3. Review by experts
4. Content validity
5. The first draft of the instrument
6. Forward translation of English instruments to Hindi
7. Review of forward translation
8. Back translation of Hindi instrument to English
9. Review of backward translation
10. Finalizing the translated instrument
11. Preliminary pilot testing.

The questionnaire was framed in both English and local languages (as many in this region are not in knowledge of English).

Generate item pool

Depending on the need of the study, 20 items were created and subjected to the expert review.[8] All the items were prepared to assess the knowledge domain of the target population.

Prepare instrument pattern

All the items in the instrument were designed to elicit only two responses – either yes or no by a number coding. For example, if the response for an item is "yes," then the number code is one, and if the response for an item is "no," then the number code is zero.

Example 1: Do you know that the human body is used for medical teaching?

Response	Score
Yes	1
No	0.

Review by experts

An expert committee of five members evaluated the 20 items, and they accepted 13 items as suitable for the study. Then, the content validity index (CVI) of the 13 items was calculated.

Content validity

The CVI of the 13 items was calculated using the following formula:[9]

$$\frac{(\text{Sum of proportion relevance rating})}{(\text{Number of experts})}$$

As an example, in this study, 5 (five) experts were involved and if 4 (four) experts scored an item as relevant and one expert scored the item as not relevant then the content validity index of that item is -

The sum of proportion relevance rating = 4

Total number of experts = 5

CVI = 4/5 = 0.8.

Standard suggestions from the review of the literature for CVI are as follows:[3,5,7-9]

1. If the number of experts was 2, CVI should be at least 0.8[9,11]
2. If the number of experts was 3 to 5, CVI should be 1[9,12,13]
3. If the number of experts was 6, CVI should be at least 0.83[9,12,13]
4. If the number of experts was 6–8, CVI should be at

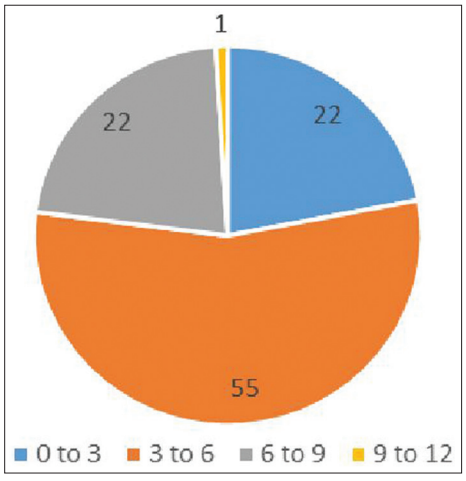

Figure 1: Frequency distribution of scores of the study participants in preliminary pilot testing

Table 1: A back-translated version of the instrument

Item	Response Code 1	Response Code 0	Participant response
Do you know that the human body is used for medical teaching?	Yes	No	
Do you know about the body donation program for medical education?	Yes	No	
Is any of your family members or a familiar person registered with the medical school for voluntary body donation?	Yes	No	
Do you know the difference between body donation and organ donation?	Yes	No	
Do you know that a pledge can be taken to donate a body for medical education?	Yes	No	
Do you know which department in a medical school provided the facility for voluntary body donation?	Yes	No	
Do you know the procedure for donating a dead body to a medical school?	Yes	No	
Do you know any organization which provides a facility for voluntary body donation in Uttar Pradesh?	Yes	No	
Did you register for voluntary body donation?	Yes	No	
Did you attend any program on voluntary body donation?	Yes	No	
Have you seen someone in your acquaintance donate a dead body to an autopsy school?	Yes	No	
Do you know that voluntary body donation is legal in India?	Yes	No	

Table 2: Correlation between educational status of the participant and the total score in preliminary pilot testing

	Education	Total score
Education	1	0.11
Total score	0.11	1

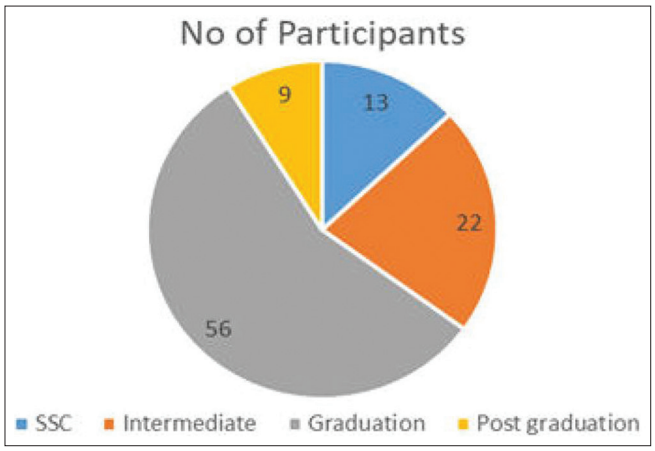

Figure 2: Distribution of participants in relation to educational qualification in preliminary pilot testing

least 0.83[9,14]

5. If the number of experts was 9, CVI should be at least 0.78.[9,14]

Out of the 13 items for which CVI was calculated, 12 items scored 1 and 1 item scored 0.4. Only 12 items with CVI 1 were utilized in drafting the instrument.

Forward translation of instrument in English to the Hindi language

One expert who was good in both Hindi and English languages and was not related to the medical fraternity was chosen to forward translate the English version of the instrument to the Hindi version.

Review of forward-translated instrument

Two experts who were good in Hindi and English languages were chosen to review the forward-translated version of the instrument.

Back translation of the Hindi version of the instrument to the English version

One neutral expert was chosen to translate the Hindi version of the Instrument back to English and the expert was unaware of the first draft of the instrument which was prepared in English [Table 1].

Review of a back-translated version of the instrument

Two neutral experts reviewed the back-translated version of the instrument and compared the back-translated version with the first draft in English version and accepted that the instrument is ready for surveying the target population.

Finalizing the translated instrument

As a majority of the population who were included in the study were speaking the Hindi language, the Hindi version of the instrument was utilized for conducting the study.

Preliminary pilot testing

The participants were able to interpret the items in the questionnaire and were able to answer them and their scores were recorded [Figure 1]. Before applying the instrument on larger population, the instrument is subjected for preliminary pilot testing on 100 participants with different educational backgrounds [Figure 2]. The summary of scores of the study participants generated in preliminary pilot testing is as follows: mean is 4.95, standard error is 0.210998, median is 5, mode is 4, standard deviation

is 2.109981, sample variance is 4.45202, range is 12, minimum score is 0, maximum score is 12, and sum of all the scores is 495.

r (Pearson correlation) value is 0.11 – clearly states that there is no or very minor linear correlation between educational status of the participant and awareness on voluntary body donation program for medical education [Table 2]. Pearson Correlation '*r*' Value should be more than 0.7 to indicate a strong linear relationship.

The validated instrument is now utilized for conducting the survey in the adult population of Raebareli.

Results

A total of 1000 participants took part in the survey. Participants of the study were from different age groups, and they had different educational backgrounds. Out of 1000 study participants, 762 were males and 238 were females [Figure 3]. Educational background of study participants is, 341 participants had SSC as educational qualification, 240 participants had intermediate as educational qualification, 328 participants were graduates, and 91 participants were postgraduates [Figure 3]. The statistical analysis of the scores of the study participants shows an average score of 5 out of 12 [Table 3]. The highest score was 12, and the lowest score was 0. The percentiles of the scores of the study participants are as follows: 25th percentile is 4, 50th percentile is 5, 75th percentile is 6, 90th percentile is 7, and 99th percentile is 11. The frequency distribution of individual scores of study participants shows that 237 (23.7%) participants scored between 0 and 3 (poor), 543 (54.3%) participants scored between 4 and 6 (average), 198 (19.8%) participants scored between 7 and 9 (good), and 22 (2.2%) scored between 10 and 12 (excellent) [Figures 4 and 5]. The correlation between educational status of the study participants and scores of the individual participants is 0.20, which means that there is a minimal or no positive correlation between educational status and knowledge regarding body donation for medical education [Table 4]. The correlation between age of the study participants and knowledge regarding body donation for medical education is 0.05, which states that there is no correlation between age of the study participants and knowledge on body donation for medical education [Table 5].

Table 3: Summary of the scores of study participants

Summary of the scores of study participants	
Variable	**Score**
Mean	4.906
SE	0.071709876
Median	5
Mode	6
SD	2.267665387
Sample variance	5.142306306
Range	12
Minimum	0
Maximum	12
Sum	4906
Count	1000

SE: Standard error, SD: Standard deviation

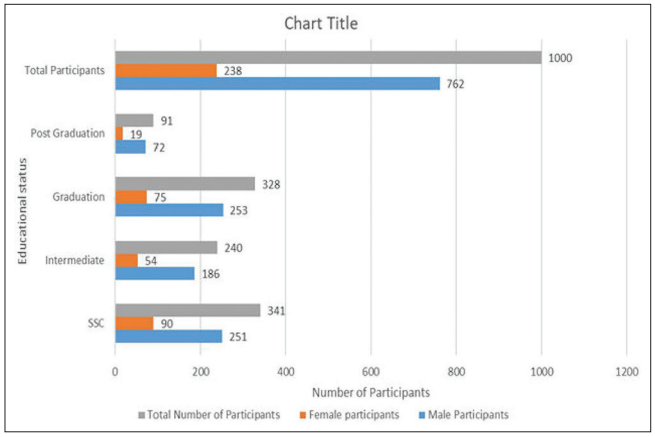

Figure 3: Educational qualification of study participants

r = 0.2, states that there is minimal or no correlation between educational status of the study participants and knowledge on body donation for medical education [Table 4]. Pearson Correlation '*r*' Value should be more than 0.7 to indicate a strong linear relationship.

r = 0.05, states that there is no correlation between age of the study participants and knowledge on body donation for medical education [Table 5]. Pearson Correlation '*r*' Value should be more than 0.7 to indicate a strong linear relationship.

Discussion

The present study was undertaken to assess the knowledge on voluntary body donation for medical education among the adult population of Raebareli, Uttar Pradesh. The aim of our study was not only to assess the knowledge but also to create awareness by asking the participants about body donation. Initially, the participants were hesitant to take part in the study due to a lack of knowledge. After the survey procedure

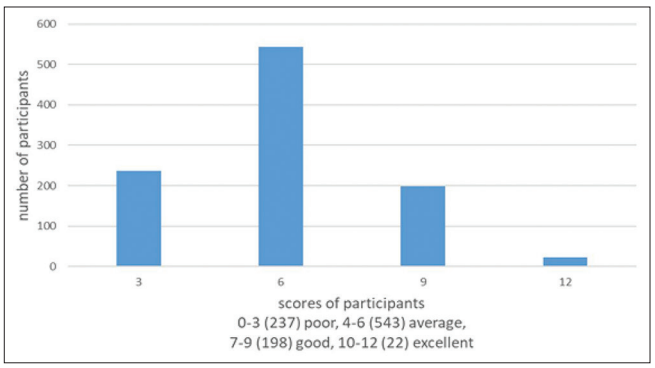

Figure 4: Frequency of the scores of study participants

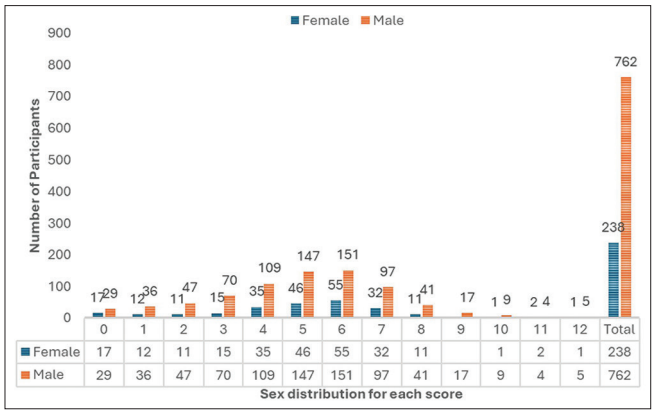

Figure 5: Frequency of scores of the study participants with respect to male and female sexes

Table 4: Correlation between educational status and scores of the study participants

	Education status	Score
Education status	1	0.20
Score	0.20	1

Table 5: Correlation between age and scores of study participants

	Age	Score
Age	1	0.05
Score	0.05	1

was explained, the participants took part in the study and also expressed their interest to attend awareness programs on voluntary body donation. We strongly believe that awareness on body donation is the best method to improve the supply of good-quality cadavers for anatomy teaching.

Literature review in relation to student–cadaver ratio in Indian medical schools shows that the average student–cadaver ratio is 20:1, whereas the ideal student–cadaver ratio is 10:1 as per the norms of the National Medical Commission of India.[15] Only 49% of medical colleges in India were following the student–cadaver ratio of 10:1.[15] Literature review with respect to the practice of voluntary body donation programs in Indian medical schools shows that 70% of the medical colleges were practicing the voluntary body donation program.[14] Saha *et al*. in their study stated that <50% of the study participants were in support of body donation, 18% were not in support of body donation, and 17% had no knowledge with respect to body donation.[16] Jacob *et al*. in their review reported that there are several factors affecting voluntary body donation among which awareness on body donation is one of the key factors.[17] Karmakar *et al*. in their study reported that there was poor knowledge and attitude regarding voluntary body donation among medical students.[18]

Saw in his study reported that the practice of silent mentor program at University of Malaya showed a positive impact on voluntary body donation.[19] Ballala *et al*. in their study stated that only 22% of the study participants (medical professionals) supported body donation by medical professionals which suggested awareness and reorientation programs on voluntary body donation for medical professionals.[20] Habicht *et al*. in their study reported that 32% of countries included in the study were using purely cadavers from voluntary body donation programs, while many countries were using sources of cadavers from both body donation and unclaimed bodies.[21]

Few studies report that using cadavers from voluntary body donation is more ethically accepted than using unclaimed bodies.[22] A study from China states that there is very minimal knowledge on body donation in ethnic minorities in China which is the reason for difficulty in procuring cadavers.[23] One study from Italy reported that religion has a significant impact on body donation in Italian medical students.[24] Naidoo *et al*. in their study stated that 71% of the study participants were not in favor of body donation, and the major factor influencing this was religion.[25] Rajasekhar *et al*. in their study elaborated the necessity for a unified Anatomy Act to be followed by all states in India to improve body donation programs.[26]

The results from the present study state that there is no or minimal correlation between educational status of the participants and the knowledge on body donation for medical education which is having "*r*" =0.2. Our study also states that there is no correlation between age of study participants and the knowledge on body donation for medical education with "*r*" =0.05. Hence, irrespective of age, sex, and educational qualification, there is very minimal knowledge on body donation for medical education among the adult population of Raebareli, Uttar Pradesh.

Conclusion

The review of literature suggests that only a well-designed awareness program for both medical professionals and also the general population is the potential practice to improve knowledge on voluntary body donation for medical education. The result from the present study shows that there is a lack of knowledge about the significance of body donation for medical education training. A study from Nigeria states that there is good awareness regarding organ donation among elderly and educated individuals,[27] but the present study concludes that the age or the educational qualification does not have a significant positive correlation with awareness on body donation. We conclude that irrespective of age, sex, and educational qualification, a large-scale awareness program can only improve the knowledge on body donation which will ensure a good supply of body cadavers for medical education. We also strongly believe that these kind of studies in all medical institutes will act as a supporting initiative to enhance voluntary body donation programs.

Study limitations

In the present study, we included participants from different age groups and different educational backgrounds, and both male and female participants took part in the study. The first limitation in our study is, number of female participants is comparatively less because female participants were reluctant to take part in the survey, maybe due to some social inhibition. The other limitation of the present study is, we assessed only the knowledge domain on body donation for medical education, and we did not assess the attitude and psychomotor domain of body donation for medical education.

Acknowledgment

We thank the Authority of AIIMS, Raebareli, Uttar Pradesh, for giving us this opportunity. We also thank all the faculty and staff members of AIIMS, Raebareli, who helped us in the present study for their support. We also convey special thanks to Mr. Basant, Nursing Officer, for his valuable effort in data collection.

Financial support and sponsorship

Nil.

Conflicts of interest

There are no conflicts of interest.

References

1. Memon I. Cadaver dissection is obsolete in medical training! A misinterpreted notion. Med Princ Pract 2018;27:201-10.
2. Ghosh SK. Cadaveric dissection as an educational tool for anatomical sciences in the 21st century. Anat Sci Educ 2017;10:286-99.
3. Estai M, Bunt S. Best teaching practices in anatomy education: A critical review. Ann Anat 2016;208:151-7.
4. Older J. Anatomy: A must for teaching the next generation. Surgeon 2004;2:79-90.
5. Flack NA, Nicholson HD. What do medical students learn from dissection? Anat Sci Educ 2018;11:325-35.
6. Cochran WG. Sampling Techniques. 3rd ed. New York: John Wiley and Sons; 1977.
7. Webair HH, Ismail TA, Ismail SB, Khaffaji AJ, Hussain NH, Kadir AA, *et al.* Patient-centered infertility questionnaire for female clients (PCIQ-F): Part I: Questionnaire development. BMC Med Res Methodol 2021;21:188.
8. DeVellis RF. Scale Development: Theory and Applications. Vol. 26. Thousand Oaks: Sage; 2016.
9. Yusoff MS. ABC of content validation and content validity index calculation. Educ Med J 2019;11:49-54.
10. Wild D, Grove A, Martin M, Eremenco S, McElroy S, Verjee-Lorenz A, *et al.* Principles of good practice for the translation and cultural adaptation process for patient-reported outcomes (PRO) measures: Report of the ISPOR task force for translation and cultural adaptation. Value Health 2005;8:94-104.
11. Davis LL. Instrument review: Getting the most from a panel of experts. Appl Nurs Res 1992;5:194-7.
12. Polit DF, Beck CT. The content validity index: Are you sure you know what's being reported? Critique and recommendations. Res Nurs Health 2006;29:489-97.
13. Polit DF, Beck CT, Owen SV. Is the CVI an acceptable indicator of content validity? Appraisal and recommendations. Res Nurs Health 2007;30:459-67.
14. Lynn MR. Determination and quantification of content validity. Nurs Res 1986;35:382-5.
15. Appaji A. A survey on the role and the status of cadavers in medical education: An Indian scenario. J Clin Diagn Res 2012;6:1132-6.
16. Saha A, Sarkar A, Mandal S. Body donation after death: The mental setup of educated people. J Clin Diagn Res 2015;9:C05-9.
17. Jacob M, Avadhani RK, Nallathamby R, Soman MA, Bindu S. Body donation as gift to medical science for better tomorrow – Literature review. J Health Allied Sci NU 2015;5:108-10.
18. Karmakar N, Chakraborty T, Datta A, Nag K, Das S, Bhattacharjee P. Knowledge, Attitude, Practice regarding voluntary whole-body donation among medicos in Northeast India. Chrismed J Health Res 2020;7:103-9.
19. Saw A. A new approach to body donation for medical education: The silent mentor programme. Malays Orthop J 2018;12:68-72.
20. Ballala K, Shetty A, Malpe SB. Knowledge, attitude, and practices regarding whole body donation among medical professionals in a hospital in India. Anat Sci Educ 2011;4:142-50.
21. Habicht JL, Kiessling C, Winkelmann A. Bodies for anatomy education in medical schools: An overview of the sources of cadavers worldwide. Acad Med 2018;93:1293-300.
22. Sasi A, Hegde R, Dayal S, Vaz M. Life after death – The dead shall teach the living: A qualitative study on the motivations and expectations of body donors, their families, and religious scholars in the South Indian City of Bangalore. Asian Bioeth Rev 2020;12:149-72.
23. Zhang X, Peng L, Li LJ, Fan W, Deng J, Wei X, *et al.* Knowledge, attitude and willingness of different ethnicities to participate in cadaver donation programs. PLoS One 2020;15:e0229529.
24. Ciliberti R, Gulino M, Gazzaniga V, Gallo F, Vellone VG, De Stefano F, *et al*. A survey on the knowledge and attitudes of Italian medical students toward body donation: Ethical and scientific considerations. J Clin Med 2018;7:168.
25. Naidoo N, Al-Sharif GA, Khan R, Azar A, Omer A. In death there is life: Perceptions of the university community regarding body donation for educational purposes in the United Arab Emirates. Heliyon 2021;7:e07650.
26. Rajasekhar SS, Aravindhan K, Gladwin V, Chand P. Body donation- consent from non-related persons: Case series, review, and recommendations. J Clin Diagn Res 2016;10:R01-4.
27. Akinyemi RO, Akinyemi JO, Olorunsogbon OF, Uvere E, Jegede AS, Arulogun OS. Gender and educational attainment influence willingness to donate organs among older Nigerians: A questionnaire survey. Pan Afr Med J 2020;36:288.

Original Article

A Study on the Morphometric Dimensions of the Intercondylar Notch of the Femur Using UTHSCA Image Tool Software and Its Clinical Significance

B. Santhosh Kumar, K. Devi Sankar[1], S. Rahini[2], Ravichandran Doraiswamy[3]

Sri Venkateswaraa Medical College Hospital and Research Institute, Departments of [2]Community Medicine, [3]Anatomy, Sri Venkateswaraa Medical College Hospital and Research Institute, Chennai, [1]Department of Anatomy, Sri Balaji Medical College Hospital and Research Institute, Tirupati, Andhra Pradesh, India

Abstract

Introduction: Anterior cruciate ligament (ACL) injuries are common among athletes, with intercondylar notch (ICN) anatomy playing a significant role in influencing risk. Understanding notch morphology aids orthopedic surgeons in optimizing ACL reconstruction techniques and developing effective injury prevention strategies. This study investigates ICN symmetry and morphology to evaluate anatomical risk factors relevant to ACL injuries and optimize surgical reconstruction strategies. **Materials and Methods:** A total of 134 ethically sourced dried femurs were analyzed, excluding specimens with deformities, abnormalities, or from infants. Standardized digital photographs were taken using a Sony DCR-W270 camera at a fixed distance of 10 cm. Two views were captured: (1) a frontal image to classify notch shape as inverted U or V, and (2) a lateral image to measure the notch roof angle. Additional parameters assessed included ICN width, notch depth, bicondylar width, and notch width index. All measurements were done using UTHSCA Image Tool Software. **Results:** The study provides baseline anatomical data useful for comparing with imaging findings (computed tomography/magnetic resonance imaging) in ACL-injured knees. Observations suggest that stenotic notches may correlate with increased susceptibility to ACL tears. These insights assist orthopedic surgeons in preoperative planning, graft selection, and refinement of surgical techniques, aiming to improve reconstruction outcomes and reduce injury recurrence. **Conclusion:** By elucidating the relationship between ICN morphology and ACL injury risk, this study provides actionable evidence to support injury prevention strategies and surgical precision in athletes.

Keywords: *Anterior cruciate ligament reconstruction, bicondylar width, intercondylar notch depth, intercondylar notch width, morphometric dimensions, notch roof angle, notch width index, UTHSCA image tool software*

Introduction

Anterior cruciate ligament (ACL) injuries are most frequently seen in athletes and individuals with osteoarthritis knee. Between 2002 and 2014, approximately 283,810 ACL reconstructions were performed in the United States, and the rate of ACL reconstruction increased by 22%, rising from 61.4 per 100,000 PYs in 2002 to 74.6 per 100,000 PYs in 2014.[1] ACL is a major ligament which stabilizes the knee joint.[1] The cruciate ligaments share a functional and anatomical relationship to the intercondylar notch (ICN). The notch's dimensions, particularly bicondylar width (BCW), ICN depth (ICND), ICN width (ICNW), notch width index (NWI), notch roof angle (NRA) and notch's shape, define the space available for the ACL within the knee joint.[2]

The ICN plays a critical role in ACL injuries and their surgical reconstruction. A narrow notch can increase the risk of graft impingement, potentially leading to graft failure.[3] The NWI, expressed as the ratio of the ICNW and BCW, is used to identify narrow notches. Normal NWI values typically range from 20 to 25, and NWI below 20 are considered stenosed or narrowed.[4] The stenosis of the notch is associated with a higher incidence of ACL ruptures, especially in young athletes and in the older population with degenerative arthritis.[5] The ICN was reported to be smaller in knees with extensive osteoarthritis as a result of osteophytic growth within the notch.[2]

How to cite this article: Kumar BS, Sankar KD, Rahini S, Doraiswamy R. A study on the morphometric dimensions of the intercondylar notch of the femur using UTHSCA image tool software and its clinical significance. J Anat Soc India 2025;74:326-31.

Article Info

Received: 28 August 2025
Revised: 11 November 2025
Accepted: 21 November 2025
Available online: 31 December 2025

Address for correspondence:
Dr. Ravichandran Doraiswamy, Department of Anatomy, Sri Venkateswaraa Medical College Hospital and Research Institute, Chennai, Tamil Nadu, India.
E-mail: ravichandransvmc@gmail.com

Access this article online

Website: https://journals.lww.com/joai
DOI: 10.4103/jasi.jasi_135_25

Quick Response Code:

A steeper NRA increases the likelihood of impingement, as the ACL comes into contact with the bony roof of the ICN. This impingement is especially pronounced during knee extension, placing increased stress and strain on the ACL. Notch's shape, particularly the "inverted V" shape, alters the way forces are distributed across the ligament, potentially increasing stress and strain during certain movements. This leads to the ACL physically getting hit against the bony walls of the notch during movements involving twisting, pivoting, or hyperextension, recalling the ACL tear.[6]

Preoperative knowledge of the dimensions of the notch obtained using advanced imaging techniques, including three-dimensional reconstructions from magnetic resonance imaging (MRI), is essential for personalized surgical planning, including graft selection, proper tunnel placement and tailored notchplasty.[7,8] Patellar tendon and hamstring grafts, each with varying diameters and stiffness, must be appropriately sized relative to the dimensions of the notch to avoid impingement.[9] A notchplasty is often performed to widen the notch, allowing adequate space for the graft and optimizing its placement.[10]

ACL rupture is often the presage of the knee. Given the prevalence of ACL injuries and the population variations, conflicting debate regarding the relationship between notch morphology and ACL rupture,[11-15] there is a need to quantify the specific morphometric characteristics of the ICN in dried femora from the local population. Establishing such baseline anatomical data may aid both preventive and reconstructive strategies for ACL injuries.

Materials and Methods

This observational research was conducted in the Department of Anatomy at Sri Venkateswaraa University, Redhills, over 3 months, following approval from the Institutional Ethics Committee. The sample size was estimated to be 134 using the standard statistical formula, considering the prevalence of stenosed notches as 9.6%. We obtained 134 adult dry femurs (57 right femurs and 77 left femurs) from Sri Venkateswaraa Medical College Hospital and Research Institute, Redhills and other medical colleges in Chennai. Bones from both sexes were included. The study excludes bones with deformity, fractures, arthritic changes, unfused epiphyses, and macerated condyles.

In a standardized position on an acrylic osteometric board, each femur was digitally photographed twice. In order to determine the BCW, ICNW, ICND, NWI, and notch shape, the initial photograph was captured directly overhead [Figure 1]. In order to determine the NRA, the second photograph was captured from the lateral perspective [Figure 2]. The camera (Sony DCR W270, Tokyo, Japan) distance from the bone was consistently maintained at 10 centimeters. Images were stored and analyzed on a computer using specialized software (UTHSCA Image Tool Software for Windows version 3.0, San Antonio, TX, USA[18]) to measure the ICN dimensions. All the measurements were calibrated in millimeters.

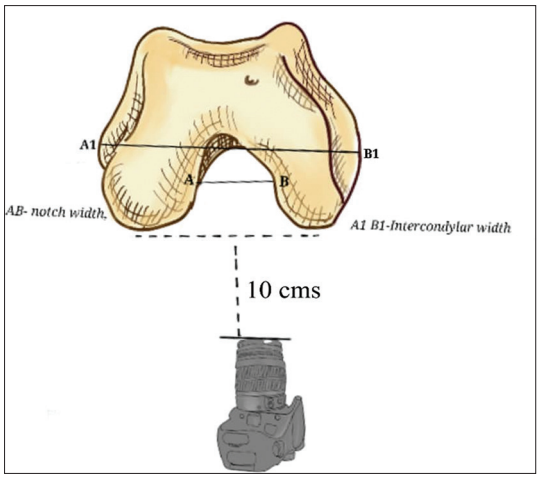

Figure 1: Shows a photograph captured from the notch's bottom. Source: Author's own illustration, adapted based on Ireland *et al*. (2001)[16] and Otsuka *et al*.

Standardized methods were followed to measure the parameters.[19,20] The parameters measured were as follows [Figures 3 and 4]:

1. BCW (AB) – Maximum distance between both femoral epicondyles
2. ICNW (EF) – Maximum distance of ICN between two condyles
3. ICND (CD) – Maximum height of the notch
4. NRA (alpha) – Angle between the lines passing through the epicondyle and posterior cortex of the shaft
5. NWI – Ratio between the ICNW and the BCW[8]
6. Notch shape – inverted "U" shape and inverted "V" shape.

The data was entered into an Excel spreadsheet and analyzed using IBM SPSS Statistics for Windows, Version 16.0 (IBM Corp. Armonk, NY, USA) measurements were obtained. The mean values of the left and right femurs were compared using the independent *t*-test. Statistical significance is considered if $P < 0.05$.

Results

Morphometric dimensions of 134 dry femurs (57 right, 77 left) were measured. The mean values for BCW, ICNW, ICND, NWI, and NRA are 65.47 ± 6.338 mm, 18.1 ± 3.428 mm, 22.65 ± 4.132 mm, 0.267° ± 0.036°, and 53.44° ±6.35°, respectively [Table 1].

The ICN shape was predominantly inverted "U" (73.1%, $n = 98$), with the remaining 26.9% ($n = 36$) exhibiting an inverted "V" shape [Table 2]. The morphometric measurements of the right and left femur did not exhibit

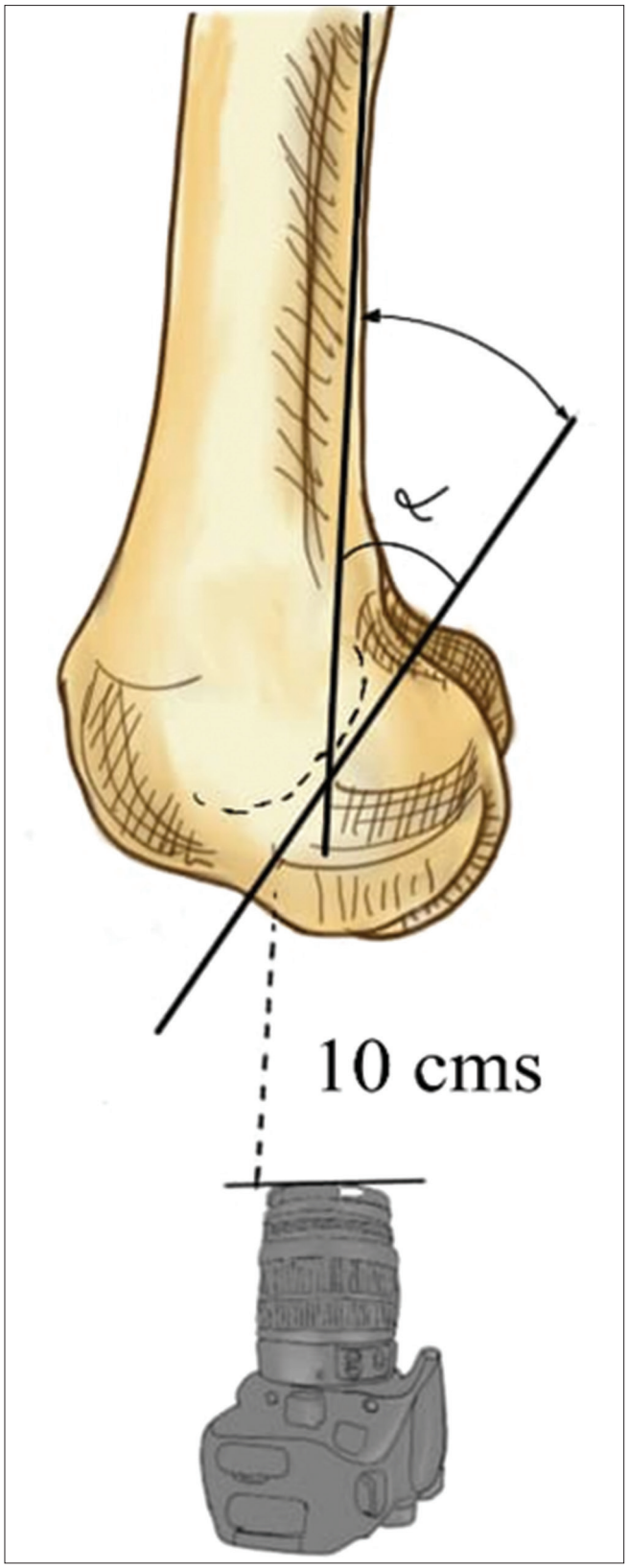

Figure 2: Shows a photograph captured from the lateral side. Source: Author's own illustration, based on the concept described by Huang *et al.* (2019)[17]

any statistically significant differences ($P > 0.05$) using an independent *t*-test [Table 3].

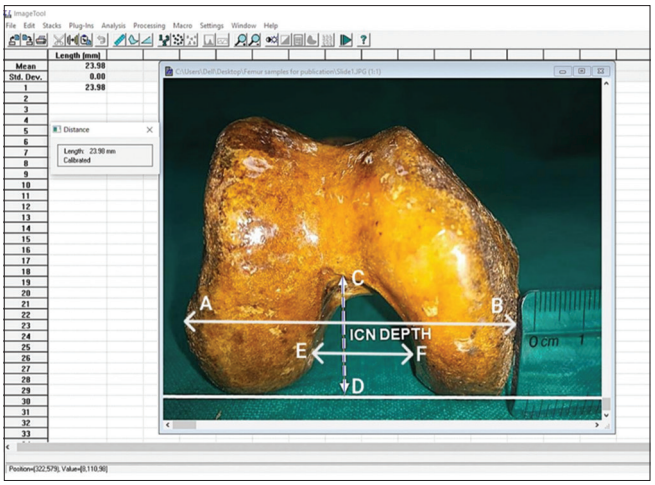

Figure 3: Showing the measurement of bicondylar width (AB), intercondylar notch (ICN) depth (CD), and ICN width (EF) in the UTHSCA image tool

Table 1: Mean and standard deviation of all the parameters (*n*=134 bones)

Parameters	Overall (mean SD)
BCW (mm)	65.47±6.338
ICN width (mm)	18.1±3.428
ICN depth (mm)	22.65±4.132
NRA (°)	53.44±6.35
NWI (mm)	0.267±0.036

SD: Standard deviation, ICN: Intercondylar notch, NWI: Notch width index, BCW: Bicondylar width, NRA: Notch roof angle

Table 2: Intercondylar notch shape

Notch shape	Left femurs (%)	Right femurs (%)	Overall (%)
U	57 (74)	41 (71.9)	98 (73.1)
V	20 (26)	16 (28.1)	36 (26.9)

Table 3: Comparison of dimensions of right and left femora

Parameters	Left femur (mean±SD)	Right femur (mean±SD)	*t*-test	*P*
BCW (mm)	65.58±6.17	65.319±6.61	0.239	0.811
ICN width (mm)	17.84±3.23	18.46±3.671	1.042	0.299
ICN depth (mm)	22.57±4.339	22.77±3.87	0.283	0.777
NRA (°)	53.36±6.441	53.55±6.28	0.164	0.87
NWI (mm)	0.263±0.033	0.272±0.038	1.28	0.194

SD: Standard deviation, ICN: Intercondylar notch, NWI: Notch width index, BCW: Bicondylar width, NRA: Notch roof angle

Discussion

The risk of ACL injuries is substantially influenced by the dimensions of the ICN at the lower end of the femur, including ICNW, ICND, notch shape, NWI, and NRA. The ACL connects the femur and tibia at an angle of 15°.[21] In a narrow notch, as evidenced by the low NWI and steep NRA, the likelihood of ACL tear is prevalent. The accurate assessment of the dimensions of the ICN

is essential, as it informs surgeons for effective graft placement and contributes to favorable surgical outcomes. Both cadaveric bone measurements and imaging techniques such as radiography and MRI have been used to investigate ICN dimensions. Given the clinical importance of these anatomical parameters, the present study focused on evaluating them within an Indian population.

The mean BCW, ICNW and ICND noted in our study were significantly lesser than that reported in previous studies. Terzidis *et al*.[22] examined Greek Caucasian bones, Taner and Murshed[23] studied Anatolian skeletal remains. Mistri[24] Ravichandran and Melanie,[25] Shweta[26] and Sangeeta *et al*.[27] had studied ethnically diverse Indian femora [Table 4].

The mean NWI in our study was 0.267 ± 0.036. The results are comparable to the findings of Biswas and Bhattacharya,[29] who documented NWI values of 0.254 ± 0.09 for the right side and 0.258 ± 0.025 for the left

Table 4: Comparison of results between various studies

Literature	BCW (mm)	ICN width (mm)	ICN depth (mm)	NWI (mm)	NRA (°)	Notch shape
Mistri, 2015[24] West Bengal *n*=127 bones (left=62, right=65)	Right=74.43±6.10 Left=73.98±5.99	Right=19.12±2.5 Left=18.65±2.8	Parameter not studied	Parameter not studied	Parameter not studied	Parameter not studied
Terzidis *et al*., 2006[22] Greek, Caucasian *n*=360 bones (right=180, left=180)	Right=84.01±0.62 Left=83.7±0.63	Right=20.5±2.3 Left=20.5±2.2	Parameter not studied	Parameter not studied	Parameter not studied	Parameter not studied
Taner and Murshed, 2002[23] Anatolian bones *n*=72 bones (right=36, left=36)	Right=76.8±5.9 Left=77.3±5.2	Parameter not studied	Parameter not studied	Parameter not studied	Parameter not studied	Parameter not studied
Ravichandran and Melanie, 2010[25] South Indian *n*=200 bones (right=106, left=94)	Right=74.58±0.57 Left=73.97±0.61	Right=18.89±0.29 Left=18.65±0.27	Parameter not studied	Parameter not studied	Parameter not studied	Parameter not studied
Ameet and Murlimanju, 2014[28] *n*=97 bones (right=45, left=52)	Right=72.5±5.3 Left=73.3±5.3	Right=18±3 Left=17.9±2.5	Right=26.3±2.3 Left=26.3±2.6	Parameter not studied	Parameter not studied	*U*=71 (73.2%) *V*=26 (26.8%)
Shweta, 2017[26] North India *n*=100 bones (right=51, left=49)	Right=73.11±6.14 Left=72.16±6.58	Right=20.82±2.57 Left=26.5±2.92	Right=26.58±2.8 Left=26.5±2.92	0.29	Parameter not studied	Parameter not studied
Biswas and Bhattacharya, 2017[29] West Bengal *n*=70 bones (right=35, left=35)	Right=71.21±4.50 Left=70.71±5.25	Right=20.86±2.52 Left=19.45±2.57	Parameter not studied	Parameter not studied	Parameter not studied	Parameter not studied
Chavada *et al*.[30] Gujarat Region *n*=74 bones (right=37, left=37)	Right=69.6±5.04 Left=69.8±4.96	Right=20.4±3.17 Left=18.7±2.52	Parameter not studied	Parameter not studied	Parameter not studied	Parameter not studied
Balgovid *et al*., 2019[31] Indian population *n*=50 (MRI)	Parameter not studied	Parameter not studied	Parameter not studied	Right=0.254±0.09 Left=0.258±0.025	53.03±5.56	Parameter not studied
Sangeeta *et al*., 2021[27] cadaveric Study *n*=32 bones (left=16, right=16)	Right=68.172±6.816 Left=69.036±7.438	Right=20.348±5.583 Left=19.264±5.161	Right=30.54±6.185 Left=30.763±7.095	Right=0.3±0.06 Left=0.28±0.05	Parameter not studied	Parameter not studied
Vinay and Vikram[32] *n*=180 bones (right=81, left=99)	Right=71.8±5.91 Left=70.8±5.95	Right=21.5±3.01 Left=21.7±2.85	Parameter not studied	Parameter not studied	Parameter not studied	Parameter not studied
Present study *n*=134 bones (right=57, left=77)	65.47±6.338	18.1±3.428	22.65±4.132	0.267±0.036	53.44±6.35	*U*=98 (73.1%) *V*=36 (26.9%)

ICN: Intercondylar notch, NWI: Notch width index, BCW: Bicondylar width, NRA: Notch roof angle, MRI: Magnetic resonance imaging

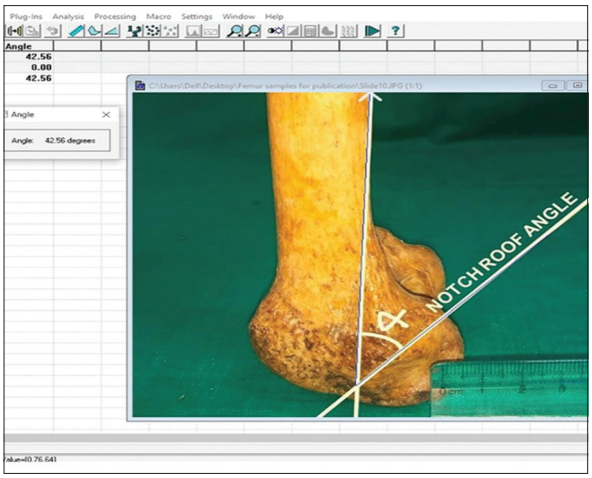

Figure 4: Showing measurement of notch roof angle in the UTHSCA image tool

side. The NWI serves as a comparative metric for assessing notch width in relation to the overall dimensions of the distal femur. An increased NWI suggests a comparatively broader notch. While various studies have reported average NWI values of 0.20 for males and 0.18 for females, below which ACL injury increases, this study did not record sex-specific values. This limits our ability to directly compare our findings to these gender-specific benchmarks.[4]

Our study showed the mean NRA to be 53.44° ±6.35°, identical to the values reported by Balgovind *et al*.[31] in their MRI analysis of an Indian cohort. This result validates the accuracy of our direct bone measurements and suggests a relatively consistent NRA within this demographic. Notably, this parameter has been infrequently reported in previous studies. The NRA is a critical factor influencing the likelihood of graft impingement after ACL reconstruction. Optimal graft positioning involves aligning it parallel to the notch roof to minimize this risk. Specifically, knees with steeper, more vertical roof angles necessitate a more posterior placement of the tibial graft to prevent impingement against the roof of the ICN.

A predominant "U" shaped (73.1%) notch was noted in our samples. The remaining 26.9% were "V" shaped. This distribution is consistent with the findings of Ravichandran *et al*.[25] The studies by Raja Balgovind *et al*.[26] and Anderson *et al*.[4] had identified an additional "W" shape while many studies have noted the inverted "U" and "V" shape only.

Population-specific differences likely account for variations in morphometric measurements. Ethnic and geographical factors, measurement techniques (direct bone measurements vs. radiographic or MRI evaluation), and differences in anatomical reference points all contribute to variability across studies.

This study employed a meticulous morphometric analysis of the ICN of the femur utilizing the (UTHSCA Image Tool Software for Windows version 3.0, San Antonio, TX, USA) a digital image analysis platform. The application of this specific software for detailed quantitative assessment of these bony dimensions, particularly within the studied population, represents a novel methodological approach.

The study has a few limitations. The age of the femur samples could not be determined, hindering the analysis of age-related variations in morphometry. The sex of the samples was also unidentifiable, preventing the exploration of sexual dimorphism in femoral characteristics. The ability to draw conclusions about population-specific differences was restricted by the impossibility of definitive classification based on ethnicity. The study's small sample size restricts the statistical power and may not accurately represent the broader population. Future continuation of this research study using MRI data offers a promising avenue to overcome the current limitations.

Conclusion

Our study's morphometric analysis of the ICN revealed BCW measurements were consistent with findings from cadaveric studies, affirming the reliability of dry bone analysis. However, significant inter-population variability was observed in ICND, highlighting the importance of ethnic-and population-specific data. Notably, both NWI and NRA demonstrated close concordance with MRI-based studies within the Indian population, validating our measurement techniques. The predominant inverted U shape of the notch, while consistent with some studies, showed slight variations in others, emphasizing the nuanced nature of notch morphology. These findings emphasize the significance of detailed morphometric analysis in understanding of femoral anatomy and its implications for ACL injury risk assessment and surgical planning.

Acknowledgment

The authors acknowledge the invaluable support of SRM Medical College Hospital and Research Centre, Kattankulathur, for their permission to collect femur samples, which were essential for the completion of this study. Their cooperation and provision of resources significantly contributed to the success of this research.

Financial support and sponsorship

This research was funded by the ICMR Short Term Studentship (STS) program (Reference ID: STS2024-11764).

Conflicts of interest

There are no conflicts of interest.

References

1. Herzog MM, Marshall SW, Lund JL, Pate V, Mack CD, Spang JT. Trends in incidence of ACL reconstruction and concomitant procedures among commercially insured individuals in the United States, 2002-2014. Sports Health 2018;10:523-31.
2. Wada M, Imura S, Baba H, Shimada S, Sasaki T. Femoral intercondylar notch measurements in osteoarthritic knees.

Rheumatology 1999;38:554-8.
3. Li Z, Li C, Li L, Wang P. Correlation between notch width index assessed via magnetic resonance imaging and risk of anterior cruciate ligament injury: An updated meta-analysis. Surg Radiol Anat 2020;42:1209-17.
4. Gupta R, Jhatiwal S, Kapoor A, Kaur R, Soni A, Singhal A. Narrow notch width and low anterior cruciate ligament volume are risk factors for anterior cruciate ligament injury: A magnetic resonance imaging-based study. HSS J 2022;18:376-84.
5. Jha S, Chauhan R. Morphometric analysis of condyles and intercondylar notch of femur in North Indian population and its clinical significance. J Evol Med Dent Sci 2017;20:2605-8.
6. Palmer WE, Brown RA, Rosenthal DI. Magnetic resonance imaging of the femoral notch in anterior cruciate ligament injury. Skeletal Radiol 1993;22:533-8.
7. Eggerding V, van Kuijk KS, van Meer BL, Bierma-Zeinstra SM, van Arkel ER, Reijman M, *et al.* Knee shape might predict clinical outcome after an anterior cruciate ligament rupture. Bone Joint J 2014;96-B: 737-42.
8. Anderson AF, Lipscomb AB, Liudahl KJ, Addlestone RB. Analysis of the intercondylar notch by computed tomography. Am J Sports Med 1987;15:547-52.
9. Orsi AD, Canavan PK, Vaziri A, Goebel R, Kapasi OA, Nayeb-Hashemi H. The effects of graft size and insertion site location during anterior cruciate ligament reconstruction on intercondylar notch impingement. Knee 2017;24:525-35.
10. Rilk S, Goodhart GC, O'Brien R, DiFelice GS. Arthroscopic anatomic anterior cruciate ligament primary repair restores anterior tibial translation intraoperatively at time zero with no additional effect of suture augmentation. Arthroscopy 2024;40:2862-71.e2.
11. Muneta T, Takakuda K, Yamamoto H. Intercondylar notch width and its relation to the configuration and cross-sectional area of the anterior cruciate ligament. A cadaveric knee study. Am J Sports Med 1997;25:69-72.
12. Teitz CC, Lind BK, Sacks BM. Symmetry of the femoral notch width index. Am J Sports Med 1997;25:687-90.
13. Arimaa A, Salminen T, Knifsund J, Kytö V, Lankinen P, Laaksonen I. Anterior cruciate ligament reconstruction and concomitant procedures in Finland between 2004 and 2018 based on national registers. Acta Orthop 2023;94:45-50.
14. Ojeda LH, Ojeda JH, Ojeda JG, Ojeda JF. Intercondylar notch stenosis in degenerative arthritis of the knee. Am J Sports Med 2005;33:347-52.
15. Souryal TO, Freeman TR. Intercondylar notch size and anterior cruciate ligament injuries in athletes. A prospective study. Am J Sports Med 1993;21:535-9.
16. Ireland ML, Ballantyne BT, Little K, McClay IS. A radiographic analysis of the relationship between the size and shape of the intercondylar notch and anterior cruciate ligament injury. Knee Surg Sports Traumatol Arthrosc 2001;9:200-5.
17. Huang M, Li Y, Guo N, Liao C, Yu B. Relationship between intercondylar notch angle and anterior cruciate ligament injury: a magnetic resonance imaging analysis. J Int Med Res 2019;47:1602-09.
18. Sousa AT, Vasconcelos JD, Soares MJ. Software image tool 3.0 as an instrument for measuring wounds. J Nurs UFPE Online 2012;6:2569-73.
19. Schikendantz MS, Weiker GG. The predictive value of radiographs in the evaluation of unilateral and bilateral anterior cruciate ligament injuries. Am J Sports Med 1993;21:11-3.
20. Herzog RJ, Silliman JF, Hutton K, Rodkey WG, Steadman JR. Measurements of the intercondylar notch by plain film radiography and magnetic resonance imaging. Am J Sports Med 1994;22:204-10.
21. Farrow LD, Chen MR, Cooperman DR, Victoroff BN, Goodfellow DB. Morphology of the femoral intercondylar notch. J Bone Joint Surg Am 2007;89:2150-5.
22. Terzidis IP, Christodoulou A, Ploumis A, Givissis P, Natsis K, Koimtzis M. Meniscal tear characteristics in young athletes with a stable knee: Arthroscopic evaluation. Am J Sports Med 2006;34:1170-5.
23. Taner Z, Murshed KA. An analysis of Anatolian human femur anthropometry. Turk J Med Sci 2002;32:231-5.
24. Mistri S. A study of femoral condylar morphometry. Indian J Basic App Med Res 2015;4:500510.
25. Ravichandran D, Melanie R. Morphology of the intercondylar notch and its clinical significance. IJAS 2010;1:26-30.
26. Shweta T. Morphometric analysis of condyles and intercondylar notch of femur in North Indian population and its clinical significance. J Evol Med Dent Sci 2017;6:2605-8.
27. Sangeeta M, Afroze MK, K L Varalakshmi. Association between intercondylar notch dimensions and morphometry of anterior cruciate ligament – A cadaveric study. J Med Sci Health 2021;10:7.
28. Ameet KJ, Murlimanju BV. A morphometric analysis of intercondylar notch of femur with emphasis on its clinical implications. Med Health 2014;9:103-8.
29. Biswas A, Bhattacharya S. A morphometric and radiological study of the distal end of femur in West Bengal population. IJAE 2017;122:39-48.
30. Chavda HS, Jethvar NK, Gupta S. A study of morphometric analysis of condyles of adult dry femur of humans in Gujarat region. Int J Anat Radiol Surg 2019;8:1.
31. Balgovind SR, Raunak B, Anusree A. Intercondylar notch morphometrics in Indian population: An anthropometric study with magnetic resonance imaging analysis. J Clin Orthop Trauma 2019;10:702-5.
32. Vinay G, Vikram S. A study of morphometric analysis of distal end of femur and its clinical importance. IP Indian J Anat Surg Head Neck Brain 2019;5:114-7.

Original Article

Morphology and Topography of Fossa Ovalis, Limbus Fossa Ovalis, and Probe Patency of Foramen Ovale in Formalin-fixed Hearts

Latha V. Prabhu, B. V. Murlimanju, Shubhangi Yadav[1], Yelluru Lakshmisha Rao, Rajanigandha Vadgaonkar, Mangala M. Pai, Aradhana Marathe[2], Jagadish Rao Padubidri[3]

Departments of Anatomy, [2]Biochemistry and [3]Forensic Medicine and Toxicology, Kasturba Medical College, Manipal Academy of Higher Education, Mangalore, Karnataka, [1]Department of Anatomy, All India Institute of Medical Sciences, Raebareli, Uttar Pradesh, India

Abstract

Introduction: Understanding the location and morphology of the fossa ovalis (FO) is crucial for radiographic and interventional cardiac procedures. **Objective:** The aim was to explore the morphology and topography of FO and limbus FO and to correlate them with the dimensions of the heart. The objective was to determine the frequency of congenital disabilities of the interatrial septum (IAS) in our sample population. **Materials and Methods:** The study included 57 formalin-fixed adult cadaveric hearts. The topography and morphological variants of different shapes of FO and limbus FO were noted. Pearson's correlation test was performed to assess the association between the dimensions of FO and the heart. **Results:** In our study, 33 hearts (57.89%) had oval-shaped FO, round in 20 hearts (35.1%), and in 4 hearts (7.01%), it was elliptical in shape. The limbus FO was raised in 46 hearts (80.7%) and this had flat in morphology in 11 hearts (19.3%). The probe patency of the foramen ovale was observed in 10 hearts (17%). The atrial septal defect (ASD) was observed in 12 hearts (21.05%) and one among them had an ostium secundum defect. The length of IAS was 52.5 ± 7.2 mm and the distance between the left margin of the superior vena caval opening and limbus FO was 22.7 ± 5.4 mm. **Conclusion:** This study provided additional information about the morphological and topographical variations of FO and limbus FO. This knowledge is helpful to cardiologists for diagnosing and correlating the embryological basis of ASDs.

Keywords: *Atrial septal defect, atrial septum, congenital heart defect, foramen ovale*

Introduction

The foramen ovale is an embryonic defect in the interatrial septum (IAS), communicating the blood from the right atrium to the left atrium in fetal life. It is a one-way flap valve formed by the septum primum and septum secundum. In about 75% of people, this foramen spontaneously closes after birth, due to the flow of blood from the lungs to the left atrium, leading to increased pressure in the left atrium. However, in 15%–35% people, this defect persists and is called patent foramen ovale (PFO).[1,2] This defect could be probe patency or may show varying degrees of patency, leading to mixing of deoxygenated and oxygenated bloods.[3] Although most of the PFO cases are asymptomatic, it could cause serious clinical disorders such as ischemic stroke, migraine, and hypoxemic medical conditions like chronic obstructive pulmonary disease, pulmonary hypertension, and platypnea-orthodeoxia.[4-6] It was reported that the severity of the disease depends directly on the size of the PFO.[7]

After the birth, once the foramen ovale is closed, it persists as the fossa ovalis (FO). FO is a depressed structure located in the lower part of the right surface of IAS. FO is an important anatomical landmark in the heart, which helps in locating the other vital structures of the right atrium including the opening of inferior vena cava, coronary sinus and bundle of His.[7] Basically, it is a three-dimensional structure, which is made up of septum primum, septum secundum and a raised margin called limbus FO. Hence, it is suggested that the knowledge of location and morphology of FO is essential during the interventional cardiac procedures like trans septal puncture as well as radiological procedures of the heart. In addition to this, FO is one of the common sites of cardiac pathology, involving premature closure of FO, PFO, atrial septal defects (ASDs), and tumors.[7] Another ASD, which can be found in the heart, is the atrial septal aneurysm or FO membrane aneurysm, which is found

How to cite this article: Prabhu LV, Murlimanju BV, Yadav S, Rao YL, Vadgaonkar R, Pai MM, *et al.* Morphology and topography of fossa ovalis, limbus fossa ovalis, and probe patency of foramen ovale in formalin-fixed hearts. J Anat Soc India 2025;74:332-7.

Article Info

Received: 30 October 2025
Revised: 17 November 2025
Accepted: 23 November 2025
Available online: 31 December 2025

Address for correspondence:
Dr. Yelluru Lakshmisha Rao, Department of Anatomy, Kasturba Medical College, Mangalore - 575 004, Karnataka, India.
E-mail: lakshmisha.rao@manipal.edu

Access this article online

Website: https://journals.lww.com/joai
DOI: 10.4103/jasi.jasi_170_25
Quick Response Code:

due to the redundancy of the valve of FO. In such cases, the hypermobile septum primum causes a prominent bulge during each cardiac cycle, resulting in potential shunting of blood from the left atrium to the right atrium, which could be one of the risk factors for stroke.[8]

Previous studies have demonstrated the variation in location and morphology of FO[9] and the clinical significance of these variants was also described. The shape of FO may vary from ovoid to round, and even sometimes it may be elliptical in shape. It is also reported that a positive correlation exists between the size of the heart and the size of the FO.[10] However, the dimensions of the FO may vary depending on the measuring tool. Structure and dimension of the FO are also altered in some pathologies such as rheumatic heart disease, amyloidosis, and cardiac myxomas.[11-13] When viewed from the right surface of the IAS, though the septal wall looks extensive, the true wall is relatively smaller, including FO and the muscular rim around it.[14] The literature review was suggesting a lack of cadaveric studies with respect to the morphology of IAS and the topography of FO. In this context, this study aims to explore the morphology of FO and limbus FO, including its shape, dimensions, topography, patency, and correlation with the dimensions of the heart. The objective was to determine the frequency of congenital disabilities of the IAS in our sample population.

Materials and Methods

The present study included 57 formalin-fixed heart specimens, which were available in the department of anatomy. The hearts with pathological changes were excluded. The age and sex of the hearts were not taken into consideration. This study has the approval of our institutional review board. IAS was studied from its right surface, after exposing the right atrium by dissecting the sulcus terminalis, extending between the openings of the superior vena cava and the inferior vena cava. Digital Vernier caliper (Mitutoyo, Japan) was used to perform the measurements, and a plastic probe measuring 1 mm was used to check the probe patency of the foramen ovale (PPFO) [Figure 1]. The different borders of the heart were measured to assess the size of the heart [Figure 2 and Table 1].

The topographical location of FO was studied by measuring the distance between the left margin of the opening of the superior vena cava and the upper margin (limbus) of FO [Figure 3a]. The morphological variants of different shapes of FO and limbus FO were noted in all the specimens. The FO were scrutinized for any visible patency or defects. The vertical and transverse dimensions of FO were also measured [Figure 3b]. The FO was observed for any patency or defects. The frequency of PFO and probe patency was noted. The length of IAS was measured between the opening of the superior vena cava and the posterior border of the septal atrioventricular valve [Figure 3a].

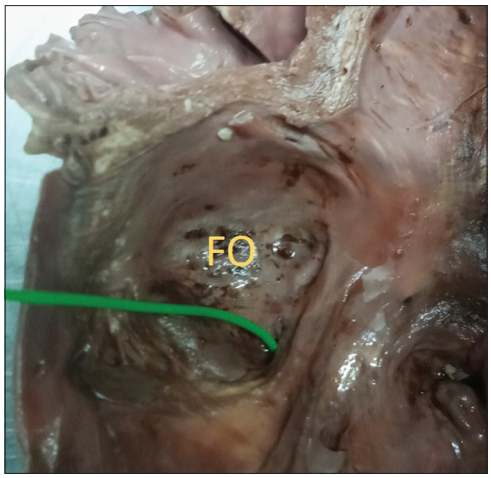

Figure 1: The probe patency of the foramen ovale (1 mm plastic probe was utilized for the probing)

Figure 2: Measurement of dimensions of the heart (right border-AB; inferior border-BC; superior border-AD; left border-CD; oblique diameter-AC)

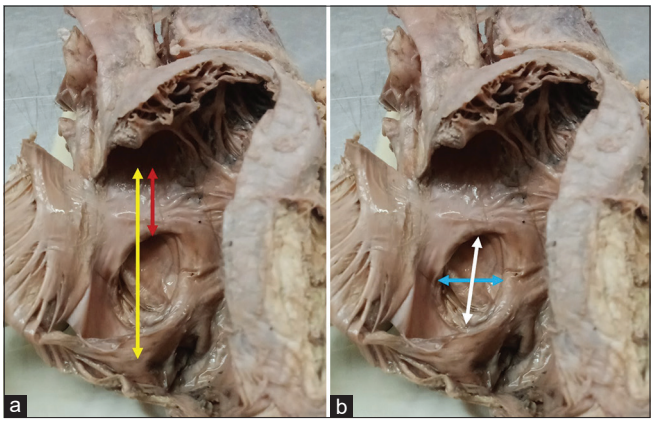

Figure 3: (a) The measurement of the interatrial septum (yellow arrow) and distance between the opening of the superior vena cava and upper margin (limbus) of the fossa ovalis (FO) (red arrow), (b) measurement of vertical (white arrow) and transverse (blue arrow) dimensions of FO

The statistical analysis was performed using the "jamovi" online software, [Amsterdam, North Holland, Netherlands] and Pearson's correlation test was applied

to assess the association between the dimensions of FO, IAS and the heart. The correlation was considered significant if Pearson's "*r*" ≥0.5. The Chi-square test for association was performed to see the association between the shape of FO and interatrial septal defects. This was considered statistically significant if the "*p*" ≤0.05.

Results

Fossa ovalis and limbus fossa ovalis

In our study, round-shaped FO [Figure 4a] was observed in 20 hearts (35.1%), 33 hearts (57.89%) had oval shape [Figure 4b], and in 4 hearts (7.01%), the FO was elliptical in shape [Figure 4c]. There were two specimens, which had fenestrated FO, and one among them had an associated fibrous band [Figure 4d]. The frequency of shapes of FO observed in this study is given in Figure 4e. The limbus FO was raised [Figure 5a] in 46 hearts (80.7%), and in the remaining hearts, this had flat [Figure 5b] morphology (19.3%). The frequency of these two types is represented in Figure 5c. The vertical length of FO was 21.4 ± 5.8 mm, and the transverse diameter was 19.5 ± 4.3 mm [Table 2].

Interatrial septum

The ASD was observed in 12 hearts [21.05%, [Figures 6 and 7], and among them, the PPFO [Figures 6a-k] was observed in 11 hearts (19.2%), and one heart showed an ostium secundum type [Figure 7] of ASD (1.75%). The mean length of IAS was 52.5 ± 7.2 mm and the mean distance between the left margin of the superior vena caval opening and the limbus FO was 22.7 ± 5.4 mm [Table 2].

The dimensions of different borders of the heart are represented in Table 1. The Pearson's correlation test [Figures 8a-i] revealed a significant association only between the lengths of the right border of the heart and IAS [Figure 8c]. Table 3 shows the Chi-square test analysis of the association between the frequency of interatrial septal defects and the shape of the FO. However, this did not reveal any statistical significance ($P > 0.05$).

Discussion

Defects in the IAS are the most common congenital heart disorders encountered in clinical practice, which have a prevalence of 1.65 per 1000 live births.[15] The basic knowledge about the development and morphology of the true inter-atrial septum gives a clear concept of interatrial defects, which is essential for clinicians to diagnose and treat congenital heart disorders. Embryologically, atrial septation starts from the appearance of a thin crescent of tissue at the atrial roof, which is called the septum primum. The free edge of this septum is covered by mesenchymal cells derived from the embryonic endocardium.[16] The septum grows downward toward the atrio-ventricular junction to fuse with the endocardial cushion. The gap between the endocardial

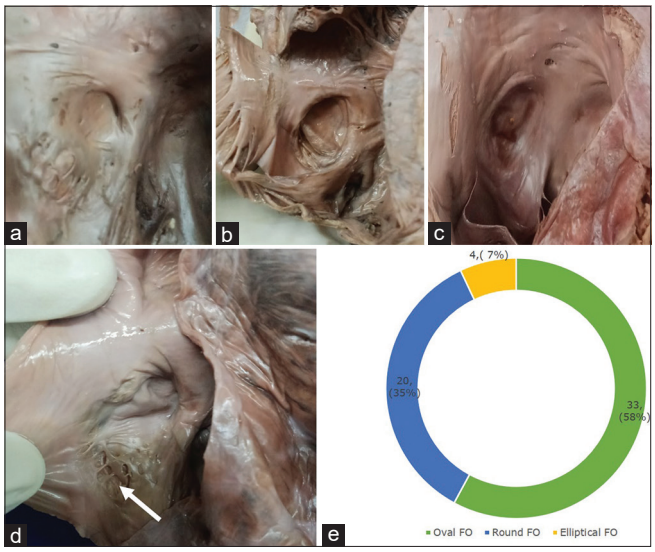

Figure 4: Morphological variants of the shapes of fossa ovalis (a) round shape, (b) oval shape, (c) elliptical shape, (d) fenestrated with fibrous band, (e) frequency of the shapes

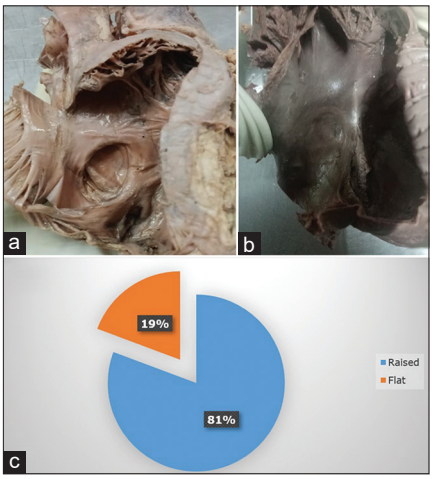

Figure 5: Morphological variants of the limbus fossa ovalis (a) raised, (b) flat, (c) frequency of the two

Table 1: The measurement of dimensions of the heart, performed in this study (*n*=57)

Dimensions of the heart	Measurements taken	in millimeter ± standard deviation
Right border (AB)	From the opening of the SVC to opening of the inferior vena cava	72.8±9.9
Inferior border (BC)	From the opening of the inferior vena cava to the apex	102.6±11
Superior border (AD)	From the opening of the SVC to the left auricle	83.8±11
Left border (CD)	From the apex of the heart to the left auricle	101.4±14.1
Oblique diameter (AC)	From the opening of SVC to the apex	121.4±21.6

SD: Standard deviation, SVC: Superior vena cava

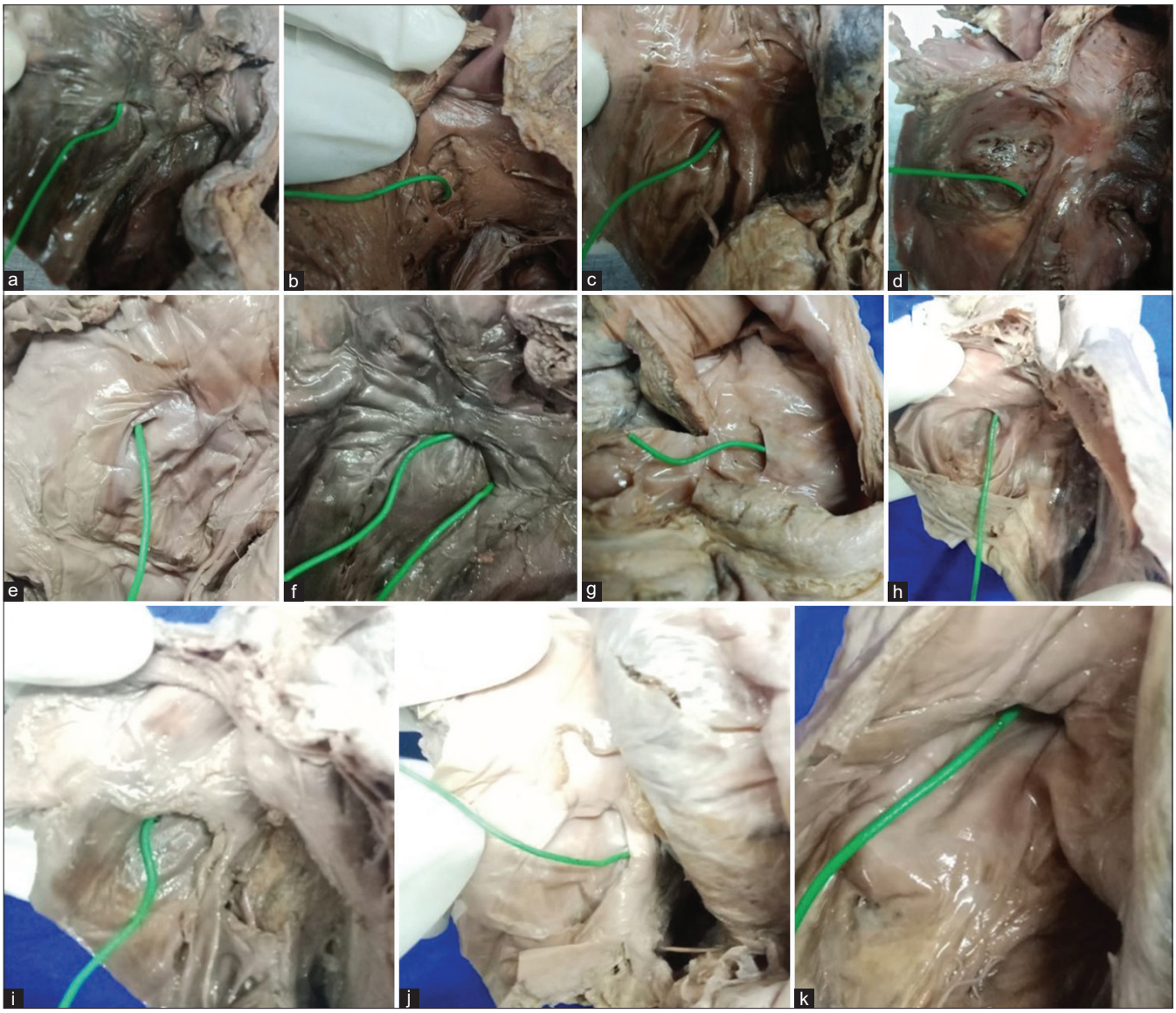

Figure 6: Cadaveric hearts of this study showing the interatrial septal defects *n* = 12, 21%, (a-k) probe patency of foramen ovale

Table 2: The measurement of dimensions of the fossa ovalis, performed in this study

Dimension	in millimeter ± standard deviation
FO vertical diameter	21.4±5.8
FO transverse diameter	19.5±4.3
Length of IAS	52.5±7.2
SVC and limbus FO	22.7±5.4

SVC and limbus FO-distance between SVS opening and limbus FO. FO: Fossa ovalis, IAS: Interatrial septum, SVC: Superior vena cava, SD: Standard deviation

cushion and the lower margin of septum primum is called the ostium primum. At the age of 6th week of embryonic life, the septum primum fuses with the atrioventricular cushion, leading to closure of the septum primum. Meanwhile, the upper part of the septum primum, near the roof of the atria, disintegrates to leave an opening called the ostium secundum. During the 7th week, from the roof of the atria, between the opening of the superior vena cava and septum primum, an in folding of the atrial wall appears and grows downwards as septum secundum. Infolded septum secundum overlaps the septum primum on its right side and forms the superior, anterosuperior, and posterior margin of the foramen ovale. Now, the septum primum forms flap-like valve to allow the blood flow from right atrium to left. After birth, the increased pressure in the left atrium pushes the septum primum toward the septum secundum and forms adhesion, leading to closure of the slit like opening. Then, the right surface of septum primum, forms the FO, and the raised margins formed by the septum secundum form the limbus FO. On a few occasions, failure of formation of adhesion between the septum primum and secundum leads to PPFO.[15]

The IAS contains two components called the anatomic septum and the true septum. The anatomic IAS is the entire partition between the right and left atria, and most of this part is formed

by infolding of the right atrial wall and extra-cardiac space filled with adipose tissue. This extra-cardiac space is also called the thick portion of IAS. The true IAS includes only FO and limbus. The trans-septal puncture performed at other than the true septum, will pass through extracardiac space, before reaching the left atrium, leading to the risk of cardiac tamponade.[15] Hence, the length of the anatomical septum and true septum and the distance between the upper border of the septum and the limbus FO, will have a great surgical importance during the trans-septal puncture procedures.

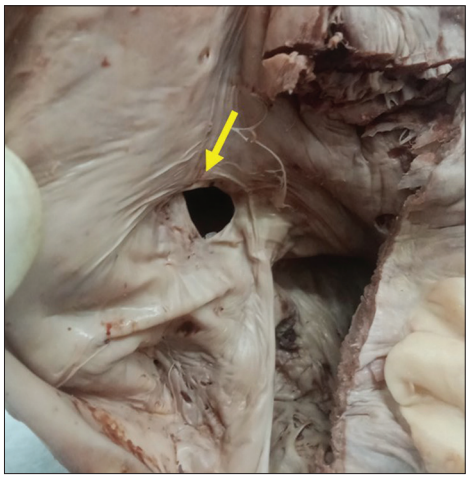

Figure 7: The ostium secundum variety of atrial septal defect (arrow), which was observed in only one heart in this study

According to Bradley and Zaidi,[17] 80% of the ASDs are ostium secundum defects. However, in our study, only one heart among the 12 hearts, which had inter ASDs showed a septum secundum defect, and this gave the frequency of 8.3%, which is smaller in comparison to the findings of Bradley and Zaidi.[17] However, a study with a larger sample size may reveal higher incidences of septum secundum defects. Kishve and Motwani[3] found that, mean transverse diameter of FO is 24.2 mm and vertical diameter was 26.8 mm. In our study also, we have found that the transverse diameter was 19.6 ± 0.4 mm and the vertical diameter of FO was 21.4 ± 0.6 mm. In our study, limbus FO was raised in 48 hearts (84.2%), and it was flat in 9 hearts (15.8%). This result

Table 3: Contingency table showing the frequency of interatrial septal defects associated with the shape of the fossa ovalis

Shape of FO	PPFO	SSD	FSP	Total
Oval	8	1	1	10
Round	1	0	1	2
Elliptical	1	0	0	1
Total	10	1	2	13
Chi-square tests				
χ^2; df; *P*		2.47; 4; 0.65		
n		13		

Chi-square test, statistical significance at $P>0.05$. FO: Fossa ovalis, PPFO: Probe patency of foramen ovale, SSD: Septum secundum defect, FSP: Fenestrated septum

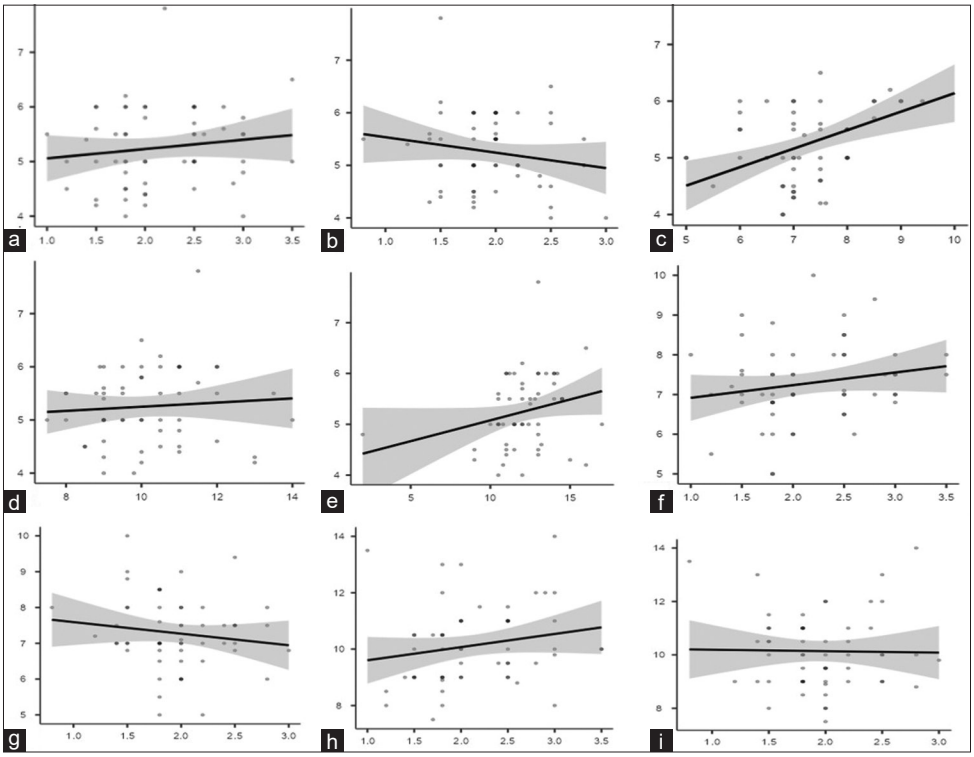

Figure 8: Graphs of the Pearson's correlation test, FO-fossa ovalis, interatrial septum (IAS)-interatrial septum (a) vertical diameter of FO versus length of IAS, (b) transverse diameter of FO versus length of IAS, (c) length of right border of heart versus length of IAS, (d) length of left border of heart versus length of IAS, (e) length of oblique border of heart versus length of IAS, (f) vertical diameter of FO versus length of right border of heart, (g) transverse diameter of FO versus right border of heart, (h) vertical diameter of FO versus length of left border of heart, (i) transverse diameter of FO versus left border of heart

is in favor of the observation of Chaudhari *et al*.[11] as they have observed raised limbus FO in 84% hearts, flat in 12% and 4% had depressed morphology. According to their study, 24% of hearts showed PFO, whereas in our study, we observed PFO in 17% hearts. In a study by Faletra *et al*.,[18] 27% of heart specimens showed PFO. According to Teo *et al*.,[19] PFO is a normal variant and will be asymptomatic if the shunting of blood is minimal. However, by the fifth decade, around 75% people will show symptoms like dyspnea on exertion, arrhythmias, pulmonary hypertension, etc.[19] Hence, early diagnosis of PFO will help in preventing and reducing the complications of cardiac disorders. Anatomical knowledge about the topography of the limbus FO will also have clinical significance during the trans-septal catheterization. Hence, this measurement was considered important and determined in this study. The mean distance of the limbus from the opening of the SVC in this study was 22.7 ± 5.4 mm.

Though there are few studies,[20-22] which recorded the external dimensions of the heart in cadavers, the detailed measurement of each border of the heart in the cadavers is not being documented in the literature. Our study is novel in measuring these dimensions of borders of heat and correlating them with the dimensions of IAS and FO. The limitation of this present study is that the formalin-fixed specimens were considered, and formalin may have some effect on the morphology of the structures and dimensions measured. Future implications of this study include studying the morphology and topography of FO, limbus FO and IAS in the autopsy specimens from which the fresh hearts can be procured.

Conclusion

The present study observed variability in the morphology and topography of FO and limbus FO. This knowledge of morphological and topographical variations of the IAS and FO is enlightening to the clinician during the cardiac interventional procedures and device implantation in congenital anomalies of heart. It is also helpful to the radiologist and cardiologist for diagnosing the ASDs and identifying the role of ASDs in other cardiac disorders like pulmonary hypertension, arrhythmias, etc., Correlating with the embryological basis for the septal defects will help in better understanding of the deformity and in the improvement of treatment strategies.

Financial support and sponsorship

Nil.

Conflicts of interest

There are no conflicts of interest.

References

1. Barik R. The three-dimensional fossa ovalis. Indian Heart J 2016;68:211-2.
2. Teshome MK, Najib K, Nwagbara CC, Akinseye OA, Ibebuogu UN. Patent foramen ovale: A comprehensive review. Curr Probl Cardiol 2020;45:100392.
3. Kishve P, Motwani R. Morphometric study of fossa ovale in human cadaveric hearts: Embryological and clinical relevance. Anat Cell Biol 2021;54:42-50.
4. Dalen JE, Stein PD, Matta F. Patent foramen ovales and cryptogenic strokes: Another look. Am J Med 2011;124:2-3.
5. Lechat P, Mas JL, Lascault G, Loron P, Theard M, Klimczac M, *et al*. Prevalence of patent foramen ovale in patients with stroke. N Engl J Med 1988;318:1148-52.
6. Mojadidi MK, Ruiz JC, Chertoff J, Zaman MO, Elgendy IY, Mahmoud AN, *et al*. Patent foramen ovale and hypoxemia. Cardiol Rev 2019;27:34-40.
7. Oduah MT, Sharma P, Brown KN. Anatomy, thorax, heart fossa ovalis. In: StatPearls. Treasure Island (FL): StatPearls Publishing; 2023.
8. Kheiwa A, Hari P, Madabhushi P, Varadarajan P. Patent foramen ovale and atrial septal defect. Echocardiography 2020;37:2172-84.
9. Vaida MA, Streian CG, Gug C, Damen NS, Jianu AM, Grigoriță A, *et al*. Morphological study of fossa ovalis in formalin-fixed human hearts and its clinical importance. Medicina (Kaunas) 2021;57:1254.
10. Reig J, Mirapeix R, Jornet A, Petit M. Morphologic characteristics of the fossa ovalis as an anatomic basis for trans-septal catheterization. Surg Radiol Anat 1997;19:279-82.
11. Chaudhari RG, Shinde SV, Deshpande JR. Morphometric analysis of fossa ovalis in rheumatic heart disease. Indian Heart J 2005;57:662-5.
12. Cohen R, Singh G, Mena D, Garcia CA, Loarte P, Mirrer B. Atrial myxoma: A case presentation and review. Cardiol Res 2012;3:41-4.
13. Munjewar C, Agrawal R, Sharma S. Cardiac amyloidosis: A report of two cases. Indian Heart J 2014;66:473-6.
14. Rana BS, Shapiro LM, McCarthy KP, Ho SY. Three-dimensional imaging of the atrial septum and patent foramen ovale anatomy: Defining the morphological phenotypes of patent foramen ovale. Eur J Echocardiogr 2010;11:i19-25.
15. Naqvi N, McCarthy KP, Ho SY. Anatomy of the atrial septum and interatrial communications. J Thorac Dis 2018;10:S2837-47.
16. Mommersteeg MT, Soufan AT, de Lange FJ, van den Hoff MJ, Anderson RH, Christoffels VM, *et al*. Two distinct pools of mesenchyme contribute to the development of the atrial septum. Circ Res 2006;99:351-3.
17. Bradley EA, Zaidi AN. Atrial septal defect. Cardiol Clin 2020;38:317-24.
18. Faletra FF, Leo LA, Paiocchi VL, Schlossbauer SA, Pedrazzini G, Moccetti T, *et al*. Revisiting anatomy of the interatrial septum and its adjoining atrioventricular junction using noninvasive imaging techniques. J Am Soc Echocardiogr 2019;32:580-92.
19. Teo KS, Disney PJ, Dundon BK, Worthley MI, Brown MA, Sanders P, *et al*. Assessment of atrial septal defects in adults comparing cardiovascular magnetic resonance with transoesophageal echocardiography. J Cardiovasc Magn Reson 2010;12:44.
20. Mannan S, Khalil M, Rahman M, Ahmed MS. Measurement of different external dimensions of the heart in adult Bangladeshi cadaver. Mymensingh Med J 2009;18:175-8.
21. Raveendran S, Vidanapathirana M, Hulathduwa SR. An autopsy study of the quantitative anatomy of human heart. J Adv Med Med Res 2021;33:89-99.
22. Mohammadi S, Hedjazi A, Sajjadian M, Ghoroubi N, Mohammadi M, Erfani S. Study of the normal heart size in Northwest part of Iranian population: A cadaveric study. J Cardiovasc Thorac Res 2016;8:119-25.

Original Article

Comparative Study of Oocyte Quality in Young and Advanced-aged Women

Abstract

Background: Oocyte quality is a key determinant of female fertility, influencing fertilization, embryo development, and pregnancy outcomes. Advanced maternal age (AMA) is associated with declining oocyte competence due to chromosomal abnormalities, mitochondrial dysfunction, and cytoplasmic changes. While previous studies have focused on genetic and molecular changes, a systematic classification of oocyte maturity and quality across different age groups remains underexplored. **Objective:** To compare the quality of oocytes retrieved from young and advanced-aged women by evaluating key parameters such as total oocytes retrieved, the proportion of Metaphase II (MII) oocytes, Metaphase I (MI) oocytes, Germinal Vesicle (GV) oocytes, and Atretic (ATR) oocytes to assess the impact of aging on oocyte maturity and developmental competence. **Materials and Methods:** A total of 50 women aged 25–50 years undergoing assisted reproductive treatment (ART) were included in the study. Participants were categorized into five age groups: 25–30, 31–35, 36–40, 41–45, and 45–50 years. Oocytes were retrieved, denuded, and classified based on their maturity status (MII, MI, GV, ATR). Data analysis was conducted using SPSS software, and statistical significance was determined using ANOVA with a $P < 0.05$. **Results:** The number of MII oocytes significantly declined with age (negative correlation: −0.946). MI oocytes showed a weak positive correlation with age (Spearman's correlation: 0.308). GV oocytes exhibited no correlation with age (correlation coefficient: 0.000). Atretic oocytes demonstrated a slight but nonsignificant positive correlation with age (correlation coefficient: 0.224). The overall ovarian response, indicated by the total number of retrieved oocytes, was lower in older age groups. **Conclusion:** Oocyte quality and maturity decline significantly with advancing age, particularly reflected in a reduced proportion of MII oocytes. The findings suggest that aging impacts oocyte competence, affecting ART success rates. A better understanding of age-related oocyte quality deterioration may help refine fertility treatment strategies, improve ART outcomes, and guide personalized reproductive interventions.

Keywords: *Maternal age, metaphase II oocytes, oocyte quality, ovarian aging*

Anupama Sawal, Kirti B Chaudhary, Bhumica Dang[1], Pradeep Bokariya[2]

Jawaharlal Nehru Medical College, Datta Meghe Institute of Higher Education and Research, Sawangi (Meghe), [2]Department of Anatomy, Mahatma Gandhi Institute of Medical Sciences, Sevagram, Wardha, Maharashtra, [1]BPS Govt. medical college, Haryana, India

Introduction

Oocyte quality is a fundamental determinant of female fertility, directly influencing fertilization success, embryo development, and pregnancy outcomes.[1] Maternal aging has been associated with a significant decline in oocyte competence due to chromosomal abnormalities, mitochondrial dysfunction, and cytoplasmic changes, which collectively impair reproductive potential.[2] While previous studies have extensively investigated age-related changes at the genetic and molecular levels, the systematic classification of oocyte maturity and quality across different developmental stages remains underexplored.

The rate of aneuploid blastocysts is greatly impacted by advanced maternal age (AMA), however fertilization and embryo development up to the blastocyst stage are not significantly affected.[3,4] Genetic defects in the fetus are strongly connected to maternal age, demonstrating that primary oocytes are vulnerable to harm as they age. Several disorders have been linked to decreased fertility in older women to date.[5]

In our study, we introduce a comprehensive assessment of oocyte maturity and quality by analyzing oocytes at different stages after retrieval and denudation. Unlike prior research, which has primarily focused on fertilization and embryo development, we specifically assess oocyte competence based on the following key parameters:

1. Total retrieved oocytes – Quantifying the overall oocyte yield in young and advanced-aged women to evaluate ovarian response[6]

How to cite this article: Sawal A, Chaudhary KB, Dang B, Bokariya P. Comparative study of oocyte quality in young and advanced-aged women. J Anat Soc India 2025;74:338-42.

Article Info

Received: 24 March 2025
Revised: 18 August 2025
Accepted: 23 November 2025
Available online: 31 December 2025

Address for correspondence:
Dr. Pradeep Bokariya, Department of Anatomy, Mahatma Gandhi Institute of Medical Sciences, Sevagram, Wardha - 442 102, Maharashtra, India.
E-mail: pradeepbokariya@mgims.ac.in

Access this article online

Website: https://journals.lww.com/joai

DOI: 10.4103/jasi.jasi_58_25

Quick Response Code:

2. Metaphase II (MII) oocytes – Assessing the proportion of fully matured oocytes with fertilization potential, a crucial factor in assisted reproductive technologies (ART)[7]
3. Metaphase I (MI) oocytes – Evaluating the number of oocytes that have not yet completed meiosis but may undergo *in vitro* maturation, providing insights into ovarian reserve and maturation efficiency[8]
4. Atretic oocytes (ATR) – Identifying the proportion of degenerating oocytes as an indicator of follicular health and reproductive aging[9]
5. Germinal vesicle (GV) oocytes – Determining the prevalence of immature oocytes arrested at the prophase I stage, reflecting follicular development status and potential fertility prognosis.[10]

The objective of our study is to compare the quality of oocytes in young and advanced-aged women by evaluating key parameters, including total oocytes retrieved, the proportion of MII oocytes, MI oocytes, ATR, and GV oocytes, to assess the impact of aging on oocyte maturity and developmental competence.

By integrating a detailed classification of oocyte developmental stages, our study provides a novel perspective on how aging affects oocyte quality and ovarian response. This systematic evaluation allows for a more precise understanding of reproductive aging, bridging the gap between conventional fertility assessments and detailed oocyte maturation analysis. Our findings may contribute to refining oocyte selection criteria, improving ART outcomes, and guiding individualized fertility treatment strategies.

Materials and Methods

This study included a total of 50 women between the ages of 25 and 50 years, all of whom sought medical assistance for infertility-related concerns. The participants were selected from both urban (Wardha) and nearby rural areas, with an equal distribution from each group. Written informed consent was obtained from all participants, ensuring their understanding that their medical data would be used exclusively for this comparative study.

All enrolled patients underwent an oocyte retrieval procedure as part of their assisted reproductive treatment (ART). Following retrieval, the total number of oocytes collected was recorded. After oocyte denudation, an assessment of oocyte maturity was performed,

The collected data were systematically recorded and analyzed to compare oocyte quality across different age groups. Patients were categorized based on their age, and the distribution of oocyte maturity stages was examined. Statistical analysis was conducted using The jamovi project (2025). jamovi (Version 2.6) [Computer Software]. (Retrieved from https://www.jamovi.org), applying appropriate tests to determine significant differences between the groups. Descriptive statistics ANOVA were used to interpret the findings. A $P < 0.05$ was considered statistically significant.

Inclusion criteria

- Patients diagnosed with infertility
- Young women undergoing ART
- Advanced-age women undergoing ART
- Patients undergoing oocyte retrieval as part of ART.

Exclusion criteria

- Patients undergoing intrauterine insemination instead of oocyte retrieval
- Patients unwilling to proceed with an intracytoplasmic sperm injection (ICSI) cycle.

This methodological approach ensures a systematic and unbiased evaluation of oocyte quality across different age groups, contributing valuable insights into the impact of aging on reproductive outcomes.

Results

The number of total oocytes retrieved, number of MII oocytes, number of MI oocytes, number of atretic oocytes and number of GVs are noted. The data are shown in Table 1. The same data are shown graphically in Figure 1.

When correlation analysis was performed for age versus different oocyte categories (average number), the data thus analyzed were as follows MII has shown negative correlation (−0.946) meaning MII oocytes decrease significantly with age.

Similarly MI has spearman's correlation (0.308) suggesting weak positive correlation, indicating no clear trend. Whereas GV (immature oocytes) has spearman's correlation coefficient (0.000) suggesting no correlation with age. And for ATR (atretic oocytes, degenerating) spearman's correlation coefficient (0.224) which suggest slight positive correlation, but not statistically meaningful.

Discussion

Effective treatments now exist for age-related infertility caused by declining oocyte quality. Oxidative stress significantly contributes to oocyte aging, leading to

Table 1: Average number of oocytes according to their oocyte maturity

Age group	MII (average)	MI (average)	GV (average)	ATR (average)	One way ANNOVA
25–30	21	3	2	2	P=0.143
31–35	17	2	3	2	(nonsignificant)
36–40	4	6	2	5	
41–45	2	4	3	3	
45–50	1	3	2	2	

MII: Metaphase II, MI: Metaphase I, GV: Germinal vesicle, ATR: Atretic

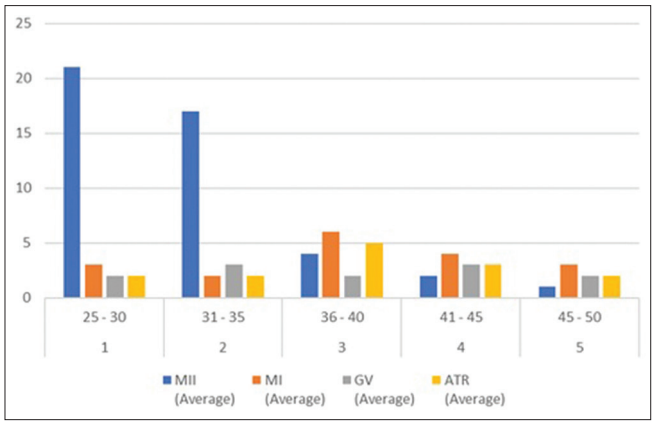

Figure 1: Grouped bar graph showing average data for metaphase II, metaphase I, germinal vesicle and atreitic oocytes according to age range of patients

mitochondrial dysfunction and chromosomal abnormalities. Various experimental therapies, particularly antioxidants, have shown promise in improving oocyte quality and mitochondrial activity. Fertility declines notably after the age of 30–35, with factors like coital patterns and male partner's age further influencing fecundity.[11] Artificial insemination using donor semen (AID) allows researchers to control these variables, reducing biases in fecundity studies.[12]

Data from the European Society for Human Reproduction and Embryology indicate an 18.9% pregnancy rate per insemination. Among women aged 25–40, 18,515 AID treatments resulted in 3498 pregnancies. In contrast, the success rate for women over 40 was only 9.2% (2053 treatments and 189 pregnancies).[13] AMA is also associated with increased miscarriage risk, attributed to deteriorating oocyte quality rather than uterine factors.[14] Lifestyle choices such as diet, exercise, stress management, substance use, and environmental exposure further influence fertility outcomes.[15] A woman's probability of conception drops from 71% under 30%–41% after 36.[16] Chromosomal abnormalities, particularly aneuploidy, heighten the risk of miscarriage and implantation failure, contributing to a sharp fertility decline in the 30s and 40s.[17]

Treatments for age-related infertility aim to shorten gestation time and enhance fecundity, but they do not directly improve oocyte quality. Oocyte donation remains the only effective option for poor oocyte quality due to aging.[18] In addition, advanced reproductive age correlates with increased pregnancy complications, including spontaneous abortion, intrauterine growth restriction, gestational diabetes, hypertension, and low birth weight.[19] Women over 40 should consider preconception testing for conditions like diabetes and hypertension before starting fertility treatments.[20]

Recent research suggests that dormant mesenchymal progenitor cells in the ovarian tunica albuginea may give rise to granulosa and germ cells, challenging the long-held belief that ovarian follicles are finite. Jonathan Tilly's team first identified ovarian stem cells in adult mice, with subsequent studies confirming their presence in humans, rabbits, and marmosets.[21] The discovery of ovarian stem cells has opened new avenues in reproductive medicine, offering potential for infertility preservation and novel treatments.[22]

Oxidative stress is a key factor in aging, affecting mitochondrial function and increasing susceptibility to various age-related diseases. During oxidative phosphorylation, mitochondria generate reactive oxygen species, which, if unbalanced, lead to cellular damage. ART is increasingly used among women with diminished ovarian reserve. Moderate ovulation induction protocols, such as letrozole or clomiphene from days 2–3 of the menstrual cycle, are commonly employed. Successful pregnancy is confirmed by ultrasound detection of a fetal sac and heartbeat at 4 weeks posttransfer.[23]

Oocyte quality is crucial for successful fertilization and embryo development. Poor oocyte quality is associated with increased chromosomal abnormalities and dysfunctional organelles, leading to lower fertilization rates, impaired embryonic growth, and higher miscarriage risks.[24] Although widely accepted, the mechanisms underlying oocyte aging remain unclear. Older oocytes often exhibit aneuploidy, contributing to failed implantation and congenital anomalies.[25] Gene expression studies indicate that aging affects about 5% of transcripts in MII-stage oocytes, with differential epigenetic modifications potentially influencing these changes.[26]

Maternal age is a primary factor in embryonic aneuploidies, with over 90% of these abnormalities originating from meiotic chromosomal missegregation.[27] The prolonged arrest of oocytes in prophase I may lead to structural deterioration over time, increasing the risk of errors in chromosome segregation during meiosis I and II.[28] Studies comparing ART outcomes among women under 25 and over 40 reveal significant age-related declines in oocyte quality, fertilization rates, and live birth rates.[29]

The success of ART depends on multiple factors, with maternal age being the most critical determinant. Fertility success rates decline sharply after 37, with an increased risk of miscarriage after 40.[30] In older women, oocytes retrieved postovarian hyperstimulation frequently display spindle and chromosomal misalignments during metaphase II. Research by Zenzes *et al*. showed that between 24 and 42 years, both the number of retrieved oocytes and mature oocytes decreased by nearly 50%.[31] Advanced-age patients also require higher gonadotropin doses yet yield fewer follicles and oocytes due to progressive ovarian follicular depletion.

Conflicting evidence exists regarding the impact of aging on oocyte quality and sperm binding capability. Some

studies report no effect of aging on cleavage rate and embryo morphology after ICSI, while others observe increased fragmentation in standard *in vitro* fertilization cycles. Most researchers agree that aged oocytes have reduced implantation and developmental potential.[32]

This study assessed zygote scores in ART patients based on maternal age. Patients under 40 exhibited a uniform distribution of zygote quality, while those over 40 had a significant decline in high-quality zygotes and an increase in lower-grade zygotes.[33] Clinical pregnancy and live birth rates were notably lower in women over 30, with a negative correlation between maternal age and ART success. These findings align with previous research indicating a steady decline in pregnancy rates with age.[34]

Conclusion

Our study confirms that as women age, their reproductive health, including ovarian function, undergoes significant decline. Younger women produce oocytes of noticeably superior quality compared to those of older women.

By analyzing oocyte quality across different age groups, we found a clear age-related impact. In younger women, the majority of recovered oocytes were at the mature MII stage, whereas in older women, immature oocytes (MI, GV, and ATR) were more prevalent.

In conclusion, younger women generate healthier, more viable oocytes, while ovarian aging negatively affects oocyte maturity and quality, potentially influencing fertility outcomes.

Financial support and sponsorship

Nil.

Conflicts of interest

There are no conflicts of interest.

References

1. Fragouli E, Wells D. Aneuploidy in the human oocyte. Cytogenet Genome Res 2012;133:168-77.
2. Tatone C, Amicarelli F. The aging ovary – The poor granulosa cells. Fertil Steril 2013;99:12-7.
3. Crosignani PG, Collins J, Diedrich K, Franks S, Geraedts JP, Jacobs PA, *et al*. Genetic aspects of female reproduction. Human Reproduction Update 2008;14:293-307.
4. Heffner LJ. Advanced maternal age – How old is too old? N Engl J Med 2004;351:1927-9.
5. Silber SJ, Kato K, Aoyama N, Yabuuchi A, Skaletsky H, Fan Y, *et al*. Intrinsic fertility of human oocytes. Fertil Steril 2017;107:1232-7.
6. Stensen MH, Tanbo T, Storeng R, Byholm T. Oocyte yield and quality in relation to age: A population-based study of 6,662 IVF cycles. Hum Reprod 2020;35:905-14.
7. Kawamura K, Cheng Y, Suzuki N. Activation of dormant follicles to generate mature eggs in infertile patients. Reprod Med Biol 2021;20:13-23.
8. Ebner T, Shebl O, Oppelt P, Mayer RB, Duba HC, Montag M. Maturation of slow-growing oocytes: A morphological and functional analysis. Fertil Steril 2016;106:724-9.
9. Tiwari D, Sharma RK, Ghosh S. Apoptosis in ovarian follicles: A marker for atretic oocytes. J Assist Reprod Genet 2022;39:319-30.
10. Combelles CM, Albertini DF, Racowsky C. Cellular and developmental control of oocyte quality: Clues from follicular dynamics. Reprod Biomed Online 2002;6:402-15.
11. Schwartz D, Mayaux MJ. Female fecundity as a function of age: Results of artificial insemination in 2193 nulliparous women with azoospermic husbands. Obstet Gynecol Surv 1982;37:548-50.
12. Balasch J. Gonadotrophin ovarian stimulation and intrauterine insemination for unexplained infertility. Reprod Biomed Online 2004;9:664-72.
13. Calhaz-Jorge C, de Geyter C, Kupka MS, de Mouzon J, Erb K, Mocanu E, *et al*. The European IVF-monitoring consortium (EIM)‡ for the European Society of Human Reproduction and Embryology (ESHRE). Hum Reprod 2016;31:1638-1652.
14. Dickey RP, Pyrzak R, Lu PY, Taylor SN, Rye PH. Comparison of the sperm quality necessary for successful intrauterine insemination with World Health Organization threshold values for normal sperm. Fertil Steril 1999;71:684-9.
15. Sharma R, Biedenharn KR, Fedor JM, Agarwal A. Lifestyle factors and reproductive health: Taking control of your fertility. Reprod Biol Endocrinol 2013;11:66.
16. Mutsaerts MA, Groen H, Huiting HG, Kuchenbecker WK, Sauer PJ, Land JA, *et al*. The influence of maternal and paternal factors on time to pregnancy – A Dutch population-based birth-cohort study: The GECKO Drenthe study. Hum Reprod 2012;27:583-93.
17. Stewart AF, Kim ED. Fertility concerns for the aging male. Urology 2011;78:496-9.
18. Liu K, Case A, Cheung AP, Sierra S, AlAsiri S, Carranza-Mamane B, *et al*. Advanced reproductive age and fertility. J Obstet Gynaecol Can 2011;33:1165-1175.
19. Dovey S, Sneeringer RM, Penzias AS. Clomiphene citrate and intrauterine insemination: Analysis of more than 4100 cycles. Fertil Steril 2008;90:2281-6.
20. Stein ZA. A woman's age: Childbearing and child rearing. Am J Epidemiol 1985;121:1638-1652.
21. Hook EB. Rates of chromosome abnormalities at different maternal ages. Obstet Gynecol 1981;58:282-5.
22. Gilbert WM, Nesbitt TS, Danielsen B. Childbearing beyond age 40: Pregnancy outcome in 24,032 cases. Obstet Gynecol 1999;93:9-14.
23. Johnson J, Canning J, Kaneko T, Pru JK, Tilly JL. Germline stem cells and follicular renewal in the postnatal mammalian ovary. Nature 2004;428:145-50.
24. Hamatani T, Falco G, Carter MG, Akutsu H, Stagg CA, Sharov AA, *et al*. Age-associated alteration of gene expression patterns in mouse oocytes. Hum Mol Genet 2004;13:2263-78.
25. Ramalingam M, Kim SJ. Reactive oxygen/nitrogen species and their functional correlations in neurodegenerative diseases. J Neural Transm (Vienna) 2012;119:891-910.
26. Miao YL, Kikuchi K, Sun QY, Schatten H. Oocyte aging: Cellular and molecular changes, developmental potential and reversal possibility. Hum Reprod Update 2009;15:573-85.
27. Bentov Y, Yavorska T, Esfandiari N, Jurisicova A, Casper RF. The contribution of mitochondrial function to reproductive aging. J Assist Reprod Genet 2011;28:773-83.
28. Capalbo A, Hoffmann ER, Cimadomo D, Ubaldi FM, Rienzi L. Human female meiosis revised: New insights into the mechanisms of chromosome segregation and aneuploidies

from advanced genomics and time-lapse imaging. Hum Reprod Update 2017;23:706-22.
29. Duncan FE, Hornick JE, Lampson MA, Schultz RM, Shea LD, Woodruff TK. Chromosome cohesion decreases in human eggs with advanced maternal age. Aging Cell 2012;11:1121-4.
30. Repokari L, Punamäki RL, Unkila-Kallio L, Vilska S, Poikkeus P, Sinkkonen J, *et al*. Infertility treatment and marital relationships: A 1-year prospective study among successfully treated ART couples and their controls. Hum Reprod 2007;22:1481-91.
31. Zenzes MT, Reed TE, Casper RF. Effects of cigarette smoking and age on the maturation of human oocytes. Hum Reprod 1997;12:1736-41.
32. Chen HL, Copperman AB, Grunfeld L, Sandler B, Bustillo M, Gordon JW. Failed fertilization *in vitro*: Second day micromanipulation of oocytes versus reinsemination. Fertil Steril 1995;63:1337-40.
33. Nicoli A, Capodanno F, Moscato L, Rondini I, Villani MT, Tuzio A, *et al*. Analysis of pronuclear zygote configurations in 459 clinical pregnancies obtained with assisted reproductive technique procedures. Reprod Biol Endocrinol 2010;8:77.
34. Balasch J, Fábregues F, Jové IC, Carmona F, Vanrell JA. Infertility factors and pregnancy outcome in women above age 35. Gynecol Endocrinol 1992;6:31-5.

Original Article

Precaval Right Renal Artery – A Path Less Traveled

C. S. Ramesh Babu, Vinay Sharma, Arjun Kumar[1], Om Prakash Gupta[2]

Department of Anatomy, Muzaffarnagar Medical College, Muzaffarnagar, [1]Department of Anatomy, Ajay Sangaal Institute of Medical Sciences and Research, Shamli, [2]Dr. O.P. Gupta Imaging Center, Meerut, Uttar Pradesh, India

Abstract

Introduction: A Thorough understanding of normal and variant anatomy of the kidneys and renal and retroperitoneal vasculature is most essential for the successful outcome of laparoscopic, robotic, urological, oncogynecological, endovascular, and other interventional procedures. One of the important factors that affects the selection of a renal donor is the presence of multiple renal vessels. Nearly one-third of the population exhibits the presence of supernumerary or accessory renal arteries, and inadvertent damage to such an artery results in segmental renal infarction. **Aim:** Although a lot of attention was paid to analyze the prevalence of accessory right and left renal arteries, scant attention has been given to the study of a surgically important variant of "precaval" right renal artery (RRA) passing anterior to the inferior vena cava. The present study aims to analyze the prevalence of the precaval RRA (PRRA). **Study Design:** The present retrospective study was designed to analyze multidetector computed tomographic scans of 732 subjects for the presence of PRRAs and any other associated renal anomalies. **Results:** The present study detected 37 PRRAs in 34 cases with an incidence of 4.64%. One PRRA was seen in 32 subjects, two in one and three in one case. More commonly, the right inferior polar arteries had a precaval course, and no gender difference was noted. The presence of associated anomalies such as horseshoe kidney, crossed renal ectopia, duplicated pelvicalyceal system, and congenital anomalies of the left renal vein was observed. **Conclusion:** Preoperative contrast-enhanced computed tomography clearly depicts PRRAs and provides a road map for the successful accomplishment of retroperitoneal surgeries.

Keywords: *Accessory hilar artery, accessory renal arteries, contrast-enhanced computed tomography, inferior polar artery, precaval right renal artery, right kidney, supernumerary renal arteries*

Introduction

Normally, each kidney is nourished by a single renal artery arising as a lateral branch of the abdominal aorta just below the origin of the superior mesenteric artery. The right renal artery (RRA) passes posterior to the inferior vena cava (IVC) (retrocaval course), whereas the left renal artery (LRA) courses posterior to the left renal vein (LRV). A recent systematic review with meta-analysis estimated the pooled prevalence of typical single renal arteries bilaterally as 78.92% and that of accessory renal arteries as 21.10%.[1] The accessory renal arteries are designated as superior polar, accessory hilar, and inferior polar. Frequently, lower origin inferior polar arteries have an oblique course and cross the ureter and are believed to be one of the factors responsible for hydronephrosis caused by compression of the ureter. Such low origin accessory RRAs (accessory hilar and inferior polar) infrequently cross the IVC anteriorly instead of posteriorly and are named as "precaval" RRAs.[2-4] Extremely rarely, the single main RRA can also have a "precaval" course as suggested by sporadic case reports.[5]

The presence of a crossing artery anterior to IVC can be misinterpreted as the right gonadal artery, colic branches of the superior mesenteric, and can be damaged inadvertently during laparoscopic retroperitoneal surgeries, such as para-aortic lymph node clearance, where the precaval accessory RRA was mistaken as a feeder supplying enlarged lymph nodes, resulting in renal infarction.[6] Preoperative assessment of the presence of renal vascular variants, such as precaval RRA (PRRA) and other anomalies, presents a road map for the surgeon to successfully accomplish minimally invasive retroperitoneal surgeries. The present, retrospective, multidetector computed tomography (MDCT) study was conducted to assess the prevalence of PRRAs and to increase the awareness of this rare but important arterial variant.

How to cite this article: Babu CS, Sharma V, Kumar A, Gupta OP. Precaval right renal artery – A path less traveled. J Anat Soc India 2025;74:343-8.

Article Info

Received: 01 October 2025
Revised: 12 November 2025
Accepted: 23 November 2025
Available online: 31 December 2025

Address for correspondence:
Prof. C. S. Ramesh Babu, Department of Anatomy, Muzaffarnagar Medical College, Muzaffarnagar, Uttar Pradesh, India.
E-mail: csrameshb@gmail.com

Access this article online

Website: https://journals.lww.com/joai
DOI: 10.4103/jasi.jasi_154_25
Quick Response Code:

Materials and Methods

The present study was carried out by retrospectively analyzing MDCT scans of the abdomen and pelvis of 732 patients (males 374:females 368) from the archives of a single imaging center for the major branches of the abdominal aorta. The institutional ethics committee approval was granted vide letter no. MMC/IEC/2024/178 dated November 18, 2014. The patients underwent contrast-enhanced computed tomography (CT) scanning for suspected abdominal and pelvic pathologies, and the imaging center routinely obtains written informed consent from all patients before scanning. The scanning was done by a 64-channel MDCT scanner (GE Optima-60), and 85–100 ml of nonionic contrast (Omnipaque 300 mg I/ml) medium was injected intravenously at a rate of 5 ml/s. Scans obtained from the diaphragm to the upper part of the thigh were analyzed in a separate work station (AW Volume Share 4.5) with multiplanar reformatting, and volume rendered and maximum intensity projection images were obtained.

Results

Thirty-four patients (17 males and 17 females) had a total of 37 PRRAs with an estimated prevalence of 4.64%. One PRRA was noted in 32 patients (main RRA – 1, accessory hilar – 12, and inferior polar – 19), two arteries (one hilar and one inferior polar) in one male, and three arteries (one main, two accessory hilar) in a female patient. Normal RRA issues from the lateral aspect of the abdominal aorta and passes to the right posterior to IVC (retrocaval), whereas PRRA arises from the anterior/anterolateral aspect of the aorta and passes anterior to IVC [Figures 1 and 2].

We have also observed associated renal positional and fusion anomalies. Horseshoe kidney with PRRA was detected in five cases [Figure 3]. Crossed renal ectopia with fusion in one case and without fusion in one case was noted [Figures 4 and 5], both cases having PRRA. In one case, a rare association of right renal ectopia with absent left renal fossa was found with PRRA [Figure 6]. In another case, an ectopic right kidney with a duplicated pelvicalyceal system with a single ureter was noted, supplied by a PRRA. Incidentally, the left renal fossa was empty [Figure 7]. LRV anomalies in the form of circumaortic LRV in one case and retroaortic LRV in four cases were noted, associated with PRRA [Figure 8].

Discussion

A wide array of published literature examined the occurrence of numerical variations, level of origin, mode of entry, and prehilar branching pattern of renal arteries by cadaveric, surgical, and radiological methods, but less attention was paid to the normal and variant course and relations of renal vessels. One such rarely recognized and reported variant is the course of RRA passing anterior to IVC (precaval course) to reach the hilum. In their cadaveric study on 200 cadavers, Anson *et al*. illustrated a case of the main RRA passing anterior to the IVC.[7] Later, Pick and Anson reported four cases of "precaval" RRAs in their illustrations, and all four cases had multiple RRAs.[2] The reported prevalence of PRRAs in the published literature ranges from 0.5% to 12.0%, as given in Table 1.

Although in the present study, no gender difference was noted in the presence of PRRA, some earlier studies have mentioned that PRRAs occur more frequently in males than in females.[9,14,16] Yeh *et al*. noted in their prospective study of 3200 subjects, 23 males and 16 females (total 39/3200 cases, 1.2%) presenting PRRA.[9] Bouali *et al*. observed PRRAs in 8 males and 3 females (total 11/120).[14] Similarly, Babu *et al*. observed PRRAs in 13 males and 7 females (total 20/225) and also noted gender difference in published single case reports (11 males versus 5 females) thus far.[16] No gender difference was seen in the present study, probably due to the inclusion of nearly an equal

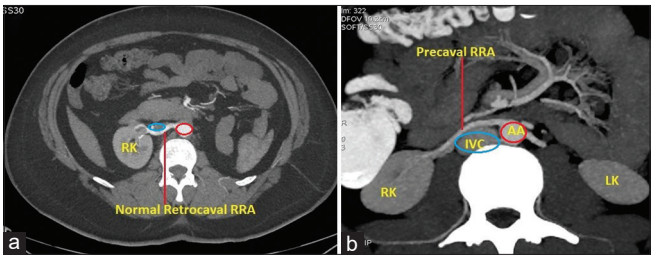

Figure 1: Axial images showing (a) normal retrocaval course of an accessory hilar right renal artery and (b) showing a variant precaval course of an inferior polar artery. AA: Abdominal aorta (red circle), IVC: Inferior vena cava (blue circle), RK: Right kidney, LK: Left kidney, RRA: Right renal artery

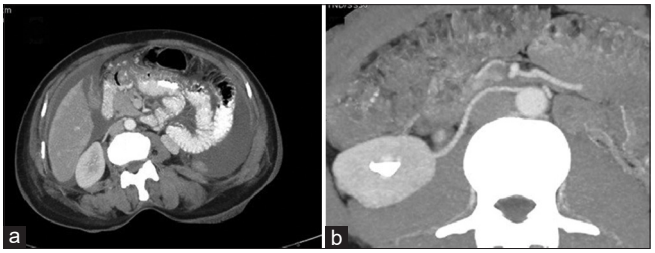

Figure 2: Axial images. (a) Precaval inferior polar right renal artery. (b) Precaval accessory hilar right renal artery

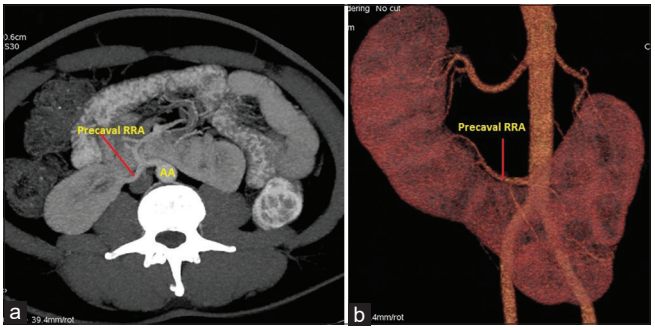

Figure 3: (a) Axial image and (b) volume rendered image showing a precaval right renal artery supplying both moieties of the horseshoe kidney in a male. AA: Abdominal aorta, RRA: Right renal artery

Table 1: Prevalence and nature of precaval right renal artery

Name of author and year	Modality of study	Total cases	Number of cases with PRRA (%)	Nature of PRRAs
Anson *et al*., 1936[7]	Cadaveric	200	1 (0.5)	Single main
Pick and Anson, 1940[2]	Cadaveric	215	4 (1.86)	5 arteries 4 accessory hilar 1 inferior polar
Petit *et al*., 1997[3]	CECT/USG	380	3 (0.78)	Main single
Meng *et al*., 2002[8]	Intraoperative-CT	500	3 (0.6)	Inferior polar
Yeh *et al*., 2004[9]	Spiral CT	186 (Retro) 3200 (Prosp)	9 (4.83) 39 (1.2)	52 PRRAs in 48 cases 4 main, 48 accessory
Holden *et al*., 2005[10]	MDCT Live donors	100	1 (1.0)	Single main RRA
Holt *et al*., 2007[11]	Intraoperative	278 (with testicular tumors)	4 (1.44)	NA
Chai *et al*., 2008[12]	Live donors	153	1 (0.65)	
Gupta *et al*., 2011[4]	Cadaveric	50	3 (6.0)	2 dominant, 2 accessory. One case, single dominant artery
Apisarnthanarak *et al*., 2012[13]	CT A renal donors	65	3 (4.6)	1 single dominant 2 accessory
Bouali *et al*., 2012[14]	Spiral CT	120	11 (9.17)	1 both dominant and accessory; 10 lower polar
Srivastava *et al*., 2013[15]	MDCT	73	4 (5.48)	1 single dominant, 1 both dominant and accessory, 2 lower polar
Babu *et al*., 2014[16]	MDCT	225	20 (8.8)	
Famurewa *et al*., 2018[17]	CT	200	9 (4.5)	
Ciner *et al*., 2021[18]	MDCT	550	3 (0.6)	
Mihaylova *et al*., 2023[19]	MDCT	561	49 (6.9)	3 main 46 accessory
Damen *et al*., 2025[20]	CT angio	200	24 (12.0)	
Present study 2025	MDCT	732	34 (4.64)	1 single main RRA

PRRA: Precaval right renal arteries, CT: Computed tomography, NA: Not available, MDCT: Multidetector computerized tomography, RRA: Right renal artery, CECT: Contrast-enhanced CT, USG: Ultrasonography

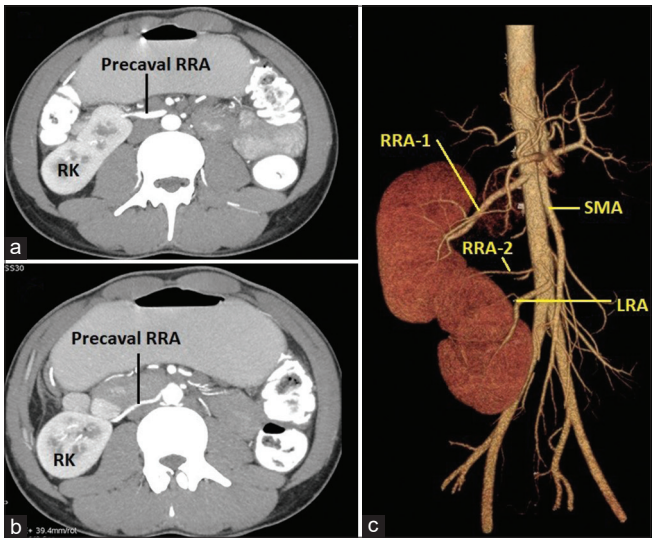

Figure 4: (a and b) Axial images; (c) volume rendered (VR) image. A case of crossed renal ectopia with fusion in a male. The orthotopically located right kidney is supplied by a main (right renal artery [RRA]-1) and an accessory RRA (RRA-2), both having a precaval course. In (c) VR image showing a crossed ectopic left kidney fusing with the lower pole of the right kidney, with the hilum facing anterolaterally. The hilum of the right kidney is facing medially. Both main (RRA-1) and accessory (RRA-2) were having precaval course. SMA: Superior mesenteric artery, LRA: Left renal artery, RK: Right kidney, RRA: Right renal artery

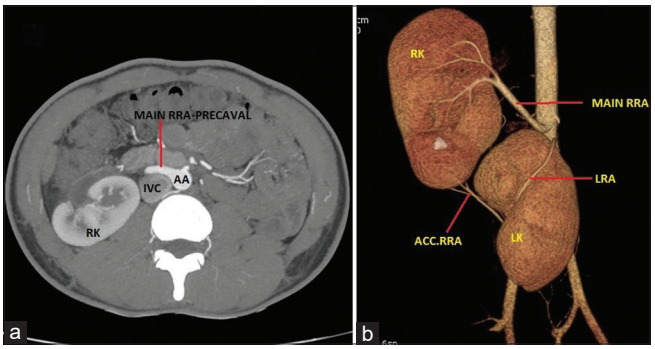

Figure 5: (a) Axial image showing the main right renal artery having precaval course. (b) Volume rendered image depicting crossed unfused left renal ectopia with anterolaterally facing right hilum and posterolaterally directed left hilum. Acc.RRA arises from the right common iliac artery and enters the lower pole of the right kidney. RRA: Right renal artery, ACC.RRA: Accessory RRA, RK: Right kidney, LRA: Left renal artery, IVC: Inferior vena cava, LK: Left kidney, AA: Abdominal aorta

number of males and females (374 males vs. 358 females; total 732 cases).

Precaval course of single main RRA is extremely rare, and about 15 cases were reported in the literature, and some of the reported cases are included in Table 1.[3,4,9,10,13,15,16,19] In addition, Lee *et al*., Pai *et al*. (2020), Al-Sharif *et al*., Farahzadi *et al*., and Schröder *et al*., have also reported a

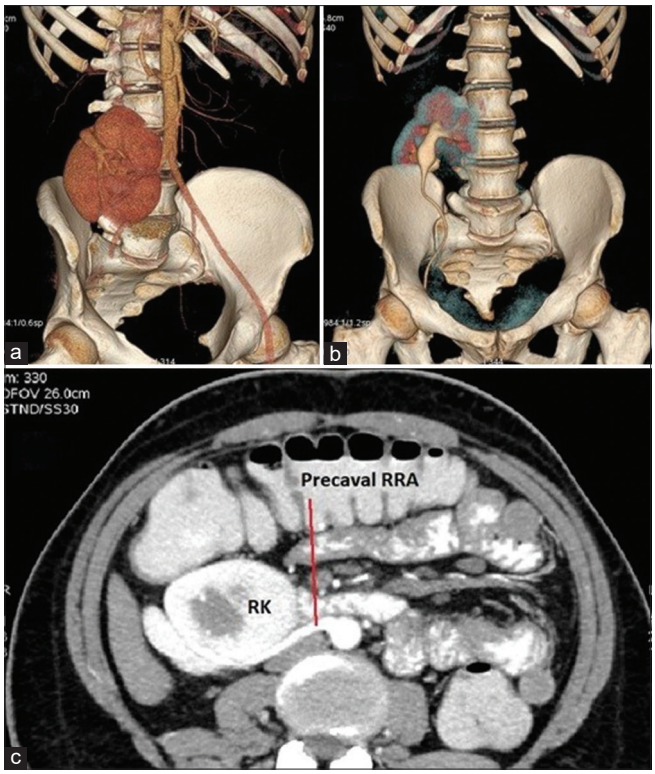

Figure 6: (a and b) Volume rendered images showing right renal ectopia with anteriorly positioned hilum with renal vessels passing posterior to the right kidney and then winding round to reach anteriorly placed hilum. (b) Urogram showing only the ectopic right kidney and absence of the left kidney. (c) Axial image showing a single main right renal artery having a precaval course and coursing posterior to the ectopic right kidney to reach the hilum. RRA: Right renal artery, RK: Right kidney

precaval course of single main RRA.[21-25] Radolinski *et al*. successfully performed right renal donor nephrectomy in the presence of a single main PRRA and suggested that the presence of a PRRA does not preclude the selection of the right kidney for transplantation.[5] Modi *et al*. have also reported successful donor nephrectomy of the right kidney with the presence of two RRAs, one precaval and one postcaval.[26] More recently, Takahashi *et al*. reported safe performance of robot-assisted partial nephrectomy in a 71-year-old woman with renal cancer aided by preoperative CT imaging revealing the anomalous course of RRA.[27] Awareness of the presence of such a rare variant by preoperative radiological studies will ensure a successful outcome of retroperitoneal surgeries.

Surgical, radiological, and cadaveric single case reports have also been published, and Babu *et al*. listed them in their article.[16] In addition, Bayazit *et al*., Raheem *et al*., Deshpande *et al*., Chakraborty *et al*., and Shakthi Kumar and Chitra have all reported the presence of RRAs passing anterior to IVC.[28-32]

Okamoto *et al*. analyzed the relationship of supernumerary right and LRAs originating from the aorta below the origin of the main renal arteries with the ureter and renal pelvis in 270 Japanese cadavers.[33] They classified them

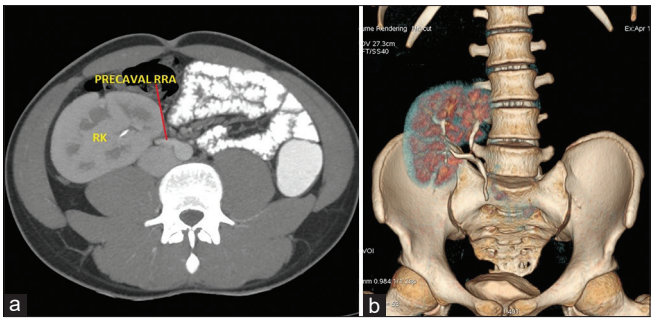

Figure 7: (a) Axial image presenting a precaval right renal artery supplying the ectopic right kidney. (b) Volume rendered urogram showing duplicated pelvicalyceal system. The left kidney was absent. RRA: Right renal artery, RK: Right kidney

into two types – type 1 arising above the level of origin of inferior mesenteric artery (IMA) and crossing the ureter anteriorly (preureteral) and type 2 arising below the origin of IMA and crossing the ureter posteriorly (postureteral). Further, type I right inferior supernumerary arteries were subdivided into type 1-a preureteral but having a normal retrocaval course and type 1-b preureteral but having an anomalous precaval course. All type 2 right inferior supernumerary arteries had a precaval course. Infrequently, on both sides, type 1 arteries give rise to gonadal branches, and type 2 arteries give rise to ureteral branches. Overall, they identified 18 inferior supernumerary RRAs having precaval course (18/270–6.6%).[33]

The embryological basis of the precaval course of RRA is ill understood, and two different theories are proposed. Hollinshead suggested that precaval course of low origin RRA was due to the development of the caudal part of IVC from the supracardinal system (located dorsal to the aorta) in contrast to higher origin RRA passing posterior to IVC was due to the development of IVC from the subcardinal vein (ventrally placed system).[34] In contrast to this view, Meng *et al*. suggested that PRRAs represent a persistent caudal set of mesonephric arteries and are formed after the development of IVC by the 8th week but before the descent of gonads, which begin during the 9th week of gestation.[8] However, none of the two theories fully explains the presence of a precaval course of the main as well as accessory renal arteries. Inferiorly positioned PRRA exhibits a variable relationship with right gonadal vessels and right ureter passing both anteriorly and sometimes posteriorly. Damen *et al*. detected a case of thoracic origin of RRA having a precaval course to reach the renal hilum, and this variant cannot be explained by the above two theories.[20]

A thorough understanding of the vascular anatomy of the retroperitoneal region and their variations is crucial for successful performance of minimally invasive laparoscopic and robotic surgeries, urogyneocological and oncological surgeries, endovascular and interventional procedures, retroperitoneal para-aortic lymph node dissection, and renal transplant surgeries.

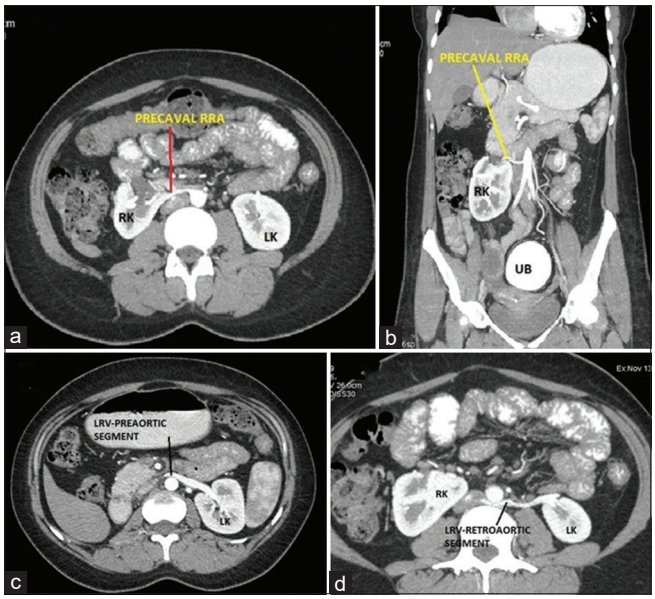

Figure 8: (a) Axial and (b) coronal image showing the precaval course of an accessory hilar artery. This female patient also had a circumaortic left renal vein. (c and d) Axial images showing the preaortic segment (c) and retroaortic segment (d) of the left renal vein. RRA: Right renal artery, RK: Right kidney, LK: Left kidney, LRV: Left renal vein, UB: Urinary bladder

Limitations of the study

One of the limitations was the retrospective nature of the study. The study was not designed to note the level of origin of the PRRAs, their relationship with the gonadal vessels, the ureter, and fine branches from them. Future studies should be planned to include these aspects of PRRAs and include to study the relationship of the precaval hilar arteries with the renal vein at the hilum.

Conclusion

PRRA, though less investigated, is an important variant to be studied in more detail, especially its relationship with gonadal vessels and renal pelvis and ureter. MDCT offers a comprehensive anatomical detail of the retroperitoneal region for critical surgical planning.

Financial support and sponsorship

Nil.

Conflicts of interest

There are no conflicts of interest.

References

1. Triantafyllou G, Paschopoulos I, Węgiel A, Olewnik Ł, Tsakotos G, Zielinska N, *et al*. The accessory renal arteries: A systematic review with meta-analysis. Clin Anat 2025;38:660-72.
2. Pick JW, Anson BJ. The renal vascular pedicle: An anatomical study of 430 body halves. J Urol 1940;4:411-34.
3. Petit P, Chagnaud C, Champsaur P, Faure F. Precaval right renal artery: Have you seen this? Am J Roentgenol 1997;169:317-8.
4. Gupta A, Gupta R, Singhal R. Precaval right renal artery: A cadaveric study. Incidence and clinical implications. Int J Biol Med Res 2011;2:1195-7.
5. Radolinski B, Diner EK, Ghasemian SR. Precaval right renal artery during laparoscopic donor nephrectomy. Transplantation 2006;82:1554-5.
6. Eitan R, Abu-Rustum NR, Walker JL, Barakat RR. Ligation of an anatomic variant of renal vasculature during laparoscopic periaortic lymph node dissection: A cause of postoperative renal infarction. Gynecol Oncol 2003;91:416-20.
7. Anson BJ, Richardson GA, Minear WL. Variations in the number and arrangement of renal vessles: A study of the blood supply of 400 kidneys. J Urol 1936;36:211-9.
8. Meng MV, Yeh BM, Breiman RS, Schwartz BF, Coakley FV, Stoller ML. Precaval right renal artery: Description and embryologic origin. Urology 2002;60:402-5.
9. Yeh BM, Coakley FV, Meng MV, Breiman RS, Stoller ML. Precaval right renal arteries: Prevalence and morphologic associations at spiral CT. Radiology 2004;230:429-33.
10. Holden A, Smith A, Dukes P, Pilmore H, Yasutomi M. Assessment of 100 live potential renal donors for laparoscopic nephrectomy with multi-detector row helical CT. Radiology 2005;237:973-80.
11. Holt PJ, Adshead JM, Filiadis I, Christmas TJ. Retroperitoneal anomalies in men with testicular germ cell tumours. BJU Int 2007;99:344-6.
12. Chai JW, Lee W, Yin YH, Jae HJ, Chung JW, Kim HH, *et al.* CT angiography for living kidney donors: Accuracy, cause of misinterpretation and prevalence of variation. Korean J Radiol 2008;9:333-9.
13. Apisarnthanarak P, Suvannarerg V, Muangsomboon K, Taweemonkongsap T, Hargrove NS. Renal vascular variants in living related renal donors: Evaluation with CT angiography. J Med Assoc Thai 2012;95:941-8.
14. Bouali O, Labarre D, Molinier F, Lopez R, Benouaich V, Lauwers F, *et al.* Anatomic variations of the renal vessels: Focus on the precaval right renal artery. Surg Radiol Anat 2012;34:441-6.
15. Srivastava S, Kumar I, Babu CS, Gupta KK, Gupta OP. Clinical insight into the precaval right renal artery: A multidetector row computed tomography angiographic study. ISRN Anat 2013;2013:250950.
16. Babu CS, Srivastava S, Gupta KK, Gupta OP. Precaval right renal artery: Is it more common? Int J Med Health Sci 2014;3:54-61.
17. Famurewa OC, Asaleye CM, Ibitoye BO, Ayoola OO, Aderibigbe AS, Badmus TA. Variations of renal vascular anatomy in a Nigerian population: A computerized tomography studys. Niger J Clin Pract 2018;21:840-6.
18. Ciner M, Karacan A, Karacan K. Evaluation of renal vascular variations with multi-section computerized tomography angiography. Int J Acad Med Pharm 2021;3:229-33.
19. Mihaylova E, Groudeva V, Nedevska M. Multidetector computed tomography angiography study of the renal arterial vasculature anatomy and its variations in a Bulgarian adult population. Surg Radiol Anat 2023;45:289-96.
20. Damen NS, Jianu AM, Rusu MC. Anatomical study and classification of the precaval right renal arteries with implications for retroperitoneal surgery. Bratisl Med J 2025;126:436-48.
21. Kim YH, Nam DH, Kim IY, *et al*. Incidental finding of a precaval right renal artery on CT: A case report. J Korean Radiol Soc 2005;52:351-3.
22. Pai E, Kumar T. Solitary precaval right renal artery. ANZ J Surg 2020;90:623-4.
23. Elamin NO, Almasaad JM, Elamin AY, *et al*. Solitary precaval right renal artery: A cadaveric case report and review. Med Sci 2021;25:347-52.

24. Farahzadi A, Mahmoodzadeh H, Gopal N. A solitary precaval right renal artery: A case report. Clin Case Rep 2022;10:e05866.
25. Schröder R, Diener MK, Taran FA. Solitary precaval right renal artery and bilateral double ureter in a patient with high-grade serous ovarian cancer. Arch Gynecol Obstet 2024;309:1107-8.
26. Modi PR, Rizvi SJ, Gupta R, Patel S, Trivedi A. Retroperitoneoscopic right-sided donor nephrectomy with pre- and postcaval renal arteries. Urology 2008;72:672-4.
27. Takahashi S, Takahashi Y, Ichimura Y, Iinuma M. A case of precaval right renal artery. Hinyokika Kiyo 2025;71:281-4.
28. Bayazit M, Göl MK, Zorlutuna Y, Tasdemir O, Bayazit K. Bilateral triple renal arteries in a patient with iliac artery occlusion: A case report. Surg Radiol Anat 1992;14:81-3.
29. Raheem O, Glacken P, O'Brien M, Hickey D, Mohan P. A single male cadaver with multiple renal arteries. Ir J Med Sci 2008;177:265-7.
30. Deshpande SH, Bannur BM, Patil BG. Bilateral multiple renal vessels: A case report. J Clin Diagn Res 2014;8:144-5.
31. Chakraborty S, Pradhan S, Paul M, Majumdar S. Bilateral supernumearary renal arteries in a single cadaver. Int J Anat Var 2016;9:64-6.
32. Shakthi Kumar R, Chitra R. Bilateral accessory renal arteries in a male cadaver of Asian origin. A case report. Ann Clin Anat 2019;1:1005.
33. Okamoto K, Kodama K, Kawai K, Wakebe T, Saiki K, Nagashima S. The inferior supernumerary renal arteries: A classification into three types. Ann Anat 2006;188:49-53.
34. Hollinshead WH, editor. Anatomy for Surgeons- The Thorax, Abdomen and Pelvis. 2nd ed., Vol. 2. New York: Harper and Row Publishers; 1971. p. 533.

Original Article

A Guide to Patellar Implant Design: Radiologic Investigation on Gender and Age-related Morphological Differences and Surgical Characteristics of the Patella

Ali Keles, Ahmet Dursun, Figen Taser

Department of Anatomy, Faculty of Medicine, Karamanoğlu Mehmetbey University, Karaman, Türkiye

Abstract

Background: The morphometry of the patella serves as a critical guide in understanding the biomechanics of the knee joint, the pathophysiology of knee disorders, gender determination, the design of patellar implants, and patellar reconstruction procedures. **Aims and Objectives:** This study aims to collect morphometric data on the patella in the Turkish population and to analyze these findings in relation to gender, laterality, and age. **Materials and Methods:** This retrospective study was conducted on computed tomography images of the knee joints from 426 patellas (141 males, 72 females) aged 20–89. Patellar parameters were measured and compared according to gender and laterality. In addition, three age groups were formed to investigate age-related differences. **Results:** Patellar height (PH), width, thickness, medial facet width, lateral facet width (LFW), and facet thickness were significantly greater in males. In contrast, the patellar medial facet ratio, patellar lateral facet ratio (PLFR), and patellar relative thickness were significantly higher in females. A significant difference in the PLFR was observed between the right and left sides. Furthermore, PH, thickness, and LFW exhibited significant differences across the age groups. **Conclusions:** The findings from this study are expected to prove valuable in procedures such as total knee arthroplasty, patellofemoral arthroplasty, prosthesis design, and enriching local anthropological records.

Keywords: *Computed tomography, knee arthroplasty, patella, patellar facets, patellofemoral joint*

Introduction

The patella, one of the largest sesamoid bones in the human body,[1] begins to develop as a cartilaginous prominence during the 3rd month of gestation. The primary ossification center begins to appear at the center of the patella between the ages of 3 and 6. Ossification is typically complete between the ages of 13 and 16 in males, whereas it occurs earlier in females.[2] The patella develops within the tendon of the quadriceps femoris muscle, acting as a pulley and significantly enhancing the efficiency of the extensor mechanism, enabling to contraction of the quadriceps femoris muscle with 33%–50% greater force.[3]

The patella has two surfaces, three edges and an apex located distally. The posterior surface features a smooth area with an oval articular surface bisected by a vertically oriented ridge, appearing flat. In addition, the patella contains two articular facets – lateral and medial – with the lateral facet typically larger.[4] The patella, positioned at the anterior aspect of the knee joint, frequently experiences trauma due to its protective function. Conditions such as osteoarthritis, fractures, chondromalacia patellae, and idiopathic patellofemoral pain syndrome also commonly affect the patella.[5,6]

Patellar morphometry can be determined using both direct and indirect measurements. Direct measurements involve assessing dry bones, skeletal remains, or intraoperative measurements taken by surgeons with calipers; however, this method is time-consuming and subject to observer variability, which may compromise accuracy.[5,7] In contrast, indirect measurement, which involves radiographic imaging, offers a simple, cost-effective, and noninvasive approach while providing digital data for future reference. Numerous studies have utilized X-ray, computed tomography (CT), and magnetic resonance ımaging (MRI) techniques to evaluate patellar morphometry.[8-11]

How to cite this article: Keles A, Dursun A, Taser F. A guide to patellar implant design: Radiologic investigation on gender and age-related morphological differences and surgical characteristics of the patella. J Anat Soc India 2025;74:349-57.

Article Info

Received: 03 March 2025
Revised: 20 September 2025
Accepted: 23 November 2025
Available online: 31 December 2025

Address for correspondence:
Dr. Ali Keles,
Department of Anatomy, Faculty of Medicine, Karamanoglu Mehmetbey University, Yunus Emre Campus, Karaman, Türkiye.
E-mail: alikeless42@gmail.com

Access this article online

Website: https://journals.lww.com/joai

DOI: 10.4103/jasi.jasi_44_25

Quick Response Code:

Knowledge of patellar morphology and morphometry is essential not only for understanding knee joint biomechanics and the pathophysiology of knee disorders but also for guiding the design of patellar implants.[12,13] Panni *et al*.[14] reported that patellar morphology could also serve as a predisposing factor for patellar instability.

The success of total knee arthroplasty or patellofemoral arthroplasty depends heavily on the appropriate sizing of the patellar implant. Variations in patellar dimensions between genders may influence implant design and its subsequent function. Most knee prostheses for total knee arthroplasty or patellofemoral arthroplasty are designed based on dimensions derived from Caucasian and Western populations.[5,15,16] Given the patella's involvement in various postures such as squatting, sitting, and kneeling, its morphometric properties may undergo changes due to cultural differences in lifestyle. In further support of this, several studies have confirmed ethnic variations in patellar morphometry.[17-20]

Some researchers have utilized the patella for gender determination.[10,21,22] Zhan *et al*.[10] reported that the patella is a crucial bone for gender determination and can be used as an alternative in forensic cases where the skull and pelvis are absent. This study aims to investigate data related to patellar morphometry, which may vary by population and gender, and to address the clinical demand for optimized patellar implant designs. In addition, the study seeks to obtain morphometric data specific to the Turkish population and investigate the variations these data may exhibit based on gender, laterality, and age.

Materials and Methods

This study was conducted retrospectively by screening the 128-slice CT (Revolution EVO; GE Healthcare Japan, Tokyo, Japan) images of knee joints obtained from the picture archiving and communication system of Karaman Training and Research Hospital between January 1 and August 31, 2022. The acquired DICOM images were converted into axial and coronal sections using the RadiAnt DICOM Viewer (Version 2023.1, Medixant Inc., Poznan, Poland), and the measurements were performed.

Patellae from 141 males and 72 females, aged between 20 and 89, were analyzed. Based on the classification of adult development stages by Santrock (2013), three age groups were used in this study (20–39 years, 40–59 years and 60 years and above).[23] Our study was approved by the Clinical Research Ethics Committee of Karamanoglu Mehmetbey University (Approval number: 09-2022/03, October 5, 2022).

Study design

Patients with congenital anomalies related to the knee, tumors, rheumatoid arthritis, severe trauma, surgeries, acute patellar dislocation, patellar fractures, or any history of knee joint infection were excluded from this study. In addition, foreigners residing in this country were not included in the study to make the results accurate and ethnicity-sensitive. The following parameters were measured:

Patellar height (PH): The longest distance between the base and apex of the patella in the coronal section [Figure 1].

Patellar width (PW): The maximum distance between the medial and lateral ends of the patella in the coronal section [Figure 1].

Patellar thickness (PT): The largest distance between the anterior and posterior surfaces of the patella in the axial section [Figure 2].

Patellar facet thickness (FT): The distance from the median line of the patellar articular facet to a line drawn from the posterior of the medial and lateral ends of the patella in the axial section [Figure 2].

Patellar medial facet width (MFW): The distance between the medial edge of the patella and the median line of the articular facet in the axial section [Figure 3].

Patellar lateral facet width (LFW): The distance between the lateral edge of the patella and the median line of the articular facet in the axial section [Figure 3].

Medial facet angle (MFA): The angle between the medial edge of the patella and the median line of the articular facet in the axial section [Figure 4].

Lateral facet angle (LFA): The angle between the lateral edge of the patella and the median line of the articular facet in the axial section [Figure 4].

Patellar angle (PA): The total of MFA and LFA [Figure 4].

Patellar medial facet ratio (PMFR = MFW/PW): The ratio of MFW to PW.

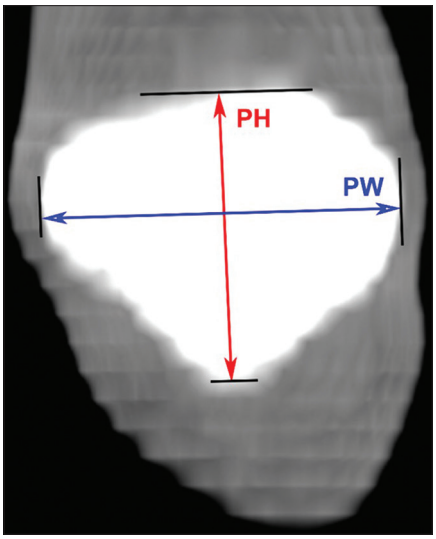

Figure 1: Coronal section of the left patella from a male subject: Patellar height is indicated by the red line, and patellar width is shown by the blue line

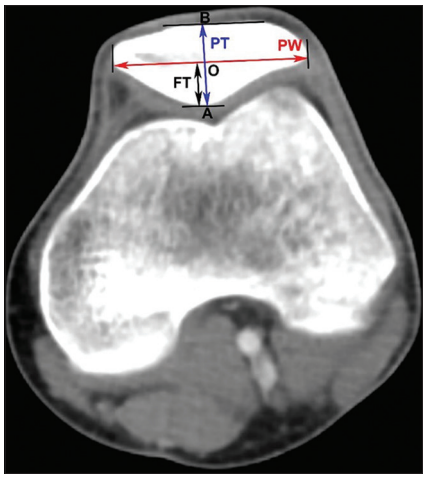

Figure 2: Axial section of the left patella from a male subject: "O" designates the patellar central point, "A" represents the central ridge of the patella, and "B" identifies the anterior point. Patellar width is shown by the red line, patellar thickness by the blue line, and patellar facet thickness by the black line

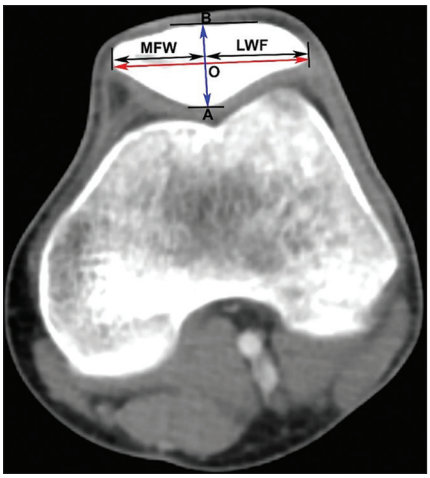

Figure 3: Axial section of the left patella from a male subject: "O" represents the central point of the patella, "A" marks the point of the central ridge, and "B" indicates the anterior point of the patella. Patellar width is denoted by the red line, patellar thickness by the blue line, patellar medial facet width, and patellar lateral facet width are also depicted

Patellar lateral facet ratio (PLFR = LFW/PW): The ratio of LFW to PW.

Patellar relative thickness (PRT = PT/PW): The ratio of PT to PW.

Patellar FT ratio (PFTR = FT/PT): The ratio of FT to PT.

Statistical analysis

Statistical analyses were performed using IBM SPSS Statistics 20.0 (IBM Corp., Armonk, NY, USA). The normal distribution of the data was determined using the Kolmogorov–Smirnov test. Arithmetic means and standard deviations of the parameters were calculated according to gender, laterality, and age groups. Since the data were normally distributed, the independent sample test was applied for comparisons by gender and laterality. One-way analysis of variance was employed for age group comparisons, and *post hoc* analyses were evaluated using the Tukey test. Pearson's correlation test was applied to assess the relationships between parameters. A significance level of $P < 0.05$ was considered statistically significant.

Results

Morphometric data were obtained from 426 patellae. When PH, PW, PT, FT, MFW, LFW, and MFA were compared by gender, the values in males were higher and statistically significant. In females, PMFR, PLFR, and PRT were significantly higher [Table 1]. LFA was found to be higher in females; however, this difference was not statistically significant. Although PA and PFTR were higher in males, no statistically significant difference was found. Only PLFR was significantly higher on the left side when the same parameters were compared by laterality. No statistically significant differences were observed in other parameters [Table 1].

Three age groups were established in our study: 20–39, 40–59, and 60 years and older. The number of individuals in these age groups was 51 (23.9%), 66 (31%), and 96 (45.1%), respectively [Table 2]. In the three-way comparison analysis among the age groups, no differences were found in PW, FT, MFW, MFA, LFA, PA, PMFR, PLFR, PRT, and PFTR parameters. However, statistically significant differences were found in PH, PT, and LFW [Table 2]. *Post hoc* analysis was conducted to determine which group originated the differences. A significant difference in PH was observed between the 40–59 and 60≤ age groups, whereas the difference in PT was between the 20–39 and 40–59 age groups. For the LFW parameter, a significant difference was observed between the 20–39 and 40–59 age groups [Table 2].

Positive correlations were observed between PH and PW, PT, and LFW; between PW and PT, MFW, and LFW; and between PT and MFW and LFW. A highly significant positive correlation was observed between PA and MFA, whereas a notable positive correlation was identified between PA and LFA. FT demonstrated a moderate negative correlation with LFA, MFA, and PA [Table 3].

Discussion

The existence of ethnic and ethnic variations in patellar morphometry has been substantiated by a multitude of studies.[17-19] Morphometric data pertaining to the patella within the Turkish population demonstrate distinct differences compared to other ethnic cohorts. Notably, prior research has identified the highest recorded PH in the South Korean population,[12] with a mean of 44.6 ± 3.7 mm, whereas the lowest PH, measuring 34.94 ± 3.68 mm, was observed in the Chinese population.[11] In our investigation, PH was determined to be 40.66 ± 3.76 mm, falling within an intermediate range. As delineated in Table 4, the PW, MFW, and LFW reached their maximal dimensions within the American population (46.1 mm, 20.5 mm,

and 27.5 mm, respectively).[24] Conversely, the Indian population[6] exhibited the lowest PW and LFW values 36.58 ± 3.0 mm and 21.09 mm, respectively, whereas the minimal MFW (18.67 ± 2.14 mm) was documented in our present study [Table 4]. In terms of PT, our findings suggest that the values observed within the Turkish cohort are lower than those reported for the Chinese,[11] American,[24] and South Korean[12] populations, yet higher than those reported for the Indian population.[6] These findings underscore the considerable influence of ethnic background and methodological discrepancies on patellar morphometric parameters.

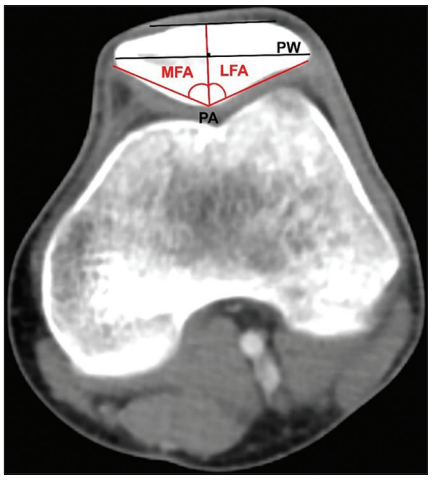

Figure 4: Axial section of the left patella from a male subject: Patellar width is indicated by the black line. The patellar angle, formed by the lateral and medial patellar facets, is measured with the central ridge of the patella as the apex. The angle between the median line of the patellar articular facet and the medial edge represents the patellar medial facet angle, while the angle between the lateral edge and the median line defines the lateral facet angle

In the context of gender-based comparisons, the majority of patellar parameters measured in our study demonstrated statistically significant differences between males and females. Male patellae were found to be significantly larger than those of females across most dimensions. Specifically, the mean values for PH, PW, PT, MFW, and LFW were consistently higher in males compared to females. These findings align with previously published data across a variety of populations, including Spanish,[25] Southern Italian,[26] South Korean,[12] Indian,[5] Chinese,[10] African American,[3] Iranian,[27] American,[24] and Turkish populations[8] [Table 5]. The cumulative evidence strongly suggests that the patella exhibits pronounced sexual dimorphism, reinforcing its utility in gender determination.[7,25,26,28,29]

Furthermore, in our study, the MFA and PA were higher in males, whereas the LFA exhibited higher values in females. However, it is noteworthy that only the difference in MFA reached statistical significance. Muhamed *et al*.,[5] in their MRI-based study of the South Indian population, reported that PA measured 127.23° ± 4.60° in males and 125.01° ± 2.87° in females. Similarly, Sharma *et al*.[30] found that, in the Northwest Indian population, using CT imaging, PA was 122.8° ± 5.65° in males and 116.6° ± 7.31° in females. Li *et al*.[31] documented PA values of 135° ± 5.2° in males and 129.2° ± 4.5° in females within the Chinese population, also employing CT scans. In our study of the Turkish population, PA values were recorded at 132.01° ± 6.88° in males and 130.58° ± 8.92° in females, indicating higher values relative to the Indian population. This variation may be attributable to intrinsic ethnic differences as well as disparities in the imaging techniques and measurement protocols employed.

Table 1: Total and gender and right-left values of patellar measurements

Patellar parameters	Total		Male		Female		*P*	Right		Left		*P*
	n	Mean±SD	*n*	Mean±SD	*n*	Mean±SD		*n*	Mean±SD	*n*	Mean±SD	
Length measurements (mm)												
PH	426	40.66±3.76	282	42.18±3.31	144	37.67±2.61	<0.001	213	40.54±3.79	213	40.77±3.73	0.530
PW	426	43.52±3.95	282	45.24±3.07	144	40.14±3.27	<0.001	213	43.55±3.90	213	43.48±4.01	0.852
PT	426	21.12±1.88	282	21.76±1.80	144	19.87±1.35	<0.001	213	21.07±1.77	213	21.17±1.99	0.610
FT	426	9.51±1.27	282	9.84±1.30	144	8.87±0.91	<0.001	213	9.51±1.19	213	9.51±1.34	0.988
MFW	426	18.67±2.14	282	19.29±2.01	144	17.45±1.85	<0.001	213	18.80±2.13	213	18.54±2.15	0.212
LFW	426	23.85±2.27	282	24.65±2.0	144	22.28±1.94	<0.001	213	23.69±2.28	213	24.0±2.26	0.162
Angle measurements (°)												
MFA	426	61.76±4.78	282	62.17±4.71	144	60.96±4.82	0.014	213	62.03±4.70	213	61.50±4.85	0.250
LFA	426	69.91±3.95	282	69.83±4.05	144	70.06±3.76	0.578	213	70.07±3.85	213	69.74±4.05	0.389
PA	426	131.52±7.65	282	132.01±6.88	144	130.58±8.92	0.069	213	131.81±8.12	213	131.24±7.16	0.448
PMFR	426	0.43±0.04	282	0.43±0.03	144	0.44±0.05	0.014	213	0.43±0.04	213	0.43±0.04	0.139
Ratios												
PLFR	426	0.55±0.04	282	0.54±0.04	144	0.56±0.04	0.005	213	0.54±0.04	213	0.55±0.04	0.022
PRT	426	0.49±0.04	282	0.48±0.03	144	0.50±0.04	<0.001	213	0.49±0.03	213	0.49±0.04	0.392
PFTR	426	0.45±0.09	282	0.46±0.10	144	0.45±0.04	0.332	213	0.45±0.05	213	0.45±0.11	0.861

P<0.05. *n*: Number of patellae, PH: Patellar height, PW: Patellar width, PT: Patellar thickness, MFW: Patellar medial facet width, LFW: Patellar lateral facet width, FT: Patellar facet thickness, PA: Patellar angle, MFA: Medial facet angle, LFA: Lateral facet angle, PMFR: Patellar medial facet ratio, PLFR: Patellar lateral facet ratio, PRT: Patellar relative thickness, PFTR: Patellar facet thickness ratio

Table 2: Mean patellar measurements distribution according to the age groups

Age groups	*n* (%)	PH (mm)	PW (mm)	PT (mm)	FT (mm)	MFW (mm)	LFW (mm)	MFA (°)	LFA (°)	PA (°)	PMFR	PLFR	PRT	PFTR
20–39	102 (23.9)	41.06±3.78	42.94±4.47	20.87±1.81	9.54±1.04	18.44±1.88	23.53±2.50	62.20±4.37	69.74±3.39	131.94±5.38	0.43±0.05	0.55±0.04	0.49±0.04	0.46±0.04
40–59	132 (31)	41.10±4.03	43.99±4.00	21.47±2.02	9.64±1.37	18.88±2.28	24.25±2.40	61.46±5.10	70.30±3.88	131.76±7.11	0.43±0.03	0.55±0.03	0.49±0.03	0.45±0.06
60≤	192 (45.1)	40.01±3.50	43.50±3.59	21.02±1.80	9.40±1.30	18.64±2.18	23.74±2.01	61.74±4.76	69.73±4.27	131.14±8.95	0.43±0.04	0.55±0.03	0.48±0.04	0.45±0.12
P		0.037	0.130	0.031	0.237	0.295	0.038	0.502	0.396	0.639	0.789	0.518	0.479	0.805

n: Number of patellae, PH: Patellar height, PW: Patellar width, PT: Patellar thickness, MFW: Patellar medial facet width, LFW: Patellar lateral facet width, FT: Patellar facet thickness, PA: Patellar angle, MFA: Medial facet angle, LFA: Lateral facet angle, PMFR: Patellar medial facet ratio, PLFR: Patellar lateral facet ratio, PRT: Patellar relative thickness, PFTR: Patellar facet thickness ratio

In the present study, patellar FT was determined to be 9.84 ± 1.30 mm in males and 8.87 ± 0.91 mm in females, with the FT values being statistically significantly higher in males ($P < 0.001$). This discrepancy may be ascribed to the generally larger bone mass observed in males. Compared to the FT values documented by Muhamed *et al*.[5] (12.21 ± 0.77 mm in males and 10.26 ± 0.99 mm in females), our results are notably lower, likely owing to variations in the radiological techniques employed.

The PMFR, defined as the ratio of MFW to PW, was recorded by Yoo *et al*.[12] as 0.43 ± 0.03 in males and 0.44 ± 0.03 in females. In the present study, PMFR was similarly identified as 0.43 ± 0.03 in males and 0.44 ± 0.05 in females, with a statistically significant difference observed between genders ($P = 0.014$).

Yang *et al*.[32] observed that a more dominant lateral articular facet of the patella is associated with an increased risk of patellofemoral cartilage lesions. The prominence of the lateral articular facet may be quantified through the PLFR, calculated as the ratio of LFW to PW. In our study, PLFR was 0.54 ± 0.04 in males and 0.56 ± 0.04 in females, and a statistically significant difference was noted between genders ($P = 0.005$). These data suggest that, within the Turkish population, the lateral articular facet is more prominent in females than in males.

Ceyhan *et al*.[33] highlighted that, between 2010 and 2014, 86% of the 39,866 knee arthroplasties performed in Turkey were undertaken in female patients, with only 14% performed in males. Furthermore, a subsequent study in Turkey revealed that, between 2013 and 2017, women underwent knee arthroplasty procedures at approximately five times the rate of men.[34] Similar trends have been observed internationally; for instance, Robertsson *et al*.[35] noted that, between 1997 and 2007, 64% of knee arthroplasties in Denmark ($n = 38,411$), 68% in Norway ($n = 26,451$), and 62% in Switzerland ($n = 86,952$) were conducted in female patients. In addition, Whitlock *et al*.[36] indicated that, in 2012, two-thirds of the over 650,000 knee arthroplasties performed in the United States involved female patients. Knee arthroplasty replacement in Turkish women is 5 times more common than in men. This rate is higher than in Europe and America. We believe that this is due to the higher PLFR in Turkish women.

Muhamed *et al*.[5] identified the PFTR (PFTR, FT/PT) as 0.60 ± 0.05 in males and 0.63 ± 0.05 in females, revealing a significant gender-based distinction. In contrast, Alsaied Ahmed *et al*.[29] asserted that PFTR exhibited no statistically significant variation across age groups or between genders. Similarly, our study also discerned no significant differences in PFTR with respect to both gender and age groups.

Alsaied Ahmed *et al*.[29] employing MRI data from the Egyptian population, observed that the PRT (PRT, PT/PW)

Table 3: Correlation coefficient between measurements of the patella

	PH	PW	PT	FT	MFW	LFW	MFA	LFA	PA	Age group
PH										
r	1	0.704**	0.630**	0.260**	0.442**	0.567**	0.240**	0.223**	0.305**	−0.109*
P		0.000	0.000	0.000	0.000	0.000	0.000	0.000	0.000	0.025
PW										
r		1	0.667**	0.282**	0.668**	0.737**	0.242**	0.238**	0.297**	0.041
P			0.000	0.000	0.000	0.000	0.000	0.000	0.000	0.397
PT										
r			1	0.331**	0.520**	0.549**	0.059	0.092	0.099*	0.008
P				0.000	0.000	0.000	0.222	0.058	0.040	0.865
FT										
r				1	0.221**	0.255**	−0.311**	−0.280**	−0.328**	−0.054
P					0.000	0.000	0.000	0.000	0.000	0.267
MFW										
r					1	0.358**	0.279**	0.074	0.219**	0.025
P						0.000	0.000	0.126	0.000	0.600
LFW										
r						1	0.129**	0.257**	0.233**	0.016
P							0.008	0.000	0.000	0.735
MFA										
r							1	0.220**	0.766**	−0.029
P								0.000	0.000	0.548
LFA										
r								1	0.647**	−0.013
P									0.000	0.796
PA										
r									1	−0.044
P										0.364
Age group										
r										1
P										

*$P<0.05$, **$P<0.001$, $r=1.00–0.76$ is a very good correlation, $r=0.75–0.51$ is a good correlation, $r=0.50–0.26$ is a moderate correlation, and $r=0.25–0.00$ is a poor correlation. *r*: Pearson correlation coefficient, PH: Patellar Height, PW: Patellar Width, PT: Patellar Thickness, MFW: Patellar Medial Facet Width, LFW: Patellar Lateral Facet Width, FT: Patellar Facet Thickness, PA: Patellar Angle, MFA: Medial facet angle, LFA: Lateral facet angle

Table 4: Comparison of patellar measurements from different populations

Authors	Data source	*n*	Population	PH (mm), mean±SD	PW (mm), mean±SD	PT (mm), mean±SD	MFW (mm), mean±SD	LFW (mm), mean±SD
Baldwin and House (2005)	During total knee arthroplasty	92	American	35.7	46.1	22.6	20.5	27.5
Yoo *et al*. (2007)	MRI	172	South Korean	44.6±3.7	45.8±3.6	22.3±1.9	19.9±1.9	-
Olateju *et al*. (2013)	Cadaveric	92	South African	43.73±3.65	45.14±3.96	-	20.38±3.36	26.02±2.68
Peng *et al*. (2014)	CT	80	Chinese	34.94±3.68	44.13±3.96	22.72±1.81	19.03±2.21	25.10±2.77
Baisakh *et al*. (2021)	Dry bone	60	Indian	36.75±3.04	36.58±3.05	18.39±1.32	18.87	21.09
Present study	CT	426	Turkish	40.66±3.76	43.52±3.95	21.12±1.88	18.67±2.14	23.85±2.27

n: Number of patellae measured, SD: Standard deviation, PH: Patellar Height, PW: Patellar Width, PT: Patellar thickness, MFW: Patellar medial facet width, LFW: Patellar lateral facet width, CT: Computed tomography, MRI: Magnetic resonance imaging

was higher in males, but gender difference significantly was restricted to the 20–30 age cohort. Meanwhile, Muhamed *et al*.,[5] studying the Indian population through MRI, also documented a significantly elevated PRT in males. However, in the current investigation, PRT was determined to be 0.48 ± 0.03 in males and 0.50 ± 0.04 in females. Contrary to the Indian and Egyptian findings, our results indicated that PRT was significantly higher in females ($P < 0.001$), potentially reflecting disparities in radiological techniques.

Taj *et al*.[20] and Doshi *et al*.,[2] in their respective studies of the Indian population, observed no significant differences

Table 5: Comparison of gender patellar measurements from different populations

Authors	Populations	PH (mm), mean±SD			PW (mm), mean±SD			PT (mm), mean±SD			MFW (mm), mean±SD			LFW (mm), mean±SD		
		Male	Female	*P*	Male	Female	*P*	Male	Female	*P*	Male	Female	*P*	Male	Female	*P*
Introna (1998)	Soutth Italians	41.2±2.9	37.0±2.9	-	43.2±2.7	39.4±3.2	-	20.4±1.9	18.2±1.7	-	16.2±3.0	14.6±2.9	-	22.4±2.5	20.5±2.4	-
Baldwin and House (2005)	American	38.6	33.9	<0.001	50.3	43.5	<0.001	23.9	21.8	-	21.1	18.8	-	29.7	25.3	-
Yoo ve *et al.* 2007	South Korean	45.6±3.0	40.0±2.6	<0.001	46.6±3.1	41.7±2.7	<0.001	22.7±1.8	20.4±1.2	<0.001	20.2±1.9	18.4±1.6	<0.001	-	-	-
Olateju *et al.* (2013)	South African	46.94±2.11	41.05±2.18	<0.001	48.03±3.41	42.71±2.52	<0.001	Right: 25.39±1.86 Left: 25.25±1.69	Right: 22.56±1.51 Left: 22.89±1.50	<0.001 <0.001	22.10±3.34	18.94±2.69	<0.001	27.20±2.52	25.04±2.46	<0.001
Peckmann *et al.* (2016)	Spanish	42.9±3.03	37.89±3.0	<0.001	44.62±3.28	40.3±2.94	<0.001	20.34±1.95	18.13±1.78	<0.001	19.19±2.26	17.02±1.8	<0.001	24.83±2.33	22.47±2.14	<0.001
Muhammed *et al.* (2017)	Indian	-	-	-	42.21±2.03	36.07±1.49	<0.001	20.30±0.89	16.24±0.92	<0.001	-	-	-	22.59±1.99	19.47±1.11	<0.001
Peckmann and Fisher (2018)	African American	44.8±3.54	39.75±3.34	<0.001	45.01±3.78	39.79±3.33	<0.001	20.8±2.0	19.16±2.04	<0.001	20.81±2.11	18.01±2.09	<0.001	24.38±2.19	21.51±2.3	<0.001
Teke *et al.* (2018)	Turkish	41.30±3.39	35.84±2.29	<0.001	46.34±3.02	40.35±2.97	<0.001	22.36±1.60	19.88±1.74	<0.001	-	-	-	-	-	-
Zhan *et al.* (2020)	Chinese	43.20±2.8	38.3±2.7	<0.001	46.2±2.6	41.4±2.7	<0.001	23.8±1.8	21.8±1.6	<0.001	-	-	-	-	-	-
Rahmani *et al.* (2020)	Iranian population	39.30±3.13	34.42±3.45	<0.001	48.23±3.60	42.34±2.83	<0.001	21.45±2.19	19.41±1.66	<0.001	-	-	-	-	-	-
Present study	Turkish	42.18±3.31	37.67±2.61	<0.001	45.24±3.07	40.14±3.27	<0.001	21.76±1.80	19.87±1.35	<0.001	19.29±2.01	17.45±1.85	*P*<0.001	24.65±2.0	22.28±1.94	<0.001

PH: Patellar height, PW: Patellar width, PT: Patellar thickness, MFW: Patellar medial facet width, LFW: Patellar lateral facet width, SD: Standard deviation

between right and left patellar measurements. In alignment with these studies, our research also demonstrated no statistically significant difference between the right and left patellae.

Out of the 13 measurement parameters examined, three (PH, PT, and LFW) showed statistically significant differences across age groups. Specifically, PH varied significantly between the 40–59 age group and the 60≤ age group; PT exhibited a significant difference between the 20–39 and 40–59 age groups; and LFW differed significantly between the 20–39 and 40–59 age groups. Alsaied Ahmed *et al*.,[29] who classified the Egyptian population into four age groups (20–30, 31–40, 41–50, and >50), reported statistically meaningful differences in four of the nine parameters assessed (PH, PW, PA, and LFW). Moreover, they highlighted a negative correlation between age and PH, PW, and PLFW parameters. By contrast, our study did not uncover any significant correlations between age groups and measurement parameters, which may be attributed to variations in the age classifications or the populations investigated.

In the cadaveric study conducted by Olateju *et al*.[37] on the South African population, a strong positive correlation was observed between PH and PW. In contrast, Alsaied Ahmed *et al*.[29] reported a negative correlation between PH and PW in their study of the Egyptian population. In the present study, we similarly identified a high positive correlation between PH and PW. To more accurately assess the correlations among patellar parameters, further research involving broader and more diverse populations is necessary.

One limitation of the current study is the inability to account for the dimensions of the articular cartilage, as the patellar measurements were performed using CT imaging. Another constraint is the relatively small sample size compared to other retrospective studies.

Conclusions

This study performed morphometric measurements of the normal patella from CT images specific to the Turkish population. The statistical analyses indicate that males have significantly larger patellae than females. There was no significant difference in measurements between the right and left knees. Given that patellar morphometry varies according to age, gender, and ethnicity, it plays a critical role in ensuring the functional success of arthroplasty by guiding the selection of appropriately sized patellar implants. Thus, our study may serve as a reference for the development of patellar implants tailored to the Turkish population. Higher PLFR in Turkish women could be a reason of more common requirement of knee arthroplasty replacement than men. Furthermore, we recognized that this ratio is higher than the European and USA populations. To better understand this situation, it is necessary to reveal the PLFR rate in other societies and to examine the correlation between this rate and the gender ratio in cases undergoing knee arthroplasty.

Financial support and sponsorship

Nil.

Conflicts of interest

There are no conflicts of interest.

References

1. Loudon JK. Biomechanics and pathomechanics of the patellofemoral joint. Int J Sports Phys Ther 2016;11:820-30.
2. Doshi B, Gautam R, Joshi H, Parmar J. A morphologic and morphometric study of articular facets of patella. Natl J Physiol Pharm Pharmacol 2022;12:8.
3. Peckmann TR, Fisher B. Sex estimation from the patella in an African American population. J Forensic Leg Med 2018;54:1-7.
4. Standring S. Gray's Anatomy: The Anatomical Basis of Clinical Practice. Churchill Livingstone Elsevier; London, UK, 2020.
5. Muhamed R, Saralaya VV, Murlimanju BV, Chettiar GK. *In vivo* magnetic resonance imaging morphometry of the patella bone in South Indian population. Anat Cell Biol 2017;50:99-103.
6. Baisakh P, Kumari S, Das SR, Nayak L, Das SR. Morphometric study of dry human patella with its clinical correlation. Indian J Forensic Med Toxicol 2021;15:430-435.
7. Akhlaghi M, Sheikhazadi A, Naghsh A, Dorvashi G. Identification of sex in Iranian population using patella dimensions. J Forensic Leg Med 2010;17:150-5.
8. Yasar Teke H, Ünlütürk Ö, Günaydin E, Duran S, Özsoy S. Determining gender by taking measurements from magnetic resonance images of the patella. J Forensic Leg Med 2018;58:87-92.
9. Jain R, Kalia RB, Das L. Anthropometric measurements of patella and its clinical implications. Eur J Orthop Surg Traumatol 2019;29:1765-9.
10. Zhan MJ, Li CL, Fan F, Zhang K, Chen YJ, Deng ZH. Estimation of sex based on patella measurements in a contemporary Chinese population using multidetector computed tomography: An automatic measurement method. Leg Med (Tokyo) 2020;47:101778.
11. Shang P, Zhang L, Hou Z, Bai X, Ye X, Xu Z, *et al*. Morphometric measurement of the patella on 3D model reconstructed from CT scan images for the Southern Chinese population. Chin Med J (Engl) 2014;127:96-101.
12. Yoo JH, Yi SR, Kim JH. The geometry of patella and patellar tendon measured on knee MRI. Surg Radiol Anat 2007;29:623-8.
13. Gracitelli GC, Pierami R, Tonelli TA, Falótico GG, Silva FD, Nakama GY, *et al*. Assessment of patellar height measurement methods from digital radiography. Rev Bras Ortop 2012;47:210-3.
14. Panni AS, Cerciello S, Maffulli N, Di Cesare M, Servien E, Neyret P. Patellar shape can be a predisposing factor in patellar instability. Knee Surg Sports Traumatol Arthrosc 2011;19:663-70.
15. Faraj AA, Nevelos AB. Ethnic factors in Perthes disease: A retrospective study among white and Asian population living in the same environment. Acta Orthop Belg 2000;66:255-8.
16. Shah DS, Ghyar R, Ravi B, Hegde C, Shetty V. Morphological measurements of knee joints in Indian population: Comparison to current knee prostheses. Open J Rheumatol Autoimmune Dis 2014;4:75-85.
17. Vaidya SV, Ranawat CS, Aroojis A, Laud NS. Anthropometric measurements to design total knee prostheses for the Indian

population. J Arthroplasty 2000;15:79-85.
18. Uehara K, Kadoya Y, Kobayashi A, Ohashi H, Yamano Y. Anthropometry of the proximal tibia to design a total knee prosthesis for the Japanese population. J Arthroplasty 2002;17:1028-32.
19. Kim TK, Chung BJ, Kang YG, Chang CB, Seong SC. Clinical implications of anthropometric patellar dimensions for TKA in Asians. Clin Orthop Relat Res 2009;467:1007-14.
20. Taj S, Raghunath G, Gurusamy K, Begum Z, Kaveripakkam V, Dharshini P. Morphometric analysis of dry human patella and patellar facets. Cureus 2022;14:e22879.
21. Kemkes-Grottenthaler A. Sex determination by discriminant analysis: An evaluation of the reliability of patella measurements. Forensic Sci Int 2005;147:129-33.
22. Michiue T, Hishmat AM, Oritani S, Miyamoto K, Amin MF, Ishikawa T, *et al*. Virtual computed tomography morphometry of the patella for estimation of sex using postmortem Japanese adult data in forensic identification. Forensic Sci Int 2018;285:206. e1- 206.e6.
23. Santrock J. Life-Span Development. New York: McGraw-Hill; 2013.
24. Baldwin JL, House CK. Anatomic dimensions of the patella measured during total knee arthroplasty. J Arthroplasty 2005;20:250-7.
25. Peckmann TR, Meek S, Dilkie N, Rozendaal A. Determination of sex from the patella in a contemporary Spanish population. J Forensic Leg Med 2016;44:84-91.
26. Introna F Jr., Di Vella G, Campobasso CP. Sex determination by discriminant analysis of patella measurements. Forensic Sci Int 1998;95:39-45.
27. Rahmani E, Mohammadi S, Babahajian A, Rahmani K, Yousefinejad V. Anthropometric characteristics of patella for sex estimation using magnetic resonance images. Forensic Imaging 2020;23:200412.
28. Bidmos MA, Steinberg N, Kuykendall KL. Patella measurements of South African whites as sex assessors. Homo 2005;56:69-74.
29. Alsaied Ahmed D, Tharwat N, Emam NM. Morphometric study of patella and its role in sex determination among Egyptians using magnetic resonance imaging. Med Clin Toxicol 2022;30:1-15.
30. Sharma M, Battan SK, Singh P, Garg M, Sharma T, Jasuja OP. Evaluating the patella bone for sex estimation in Northwest Indian subjects: A radiological study. Forensic Imaging 2024;36:200573.
31. Li M, Ji G, Fan L, Fan CY, Lin W, Yang GM, *et al*. Assessment of patellar morphology in trochlear dysplasia on computed tomography scans. Orthop Surg 2021;13:458-65.
32. Yang B, Tan H, Yang L, Dai G, Guo B. Correlating anatomy and congruence of the patellofemoral joint with cartilage lesions. Orthopedics 2009;32:20.
33. Ceyhan E, Gursoy S, Akkaya M, Ugurlu M, Koksal I, Bozkurt M. Toward the Turkish National Registry System: A prevalence study of total knee arthroplasty in Turkey. J Arthroplasty 2016;31:1878-84.
34. Aslan H. Knee arthroplasties in Turkey: A study from a health management perspective. J Health Inst Turk 2023;6:93-9.
35. Robertsson O, Bizjajeva S, Fenstad AM, Furnes O, Lidgren L, Mehnert F, *et al*. Knee arthroplasty in Denmark, Norway and Sweden. A pilot study from the Nordic Arthroplasty Register Association. Acta Orthop 2010;81:82-9.
36. Whitlock KG, Piponov HI, Shah SH, Wang OJ, Gonzalez MH. Gender role in total knee arthroplasty: A retrospective analysis of perioperative outcomes in US patients. J Arthroplasty 2016;31:2736-40.
37. Olateju OI, Philander I, Bidmos MA. Morphometric analysis of the patella and patellar ligament of South Africans of European ancestry. S Afr J Sci 2013;109:109:1-6. [doi: 10.1590/SAJS.2013/20130069].

Original Article

Sternal Angle Anatomy Redefined by Insights from CT Thorax

Abstract

Purpose: The manubriosternal angle (SA), commonly known as "Angle of Louis" (AoL), has been an important surface landmark in thoracic anatomy. Universally accepted as corresponding to T4–T5 intervertebral disc (IVD) level as well as to major mediastinal landmarks such as tracheal bifurcation (TB), main pulmonary artery (MPA) branching, and 'azygos superior vena cava (A-SVC) junction, and having clinical relevance in applied surgical anatomy, the arrival of modern era cross-sectional imaging modalities such as CT and magnetic resonance imaging have unequivocally demonstrated these thoracic landmarks in live subjects, providing objective real-time data to revisit traditionally held anatomical concepts. **Materials and Methods:** An observational study was done, including 155 adult patients undergoing CT thorax at the department of radiodiagnosis and imaging at our hospital. **Results:** The vertebral level of SA was seen at T4–T5 IVD only in 34.2% patients, whereas in 72.6% patients, it was located between T4 vertebral body (VB) and T4–T5 IVD. In addition, the location of mediastinal structures corresponding to AoL was observed as follows: TB (30.3%), A-SVC junction (38.1%) and MPA branching (9.0%). However, in majority of patients, these structures were seen located between T4–T5 IVD and T5 VB, namely TB (69.6%), A-SVC junction (63.3%), and MPA branching (45.8%). Comparison of our results with similar studies, national and international, provided correlatable inputs. **Conclusion:** It is evident from our study results that significant variation from traditionally held anatomical precepts exists in real-time thoracic anatomy at the level of SA, when live subjects undergo cross-sectional imaging. Notwithstanding the impact of limited sample size, findings of this study highlight the universal need to review and revise traditionally accepted thoracic anatomy landmarks at the AoL.

Keywords: *Angle of Louis, azygos vein–superior vena cava junction, main pulmonary artery branching, sternal angle, tracheal bifurcation*

Namrata Chitrashekhar Kolsur, Raju Augustine George, R. Nagesh, P. J. Rohan, Sujay Umesh Bani

Department of Radiodiagnosis and Imaging, BGS Global Institute of Medical Sciences, Bengaluru, Karnataka, India

Introduction

The sternal angle (SA), popularly known in the medical community as "Angle of Louis" (AoL), has always been considered a reliable surface landmark in thoracic anatomy and stated to be corresponding to level of the T4–T5 intervertebral disc (IVD) posteriorly.[1] Most popularly, the term AoL term is said to have originated from a French surgeon named Pierre Charles Alexandre Louis, but the origin of this term has been a debatable matter because there is no tangible evidence that Louis himself had ever defined it in terms of an anatomical site. It was Essom-Sherrier and Neelon (1989) who stated that Louis gave a panoptic description of the SA, which was found in a review of Louis's work by Edward Goodman in 1910.[2]

Many important anatomic occurrences have been assigned to this level, namely tracheal bifurcation (TB), branching of the main pulmonary artery (MPA) bifurcation, and junction of the azygos vein with the superior vena cava (A-SVC). These were derived from text and images depicted in anatomy textbooks since centuries which in turn were completely based on observations of anatomists during cadaveric dissections.[3] Understanding the relationship of surface anatomy to these vital internal structures is of paramount value while performing clinical assessment of patients, interpretation of thoracic imaging, and planning of interventional/surgical procedures. This study was designed to contribute *in-vivo* thoracic anatomical inputs at the level of the AoL as observed in our subset of Indian adult patients, who underwent CT scans of the thorax for a wide range of clinical indications.

Materials and Methods

Two hundred thirty consecutive adult patients underwent CT thorax in the

How to cite this article: Kolsur NC, George RA, Nagesh R, Rohan PJ, Bani SU. Sternal angle anatomy redefined by insights from CT thorax. J Anat Soc India 2025;74:358-62.

Article Info

Received: 03 March 2025
Revised: 23 November 2025
Accepted: 13 December 2025
Available online: 31 December 2025

Address for correspondence:
Dr. Namrata Chitrashekhar Kolsur,
Godrej United, Panorama C-1602, Opposite Garudacharpalya Metro Station, Mahadevapura, Bengaluru - 560 048, Karnataka, India.
E-mail: nkolsur@gmail.com

Access this article online

Website: https://journals.lww.com/joai

DOI: 10.4103/jasi.jasi_45_25

Quick Response Code:

department of radiodiagnosis at our tertiary care hospital from August 2022 to January 2024. CT thorax was performed on all patients in a SIEMENS SOMATOM MDCT 64 slice scanner at 120 KVp and 280 mAs using helical mode to acquire 5 mm display axial sections. Multiplanar sagittal and coronal reformatted images using standard reconstruction algorithms (using 1 mm recon sections) in mediastinal, lung, and bone windows were obtained [Figures 1-5]. 75 patients were excluded from the study due to evidence of congenital vertebral anomalies, vertebral deformities, major thoracic surgeries, and/or mediastinal shift. The objective imaging findings obtained from the remaining 155 patients formed the database for this observational study.

Results

The 155 patients ranged from 19 to 82 years in age, with a mean of 47.54 ± 15.88 years, of whom 53% were males and 47% were females, giving a reasonably balanced gender and age distribution to our study [Table 1].

For descriptive purposes, assuming T4–T5 IVD to be the central plane corresponding to AoL, the patient database was distributed into three arbitrary levels as depicted in Table 2. Out of 155 participants, SA was commonly seen corresponding to the T4–T5 IVD in 34.2% and at T4 vertebral body (VB) in 28%, with Level 2 accounting overall for 73.5% of the patients. Among the screened mediastinal landmarks, it was observed that TB corresponded to T4–T5 IVD level in only 30.32% and more commonly was seen at T5 VB in 39.4% of subjects, once again with Level 2 accounting for 82.6%. MPA bifurcation corresponded to T4–T5 IVD in only 9% cases, whereas in a larger subset of 36.8% patients, MPA branching was seen at T5 VB level. Level 2 only accounted for 54.2% of patients with MPA branching; instead, it was observed in 81% of patients to be located below the level of SA, ranging from T5 VB up to T7 VB.

The A-SVC junction was noted to occur at T4–T5 IVD in only 38.1% of patients, with the next common levels being T5 VB and T4 VB with 25.2% and 24.5% patients, respectively; Integrated T4–T5 IVD and T5 VB values accounted for 63.3%, and overall, 87.7% patients were within Level 2. A complete range of distribution of all the selected parameters is shown in Table 2.

Discussion

Widespread induction of real-time, cross-sectional modern imaging modalities such as computed tomography (CT) and magnetic resonance imaging (MRI) in clinical practice has opened the opportunity to potentially review and revisit traditionally held concepts in thoracic anatomy. Imaging observations, which are at variance with traditional teachings at the anatomical surface landmark of the AoL, were first reported by Chukwuemeka *et al*. in 1997 based on CT studies of thorax.[4]

Commencing with the basic parameter of SA-Vertebral level correlation, it was observed that the vertebral level of the SA varied widely between T2-T3 IVD and T6-T7

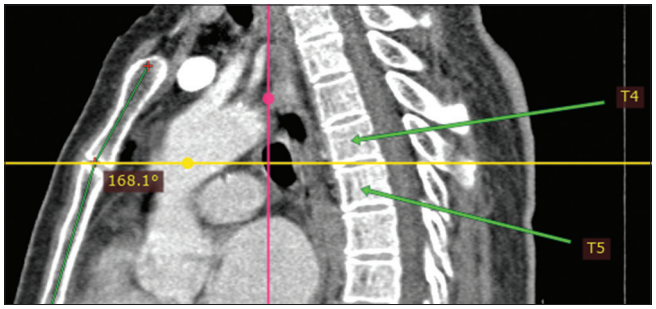

Figure 1: Sternal angle measurement (168.1°) and plane of angle of Louis intersecting at T4–T5 intervertebral disc

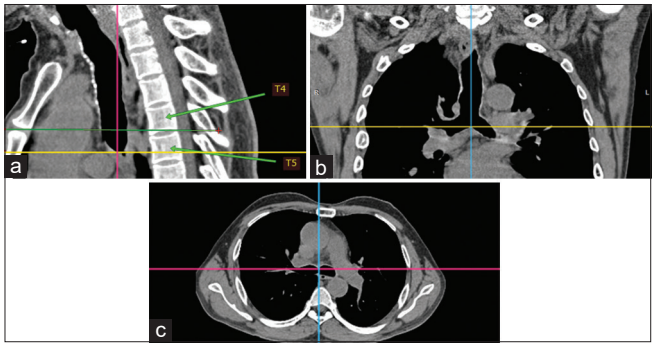

Figure 3: Use of sagittal and coronal reformats for tracheal bifurcation (TB) level assessment: (a) Sagittal reformat showing TB corresponding to T5 vertebral body (pink and yellow lines intersection), line passing sternal angle (green); (b) Coronal reformats showing TB; (c) axial section at level of TB

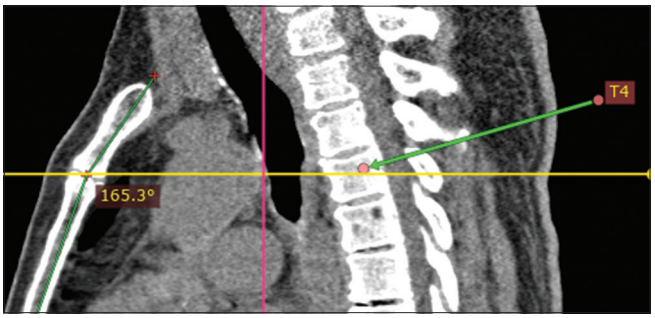

Figure 2: Sternal angle (SA) measurement (165.3°) and SA intersecting at T4 vertebral body

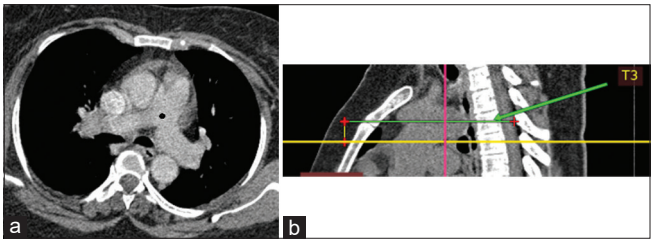

Figure 4: Main pulmonary artery bifurcation. (a) Axial section (marked as black dot); (b) Sagittal reformat: Seen passing through T4 vertebral body (yellow line), line passing through sternal angle (green)

IVD levels [Table 2], but in 73.5% patients, it is seen to be located within Level 2. However, within this subset, the SA correlated precisely with the anatomical description of T4–T5 IVD only in 34.2% patients. In addition, T4 VB was seen to be the next most common level of SA, seen in 44 (28.4%) cases of our study population. Extremely higher and lower levels (T2-T3 IVD and T6-T7 IVD) were seen only in 1.9% of the population, mostly in the elderly. Our observations on the variant vertebral levels of the AoL are in concordance with few other Indian studies [Table 3]. A CT-based study conducted by Garg *et al*.[5] and an MRI-based study by Aggarwal *et al*.[6] showed SA at T4–T5 IVD in 35 subjects (35%, study population: 100) and T4 VB/T4–T5 IVD in 85 subjects (38.8%, study population: 262), respectively. The only contrasting level was reported by Naziya *et al*.[7] on the CT study where T5 VB was found to be the most common in 33 (68%, sample size: 48) patients, whereas our study showed only 17 (11%) cases at this level.

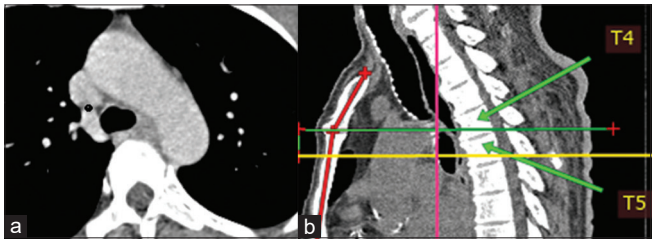

Figure 5: A-SVC junction. (a) Axial section (marked as black dot); (b) Sagittal reformat: Seen passing through T5 vertebral body (yellow line), line passing through sternal angle (green)

Table 1: Demographic details of the study population

Variables	*n* (%)
Gender	
Male	82 (52.9)
Female	73 (47.1)
Age (years)	
<30	29 (18.7)
30–60	88 (56.8)
>60	38 (24.5)

One hundred twenty-eight (82.6%) patients of the study population showed TB to lie within Level 2 as depicted in Table 2. However, on further analysis of data at this level, it was observed that only in 47 (30%) cases, the AoL corresponded exactly to T4–T5 IVD, whereas 61 (39.3%) cases of the study population showed a T5 VB predominance; combination of these two shows that they constitute the majority of the study population, i.e., 108 (70%). In addition, 88 (57%) cases showed TB to lie below the level of T4–T5 IVD. Multiple variations were also observed on comparison with international studies [Table 3]. Findings in our study closely correlate with that of Keough *et al*.[10] done in the South African population, which also showed that in 46 (60%, sample size: 76) cases, the TB occurred below the level of SA. Studies by Mirjalili *et al*.[8] and Shen *et al*.[9] have documented that larger proportions of patients showed TB to be located below the conventional SA level, with 142 cases (in New Zealanders, 93%, sample size: 153) and 91 cases (in the Chinese population, 91%, sample size: 100), respectively [Table 3]. Findings in our study closely correlate with that of Keough *et al*.[10] done in the South African population, which also showed that in 46 cases (60%, sample size: 76) the TB occurred below the level of SA.

It is clearly evident from Table 2 that Level 2 accounted for 84 (54.2%) patients of MPA branching. However, in reality, further review of this level showed that only 14 (9%) cases were at T4–T5 IVD, whereas the larger subset of subjects showed MPA branching at T5 VB (57 in number: 36.8%), suggesting that a composite of these two levels would add up to the highest percentage of study subjects having an MPA branching at and near the SA. Furthermore, in a considerable number of study

Table 2: Sternal angle and related distribution of selected Mediastinal structures

Levels	Structures							
	SA, *n* (%)		TB, *n* (%)		MPA, *n* (%)		A-SVC, *n* (%)	
Level 1								
T2–T3 IVD	23 (14.8)	1 (0.6)		-	2 (1.3)	-	8 (5.2)	-
T3 VB		7 (4.5)		-		-		-
T3–T4 IVD		15 (9.7)		-		2 (1.3)		8 (5.2)
Level 2								
T4 VB	114 (73.5)	44 (28.4)	128 (82.6)	20 (12.9)	84 (54.2)	13 (8.4)	136 (87.7)	38 (24.5)
T4–T5 IVD		53 (34.2)		47 (30.32)		14 (9.0)		59 (38.1)
T5 VB		17 (11.0)		61 (39.35)		57 (36.8)		39 (25.2)
Level 3								
T5–T6 IVD	18 (11.6)	14 (9.0)	27 (17.4)	19 (12.26)	69 (44.5)	32 (20.6)	11 (7.1)	8 (5.2)
T6 VB		2 (1.3)		5 (3.23)		29 (18.7)		2 (1.3)
T6–T7 IVD		2 (1.3)		3 (1.94)		6 (3.9)		-
T7 VB		-		-		2 (1.3)		1 (0.6)

VB: Vertebral body, IVD: Intervertebral disc, MPA: Main pulmonary artery, TB: Tracheal bifurcation, SA: Sternal angle, A-SVC: Azygos-superior vena cava

Table 3: Comparison of cross-sectional imaging anatomy findings at the sternal angle

	Current study	International studies			Indian studies			Anatomical literature	Proposed
		Mirjalili *et al*.[8]	Shen *et al*.[9]	Keough *et al*.[10]	Garg *et al*.[5] (CT)	Naziya *et al*.[7] (CT)	Aggarwal *et al*.[6] (MRI)		
SA	T4/T5 IVD (34.5%) T4 VB (28.4%)	T4 VB and T4/T5 IVD (48%)	T4 VB and T4/5 IVD (51%)	T4 VB (23%)	T4–T5 (35%) T5 (24%)	T5 (68.75%)	T4/T4–5 (38.8%) ↓ SA (58.9%)	T4/5 IVD or IB T4	T4 and T4/5 IVD
TB	T4/T5 (30%) T5 (39.35%) ↓ SA (57%)	T4/T5 (7%) T6 (46%) ↓ SA (93%)	T4–T5 (4%) T5 (40%) or T6 (35%) ↓ SA (91%)	↓ SA (60%)	T5/6 (26%) ↓ SA (46%)	T5 (52.08%)	T4/T4–5 (54.07%) ↓ SA (43.0%)	T4/5 IVD or IB T4	T4/5 IVD and T5 VB
MPA	T4/T5 (9%) T5 (36.8%) ↓ SA (82%)	T4/T5 (4%) T6 (28%) ↓ SA (96%)	T4/T5 (1%) T5/6 or T6 (56%) ↓ SA (97%)	↓ SA (76%)	T5/6 (23%) ↓ SA (73%)	-	-	T4/5 IVD or IB T4	T4/5 IVD and T5 VB
A-SVC	T4/T5 (38.1%) T5 (25.2%) ↓ SA (32%)	T4–T5 (8%) T5 (49%) ↓ SA (87%)	T4–T5 (10%) T5 (47%) ↓ SA (79%)	T4/T5 (55%)	T5 (41%) At SA (38%)	-	-	T4/5 IVD or IB T4	T4/5 IVD and T5 VB

VB: Vertebral body, MPA: Main pulmonary artery, TB: Tracheal bifurcation, SA: Sternal angle, A-SVC: Azygos-superior vena cava, MRI: Magnetic resonance imaging, IVD: Intervertebral disc, ↓ SA: implies below sternal angle

subjects, it was seen below the level of SA, i.e., T5 VB up to T7 VB in 126 (81%) subjects. Observations of the current study are closely concordant with the documentations of MPA branching levels worldwide. Shen *et al*.[9] and Mirjalili *et al*.[8] found even lesser proportions at 1 (1%) and 6 (4%) of their cases, respectively, whose MPA branching was at T4–T5 IVD level, with 97 (97%) subjects and 147 (96%) subjects, respectively, showing branching of MPA below the level of SA. Studies by Garg *et al*.[5] and Keough *et al*.[7] also reported that 73 (73%) cases and 58 (76%) cases respectively in their study population showed MPA branching below the SA [Table 3].

The A-SVC junction was noted to occur at Level 2 in 136 (87.7%) of our patients, with only 59 (38.1%) of them at T4–T5 IVD level. The next most common levels were T5 VB and T4 VB with 39 (25.2%) cases and 28 (24.5%) cases, respectively. Integrated T4–T5 IVD and T5 VB values include 98 (63.3%) cases of the population. In addition, a large proportion of patients were seen to have an A-SVC junction at or below the level of SA in 109 (70.4%) cases. Garg *et al*.[4] also found the A-SVC junction to be located at T4–T5 IVD level in 38 (38%) cases, which mirrors our findings in the current study. However, the most common level in their study was seen to be at T5 VB (41 cases, 41%), whereas T5 VB accounts for only 39 (25.2%) patients in the current study. Similarly, T5 VB was observed to be the most common level in studies by Keough *et al*.[10] and Shen *et al*.[9] with 75 (49%) cases and 47 (47%) cases, respectively. In addition, these studies also showed larger proportions of cases (more than 80%) with A SVC junctions at and below the SA.[8,10]

Observations made in our study confirm that multiple variations exist in the location of mediastinal structures at the level of SA between radiological studies in live patients versus cadaveric anatomy, which could be a result of many factors. First and foremost, respiratory variability would be a contributory factor, as CT thorax is conventionally performed during breath-holding in deep inspiration. Expansion of the chest to various degrees can affect the vertebral levels of the mediastinal structures by altering the dimensions of the thorax. Chest expansion during deep inspiration moves the manubrium–sternal joint in an upward and outward direction, resulting in its correspondence to a higher vertebral level. Concurrently, there is a downward movement of the diaphragm in deep inspiration, affecting the level of the mediastinal structures. Therefore, these movements could serve as an explanation as to why more patients have SA corresponding to the T4 VB than T4–T5 IVD, and mediastinal structures were observed to correspond lower, mainly below the T4–T5 IVD and T5 VB in our study [Table 2]. The absence of thoracic expansion in cadavers would contribute to uniformity in the vertebral levels of SA and mediastinal structures documented in anatomical studies, further reiterating the effect of respiration. Second, the imaging modality used in most of the current literature, including our study, has been centered on CT as the modality for understanding the SA and mediastinal variations. MRI Thorax has also been used in a limited number of studies, which is advantageous not only due to the absence of exposure to ionizing radiation but also because it is done in quiet breathing as opposed to breathhold in deep inspiration in CT thorax. Therefore, this aspect could explain the variation of levels in CT-based

studies as compared to MRI thorax, affecting relative levels of SA and mediastinal structures. Further studies using MRI thorax are recommended as the primary imaging modality to clarify these anatomical concepts in quiet breathing. Third, the sample size of the study for generalizing normal limits for a population involves undertaking studies with larger sample sizes, so that the data collected can be analyzed and extrapolated for the general population. Due to the limited sample size of our study, we would recommend future studies with larger sample sizes so as to further validate the variations of the SA and mediastinal structures.

CONCLUSION

At the commencement of this study, the time honored anatomical concept of the sternal angle was assumed to be correct. However, the analysis of imaging findings in this study and review of existing limited literature on this subject, both national and international, have re-confirmed the existence of multiple variations between live imaging data and cadaveric levels. These findings highlight the need to revise the currently taught anatomical concepts at the level of sternal angle.

Financial support and sponsorship

Nil.

Conflicts of interest

There are no conflicts of interest.

References

1. Last RJ. Thorax and superior mediastinum. In: Sinnatamby CS, editor. Last's Anatomy-Regional and Applied. 12th ed. Edinburgh: Elsevier; 2011. p. 189.
2. Coscione A, Dixon L, Ellis H. The angle of Louis. Eur J Anat 2013;17:190-2.
3. McGregor L. The chest wall, lungs and mediastinum. In: Decker GA, duPlessis DJ, editors. Synopsis of Surgical Anatomy. 12th ed. Bristol: John Wright and Sons; 1986. p. 137-8.
4. Chukwuemeka A, Currie L, Ellis H. CT anatomy of the mediastinal structures at the level of the manubriosternal angle. Clin Anat 1997;10:405-8.
5. Garg S, Gulati A, Aggarwal A, Gupta T, Mirjalili SA, Sahni D. Retrospective analysis of adult thoracic surface anatomy in Indian population using computed tomography scans. J Anat Soc India 2019;68:39-45.
6. Aggarwal R, Sreedhar M, Sheikh RA, Theegala VS. *In-vivo* cross-sectional topography at the sternal angle on MRI. JASI 2020;69:243-6.
7. Naziya SP, Ali AS, Bhuiyan PS. A computerized tomographic study of normal mediastinal anatomy in Indian subjects. Int J Health Sci Res 2014;4:111-6.
8. Mirjalili SA, Hale SJ, Buckenham T, Wilson B, Stringer MD. A reappraisal of adult thoracic surface anatomy. Clin Anat 2012;25:827-34.
9. Shen XH, Su BY, Liu JJ, Zhang GM, Xue HD, Jin ZY, *et al*. A reappraisal of adult thoracic and abdominal surface anatomy via CT scan in Chinese population. Clin Anat 2016;29:165-74.
10. Keough N, Mirjalili SA, Suleman FE, Lockhat ZI, van Schoor A. The thoracic surface anatomy of adult black South Africans: A reappraisal from CT scans. Clin Anat 2016;29:1018-24.

Case Report

Can External Occipital Protrusion Be the Cause of Shoulder Pain?

Abstract

The external occipital protuberance (EOP) can sometimes be felt as a palpable swelling and sometimes as a protrusion extending downward. It is also called an inion hook. EOP bony tubercle can be generally classified into three types: flat form (type 1), crest type (type 2), and protrusion type (type 3). In this report, we present a 32-year-old adult male patient with right shoulder pain. On examination, pain extending from the occipital region to the shoulder was observed. Type 3 EOP protrusion was incidentally detected on X-ray imaging. When "EOP" was searched in PubMed, anatomical and imaging studies were found. It was found to be clinically associated with headache in studies in terms of size and type. We think that this is the first case of EOP protrusion associated with shoulder pain.

Keywords: *External occipital protuberance, inion hook, occipital exostosis, occipital protrusion, occipital tubercle*

Mert Emre Aydın, Aziz Atik[1]

Department of Orthopaedics and Traumatology, Çanakkale Çan Public Hospital, Çanakkale, [1]Department of Surgical Medical Sciences, Faculty of Medicine, Balikesir University, Balikesir, Türkiye

Introduction

The external occipital protuberance (EOP) is an anatomical structure located on the posterior surface of the occipital bone at the level of the upper nuchal line. It is the insertion site of the nuchal ligament and trapezius muscle.[1] It is also called an inion hook. The trapezius muscle arises from the EOP and the medial half of the superior nuchal lines. EOP can be generally classified into three types: flat form (type 1), crest type (type 2), and protrusion type (type 3).[2] In the present study, a cranium was detected in which a bony tubercle was found projecting from the EOP. When "EOP" was searched in PubMed in the last 5 years, anatomical and imaging studies were found. It was found to be clinically associated with headache in studies in terms of size and type. We think that this is the first case of EOP protrusion associated with shoulder pain.

Case Report

We report a 32-year-old young adult male patient. He complained of pain in his right shoulder and radiating from the shoulders to the neck while lying supine and working at a desk for a long time. Sometimes he also had headaches. On physical examination, the range of motion of both shoulder joints was normal. Neurological examination was normal. Neer and Jobe tests were negative. There was tenderness on palpation over the posterior fibers of the trapezius muscle. A pea-sized swelling was palpated on EOP. There was no evidence of discharge, infection, or inflammation. There were no known comorbidities.

X-ray imaging showed no shoulder pathology. No signs of impingement were seen [Figure 1]. On cervical lateral radiography, an exophytic structure was observed in the occipital protuberance, and the distance between the two longest points was measured as 16.4 mm [Figure 2].

A brain computed tomography (CT) was ordered to examine the protrusion in detail and to rule out intracranial pathologies that could cause neurologic symptoms. Cervical CT was ordered to rule out cervical bone pathologies. No tumoral bone pathology such as osteoid osteoma, enchondroma, or traumatic degenerative changes was observed. No acute or chronic intracranial pathology was found in the brain CT, but EOP protrusion was observed. The protrusion had a longer course on the posterior fibers of the right trapezius muscle, extending from its insertion to its origin. The EOP tubercle measured 12.4 mm in length, 26 mm in width, and 11.4 mm in thickness between the two most distal points in the sagittal plane and

How to cite this article: Aydın ME, Atik A. Can external occipital protrusion be the cause of shoulder pain? J Anat Soc India 2025;74:363-5.

Article Info

Received: 07 March 2025
Revised: 13 June 2025
Accepted: 23 November 2025
Available online: 31 December 2025

Address for correspondence:
Dr. Mert Emre Aydin, Istiklal Neighbourhood, Martyr Mustafa Kaya Street No: 169, Çan 17400, Çanakkale, Turkey. E-mail: mertemreaydin9308@gmail.com

Access this article online

Website: https://journals.lww.com/joai

DOI: 10.4103/jasi.jasi_48_25

Quick Response Code:

axial plane, respectively [Figure 3]. Our findings were compatible with a type 3 EOP bone tubercle.[2]

Cervical magnetic resonance imaging (MRI) was ordered for spinal nerve compression and additional pathologies that may cause shoulder pain. No pathology requiring surgical intervention was observed. Shoulder MRI was ordered for a rotator cuff tear and additional pathologies involving the shoulder. No significant pathology was observed except for minimal effusion around the biceps tendon [Figure 4]. In addition, no pathology was observed when evaluated in terms of rheumatologic diseases such as fibromyalgia. Shoulder pain was thought to be due to EOP protrusion.

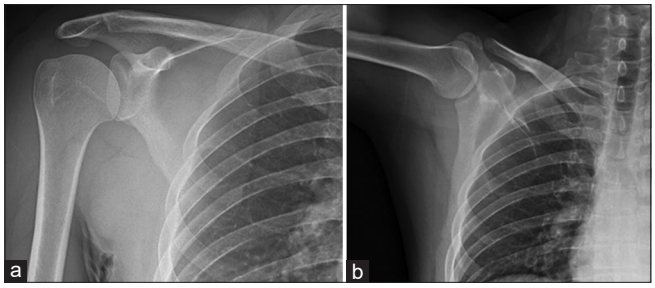

Figure 1: X-ray view of the right shoulder. (a) anterior anatomical position, (b) semiabduction position

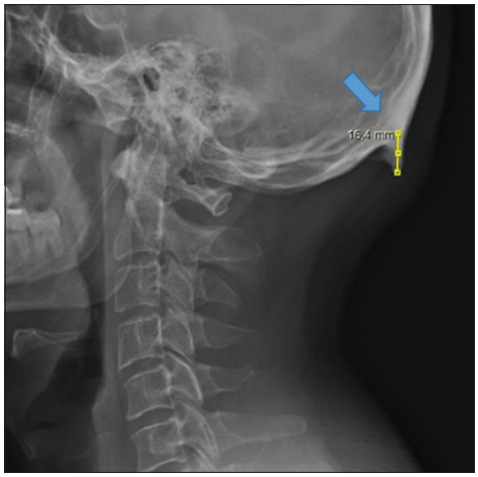

Figure 2: X-ray of the craniocervical lateral view. The tubercle structure in the occipital protrusion is shown with a blue arrow. The distance between the longest two points was measured as 16.4 mm

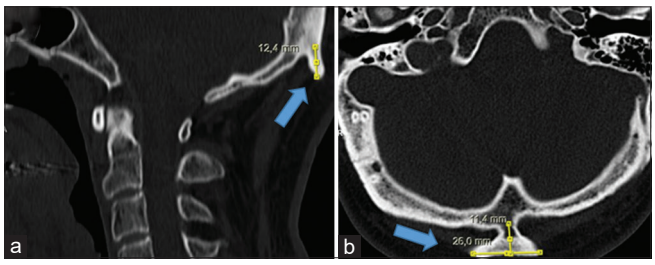

Figure 3: Computed tomography section of the cranium. The tubercle structure in the occipital protrusion is shown with a blue arrows. (a) sagittal section view of the external occipital protuberance (EOP) protrusion measured 12.4 mm in length, (b) axial section view of the EOP protrusion measured 26 mm in width and 11.4 mm in thickness between the two most distal points

The patient was given medical treatment. Oral nonsteroidal anti-inflammatory drug (NSAID, etodolac 500 mg) was administered twice daily, antispasmodic drug (tizanidine 2 mg) twice daily, and locally acting NSAID cream was applied twice daily (2 doses per day). Physiotherapy and rehabilitation were applied to the patient whose complaints regressed but did not completely resolve.

Discussion

In this study, we present the clinical outcome of a bone tubercle protruding from the EOP. This tubercle is an extra bony growth, different from a normal occiput. Therefore, vertical biomechanical movements of the neck can cause occipital headache due to this additional bony growth acting on nearby neurovascular structures. When bone protrusions rub against soft tissues such as ligaments, tendons, nerves, and blood vessels, they can cause wear and tear or pain. The most common locations for these bone protrusions are the shoulders, hands, knees, feet, and obturator foramen.[3] The literature on EOP-related tubercles is limited.

When "inion hook" was searched, one study was found. In this study, the relationship between traumatic occipital spur fracture was investigated.[4]

When "EOP" was searched in PubMed, anatomical, cadaver forensic, and imaging studies were found.[5-7] Clinical studies have focused on headaches.[5,8-11] We say that it can also be the cause of shoulder pain. If this tubercle is not identified, the headache may be misdiagnosed and lead to unnecessary diagnostic surgeries. Therefore, to prompt relevant clinicians for the management and treatment of associated diseases, the study was conducted through this case report. We believe that this is the first EOP tubercle case causing shoulder pain.

There are different opinions about EOP-related bone tubercle formation. There are different opinions that occipital protrusion is more common in young adults and is associated with postural changes (Jacques *et al*. in 2020 and Shahar and Sayers in 2016).[12,13]

Three subtypes were defined by Gülekon and Turgut: flat form (type 1), crest type (type 2), and protrusion type (type 3).[2] EOP protrusion is an anatomical problem that is mostly symptomatic and occurs during adolescence. The authors suggested that there is limited information on the evolving EOP protrusion.[14]

It can usually be treated with analgesia or other rehabilitation methods.[8] In cases that cannot be resolved despite all noninvasive methods, bony correction of the tubercle can be achieved by surgical resection.[8]

Shoulder pain may develop in young patients due to many causes. In cases with persistent shoulder pain in which

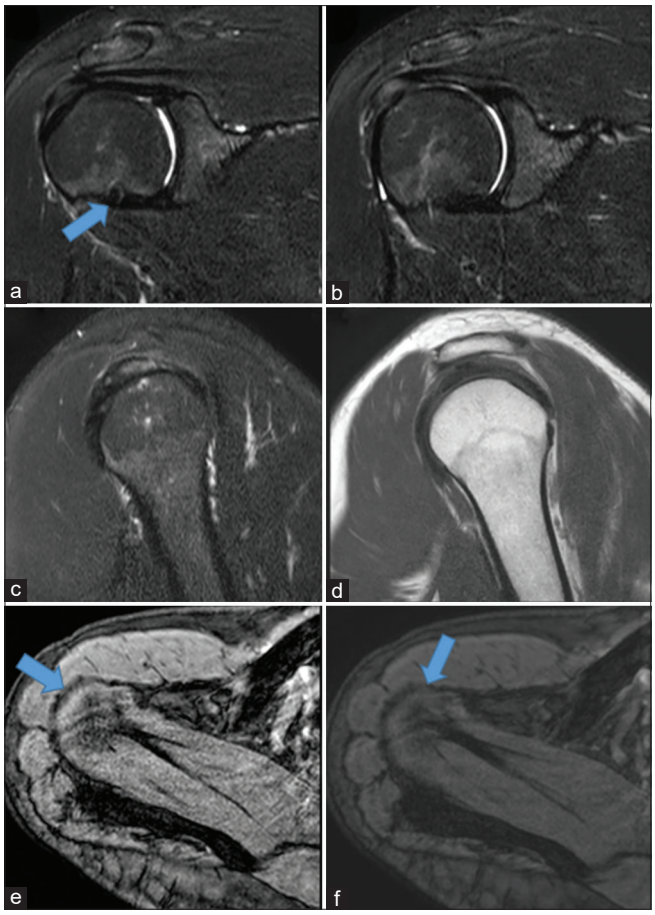

Figure 4: Sectional magnetic resonance imaging of the shoulder. (a) Coronal section view of the humeral head. (a) Biceps tendon was created with the blue arrow, (b-d) the rotator cuff is shown and intact, (e and f) an axial section view of the shoulder, and blue arrows indicate the rotator cuff attachment site

shoulder-related pathologies are not considered, we think that a good physical examination should be performed, and the source of the pain should be investigated with additional imaging studies. Although it is said that surgical treatment is reasonable in symptomatic patients in the long term, we think that the existing anatomy, adapted with analgesia and additional rehabilitation methods, should not be disturbed.

Declaration of patient consent

The authors certify that they have obtained all appropriate patient consent forms. In the form, the patient has given his consent for his images and other clinical information to be reported in the journal. The patient understands that his name and initials will not be published and due efforts will be made to conceal his identity, but anonymity cannot be guaranteed.

Financial support and sponsorship

Nil.

Conflicts of interest

There are no conflicts of interest.

References

1. Kadri PA, Al-Mefty O. Anatomy of the nuchal ligament and its surgical applications. Neurosurgery 2007;61:301-4.
2. Gülekon IN, Turgut HB. The external occipital protuberance: Can it be used as a criterion in the determination of sex? J Forensic Sci 2003;48:513-6.
3. Singh R. Bony spurs projecting in the obturator foramen. Folia Morphol (Warsz) 2012;71:125-7.
4. Sattur M, Korson C, Henderson F Jr., Kalhorn S. Presentation and management of traumatic occipital spur fracture. Am J Emerg Med 2019;37:1005.e1-2.
5. Singal A, Chaudhary P, Singh P. External occipital protuberance classification with special reference to spine type and its clinical implications. Surg Radiol Anat 2023;45:555-61.
6. Srivastava M, Asghar A, Srivastava NN, Gupta N, Jain A, Verma J. An anatomic morphological study of occipital spurs in human skulls. J Craniofac Surg 2018;29:217-9.
7. Bilge Y, Kedici PS, Alakoç YD, Ulküer KU, Ilkyaz YY. The identification of a dismembered human body: A multidisciplinary approach. Forensic Sci Int 2003;137:141-6.
8. Marshall RC, Abela C, Eccles S. Painful exostosis of the external occipital protuberance. J Plast Reconstr Aesthet Surg 2015;68:e174-6.
9. Porrino J, Sunku P, Wang A, Haims A, Richardson ML. Exophytic external occipital protuberance prevalence pre- and post-iphone ıntroduction: A retrospective cohort. Yale J Biol Med 2021;94:65-71.
10. Satyarthee GD. External occipital protuberance projecting as downward curved horn presenting with ıntractable occipital pain: Report of a first case. J Pediatr Neurosci 2019;14:173-4.
11. Tsutsumi S, Ono H, Ishii H. Emissary foramina of the external occipital protuberance: A magnetic resonance ımaging study. J Comput Assist Tomogr 2021;45:753-8.
12. Jacques T, Jaouen A, Kuchcinski G, Badr S, Demondion X, Cotten A. Enlarged External Occipital Protuberance in young French individuals' head CT: stability in prevalence, size and type between 2011 and 2019. Sci Rep 2020;10:6518. doi:10.1038/s41598-020-63554-y
13. Shahar D, Sayers MG. A morphological adaptation? The prevalence of enlarged external occipital protuberance in young adults. J Anat. 2016;229:286-291. doi: 10.1111/joa.12466.
14. Singh R. Bony tubercle at external occipital protuberance and prominent ridges. J Craniofac Surg 2012;23:1873-4.

Case Report

A Rare Case of a Pedunculated Accessory Liver Lobe Arising from Segment 3: A Radiological Insight

Abstract

Accessory liver lobes (ALLs) are rare congenital anatomical variations that may mimic pathological conditions, leading to diagnostic challenges. Among these, pedunculated ALLs are exceptionally uncommon. We report a rare case of a pedunculated ALL arising from segment 3 of the liver in a 45-year-old male patient with no known medical history. The lobe was incidentally detected on contrast-enhanced abdominal computed tomography performed for an unrelated indication. Imaging revealed a well-defined hepatic structure extending from the portal hilum toward the lesser omentum, maintaining continuity with the liver parenchyma. ALLs have been classified into different subtypes based on their anatomical connection to the liver. Their presence can lead to diagnostic confusion, as they may mimic hepatic, retroperitoneal, or even thoracic masses. While most cases are asymptomatic, complications such as torsion, rupture, or hemorrhage have been reported. Advanced imaging techniques, including cross-sectional imaging, nuclear scintigraphy, and hepatobiliary-phase magnetic resonance imaging, can aid in diagnosis. In this case, the accessory lobe could have been misinterpreted as a papillary process of the caudate lobe. Recognition of ALLs is crucial to prevent unnecessary surgical interventions and misdiagnosis. Radiologists should be familiar with this rare anatomical variant to ensure accurate interpretation of imaging findings. To our knowledge, this is the first reported case of a pedunculated ALL arising from segment 3.

Keywords: *Accessory lobe, incidentally, liver, papillary process, variation*

Halil Ibrahim Altunbulak[1,2], Ahmet Yasir Altunbulak[3], Bilal Altunbulak[4], Ahmet Poker[5]

[1]Department of Radiology, Hacettepe University, [4]Department of Radiology, Ankara Bilkent City Hospital, Ankara, [2]Department of Radiology, Ministry of Health Tatvan State Hospital, Bitlis, [3]Department of Radiology, Ministry of Health Batman State Hospital, Batman, [5]Department of Radiology, Ministry of Health Sivas State Hospital, Sivas, Türkiye

Introduction

The liver exhibits numerous congenital anatomical variations, among which the accessory liver lobe (ALL) is one of the rarest.[1] Here, we present a highly unusual case of a pedunculated ALL originating from segment 3, extending toward the lesser omentum.

Case Report

Written informed consent was obtained from the patient in accordance with ethical guidelines.

A contrast-enhanced abdominal computed tomography scan was performed on a 45-year-old male patient with no known medical history for an indication unrelated to the case. Imaging revealed an incidental finding of an ALL extending from segment 3 anterior to the caudate lobe. This lobe maintained continuity with the liver parenchyma and extended from the portal hilum toward the lesser omentum [Figure 1 and Video 1].

Discussion

Khan *et al*. classified ALLs into three types: (1) lobes continuous with the liver without a pedicle, (2) lobes connected to the liver via a pedicle, and (3) lobes completely separate from the liver.[2] Meanwhile, Colan *et al*. proposed a four-category classification: (1) an external lobe attached to intra-abdominal ligaments or the gallbladder, (2) an ectopic lobe typically undetectable on imaging, (3) a large lobe connected to the liver via a pedicle, and (4) a small lobe weighing 10–30 g.[3] More detailed classifications consider bile drainage pathways (intrahepatic vs. extrahepatic) and the presence of a common capsular structure.[4] Histologically, ALLs exhibit normal hepatic architecture. They are more commonly found in the abdominal cavity than in the thoracic or pelvic regions.[5] Most cases are incidentally detected, but

How to cite this article: Altunbulak HI, Altunbulak AY, Altunbulak B, Poker A. A rare case of a pedunculated accessory liver lobe arising from segment 3: A radiological insight. J Anat Soc India 2025;74:366-8.

Article Info

Received: 21 March 2025
Revised: 23 November 2025
Accepted: 08 December 2025
Available online: 31 December 2025

Address for correspondence:
Dr. Halil Ibrahim Altunbulak, Department of Radiology, Hacettepe University, Ankara, Türkiye.
E-mail: halil.altunbulak5806@gmail.com

Video Available on:
https://journals.lww.com/joai

Access this article online

Website: https://journals.lww.com/joai

DOI: 10.4103/jasi.jasi_57_25

Quick Response Code:

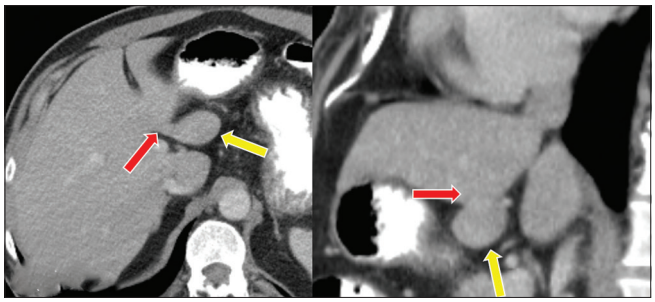

Figure 1: An accessory liver lobe (yellow arrow) arising from segment 3 of the liver and connected by a thin pedicle (red arrow) is observed

clinical symptoms may arise due to complications such as torsion, rupture, or hemorrhage.[6] Their presence can mimic mass lesions, leading to diagnostic confusion. In the thoracic region, they may be mistaken for pulmonary, pleural, or diaphragmatic tumors, whereas in the abdomen, they can resemble gastric, hepatic, splenic, retroperitoneal masses, lymphadenopathy, or even normal anatomical structures.[7]

Diagnosis is often made through cross-sectional imaging obtained for unrelated clinical indications. These lobes may differ from the main liver parenchyma in metabolic activity, sometimes showing relative preservation or susceptibility to certain pathological changes. Reports exist of aberrant venous drainage patterns in which fatty infiltration was present in the main liver parenchyma but spared in the accessory lobe.[8] In some cases, hepatocellular carcinoma has developed within an otherwise normal accessory lobe, while in cirrhotic patients, the accessory lobe remained uninvolved by malignancy.[9]

During embryonic development, these lobes may also give rise to accessory fissures and lobulations. If imaging findings are inconclusive, nuclear scintigraphy or hepatobiliary-phase magnetic resonance imaging can confirm the diagnosis.[10] In some cases, accessory lobes may be misinterpreted as other hepatic anatomical variations, such as an elongated left hepatic lobe [Figure 2b] (morphological variations of the left lobe of the liver) or a papillary process of the caudate lobe [Figure 2a].[11]

To our knowledge, this is the first reported case of a pedunculated ALL arising from segment 3.

Conclusion

ALLs are rare anatomical variations, often detected incidentally on imaging performed for unrelated reasons. Recognition of this anomaly is crucial to prevent unnecessary surgical interventions or additional diagnostic procedures. Radiologists, in particular, should be familiar with this variation to avoid misdiagnosis and ensure accurate interpretation of imaging findings.

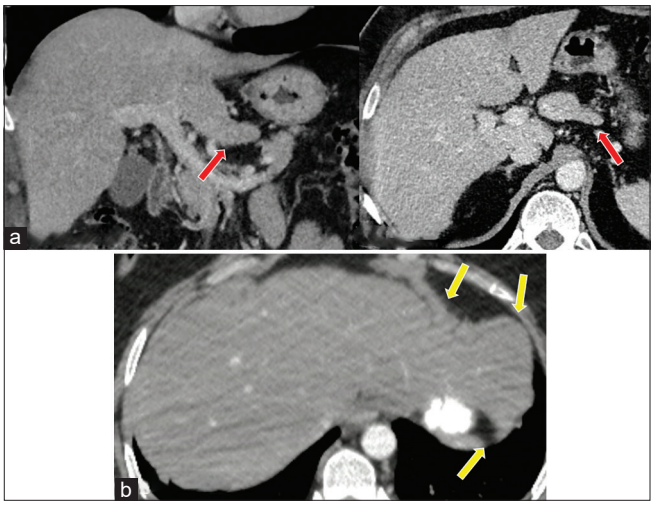

Figure 2: Differential diagnoses of an accessory liver lobe on computed tomography are demonstrated. (a) The papillary process of the caudate lobe (red arrows). (b) Elongation of the left hepatic lobe (yellow arrow)

Declaration of patient consent

The authors certify that they have obtained all appropriate patient consent forms. In the form, the patient has given his consent for his images and other clinical information to be reported in the journal. The patient understands that name and initials will not be published and due efforts will be made to conceal identity, but anonymity cannot be guaranteed.

Financial support and sponsorship

Nil.

Conflicts of interest

There are no conflicts of interest.

References

1. Nayak SB, Kumar N, Sirasanagandla SR, Shetty SD. A mini accessory liver lobe in the fissure for ligamentum teres and its clinical significance: A case report. J Clin Diagn Res 2013;7:2573-4.
2. Khan AM, Hundal R, Manzoor K, Dhuper S, Korsten MA. Accessory liver lobes: A diagnostic and therapeutic challenge of their torsions. Scand J Gastroenterol 2006;41:125-30.
3. Collan Y, Hakkiluoto A, Hästbacka J. Ectopic liver. Ann Chir Gynaecol 1978;67:27-9.
4. Goor DA, Ebert PA. Anomalies of the biliary tree. Report of a repair of an accessory bile duct and review of the literature. Arch Surg 1972;104:302-9.
5. Tancredi A, Cuttitta A, de Martino DG, Scaramuzzi R. Ectopic hepatic tissue misdiagnosed as a tumor of lung. Updates Surg 2010;62:121-3.
6. Kapoor A, Harshavardhan K, MutnuRu C. Accessory Hepatic Lobe-A ' Not so Rare ' Entity; 2017.
7. Wang Y, Junlin L, Zhang WG, Chen JH, He Y, Chen JM. Accessory lobe of right liver mimicking a pulmonary tumor in an adult male. Ann Thorac Surg 2010;89:e9-10.
8. Kawamori Y, Matsui O, Takahashi S, Kadoya M, Takashima T, Miyayama S. Focal hepatic fatty infiltration in the posterior edge

of the medial segment associated with aberrant gastric venous drainage: CT, US, and MR findings. J Comput Assist Tomogr 1996;20:356-9.

9. Arakawa M, Kimura Y, Sakata K, Kubo Y, Fukushima T, Okuda K. Propensity of ectopic liver to hepatocarcinogenesis: Case reports and a review of the literature. Hepatology 1999;29:57-61.
10. Hashimoto M, Oomachi K, Watarai J. Accessory lobe of the liver mimicking a mass in the left adrenal gland. A case report. Acta Radiol 1997;38:309-10.
11. Abdalla EK, Vauthey JN, Couinaud C. The caudate lobe of the liver: Implications of embryology and anatomy for surgery. Surg Oncol Clin N Am 2002;11:835-48.

The Editorial Process

A manuscript will be reviewed for possible publication with the understanding that it is being submitted to Journal of the Anatomical Society of India alone at that point in time and has not been published anywhere, simultaneously submitted, or already accepted for publication elsewhere. The journal expects that authors would authorize one of them to correspond with the Journal for all matters related to the manuscript. All manuscripts received are duly acknowledged. On submission, editors review all submitted manuscripts initially for suitability for formal review. Manuscripts with insufficient originality, serious scientific or technical flaws, or lack of a significant message are rejected before proceeding for formal peer-review. Manuscripts that are unlikely to be of interest to the Journal of the Anatomical Society of India readers are also liable to be rejected at this stage itself.

Manuscripts that are found suitable for publication in Journal of the Anatomical Society of India are sent to two or more expert reviewers. During submission, the contributor is requested to provide names of two or three qualified reviewers who have had experience in the subject of the submitted manuscript, but this is not mandatory. The reviewers should not be affiliated with the same institutes as the contributor/s. However, the selection of these reviewers is at the sole discretion of the editor. The journal follows a double-blind review process, wherein the reviewers and authors are unaware of each other's identity. Every manuscript is also assigned to a member of the editorial team, who based on the comments from the reviewers takes a final decision on the manuscript. The comments and suggestions (acceptance/ rejection/ amendments in manuscript) received from reviewers are conveyed to the corresponding author. If required, the author is requested to provide a point by point response to reviewers' comments and submit a revised version of the manuscript. This process is repeated till reviewers and editors are satisfied with the manuscript.

Manuscripts accepted for publication are copy edited for grammar, punctuation, print style, and format. Page proofs are sent to the corresponding author. The corresponding author is expected to return the corrected proofs within three days. It may not be possible to incorporate corrections received after that period. The whole process of submission of the manuscript to final decision and sending and receiving proofs is completed online. To achieve faster and greater dissemination of knowledge and information, the journal publishes articles online as 'Ahead of Print' immediately on acceptance.

Clinical trial registry

Journal of the Anatomical Society of India favors registration of clinical trials and is a signatory to the Statement on publishing clinical trials in Indian biomedical journals. Journal of the Anatomical Society of India would publish clinical trials that have been registered with a clinical trial registry that allows free online access to public. Registration in the following trial registers is acceptable: http://www.ctri.in/; http://www.actr.org.au/; http://www.clinicaltrials.gov/; http://isrctn.org/; http://www.trialregister.nl/trialreg/index.asp; and http://www.umin.ac.jp/ctr. This is applicable to clinical trials that have begun enrollment of subjects in or after June 2008. Clinical trials that have commenced enrollment of subjects prior to June 2008 would be considered for publication in Journal of the Anatomical Society of India only if they have been registered retrospectively with clinical trial registry that allows unhindered online access to public without charging any fees.

Authorship Criteria

Authorship credit should be based only on substantial contributions to each of the three components mentioned below:

1. Concept and design of study or acquisition of data or analysis and interpretation of data;
2. Drafting the article or revising it critically for important intellectual content; and
3. Final approval of the version to be published.

Participation solely in the acquisition of funding or the collection of data does not justify authorship. General supervision of the research group is not sufficient for authorship. Each contributor should have participated sufficiently in the work to take public responsibility for appropriate portions of the content of the manuscript. The order of naming the contributors should be based on the relative contribution of the contributor towards the study and writing the manuscript. Once submitted the order cannot be changed without written consent of all the contributors. The journal prescribes a maximum number of authors for manuscripts depending upon the type of manuscript, its scope and number of institutions involved (vide infra). The authors should provide a justification, if the number of authors exceeds these limits.

Contribution Details

Contributors should provide a description of contributions made by each of them towards the manuscript. Description should be divided in following categories, as applicable: concept, design, definition of intellectual content, literature search, clinical studies, experimental studies, data acquisition, data analysis, statistical analysis, manuscript preparation, manuscript editing and manuscript review. Authors' contributions will be printed along with the article. One or more author should take responsibility for the integrity of the work as a whole from inception to published article and should be designated as 'guarantor'.

Conflicts of Interest/ Competing Interests

All authors of must disclose any and all conflicts of interest they may have with publication of the manuscript or an institution or product that is mentioned in the manuscript and/or is important to the outcome of the study presented. Authors should also disclose conflict of interest with products that compete with those mentioned in their manuscript.

Submission of Manuscripts

All manuscripts must be submitted on-line through the website https://review.jow.medknow.com/jasi. First time users will have to register at this site. Registration is free but mandatory. Registered authors can keep track of their articles after logging into the site using their user name and password.

- If you experience any problems, please contact the editorial office by e-mail at editor@jasi.org.in

The submitted manuscripts that are not as per the "Instructions to Authors" would be returned to the authors for technical correction, before they undergo editorial/ peer-review. Generally, the manuscript should be submitted in the form of two separate files:

[1] Title Page/First Page File/covering letter:

This file should provide

1. The type of manuscript (original article, case report, review article, Letter to editor, Images, etc.) title of the manuscript, running title, names of all authors/ contributors (with their highest academic degrees, designation and affiliations) and name(s) of department(s) and/ or institution(s) to which the work should be credited, . All information which can reveal your identity should be here. Use text/rtf/doc files. Do not zip the files.
2. The total number of pages, total number of photographs and word counts separately for abstract and for the text (excluding the references, tables and abstract), word counts for introduction + discussion in case of an original article;
3. Source(s) of support in the form of grants, equipment, drugs, or all of these;
4. Acknowledgement, if any. One or more statements should specify 1) contributions that need acknowledging but do not justify authorship, such as general support by a departmental chair; 2) acknowledgments of technical help; and 3) acknowledgments of financial and material support, which should specify the nature of the support. This should be included in the title page of the manuscript and not in the main article file.
5. If the manuscript was presented as part at a meeting, the organization, place, and exact date on which it was read. A full statement to the editor about all submissions and previous reports that might be regarded as redundant publication of the same or very similar work. Any such work should be referred to specifically, and referenced in the new paper. Copies of such material should be included with the submitted paper, to help the editor decide how to handle the matter.
6. Registration number in case of a clinical trial and where it is registered (name of the registry and its URL)
7. Conflicts of Interest of each author/ contributor. A statement of financial or other relationships that might lead to a conflict of interest, if that information is not included in the manuscript itself or in an authors' form
8. Criteria for inclusion in the authors'/ contributors' list
9. A statement that the manuscript has been read and approved by all the authors, that the requirements for authorship as stated earlier in this document have been met, and that each author believes that the manuscript represents honest work, if that information is not provided in another form (see below); and
10. The name, address, e-mail, and telephone number of the corresponding author, who is responsible for communicating with the other authors about revisions and final approval of the proofs, if that information is not included on the manuscript itself.

[2] Blinded Article file: The main text of the article, beginning from Abstract till References (including tables) should be in this file. The file must not contain any mention of the authors' names or initials or the institution at which the study was done or acknowledgements. Page headers/ running title can include the title but not the authors' names. Manuscripts not in compliance with the Journal's blinding policy will be returned to the corresponding author. Use rtf/doc files. Do not zip the files. **Limit the file size to 1 MB.** Do not incorporate images in the file. If file size is large, graphs can be submitted as images separately without incorporating them in the article file to reduce the size of the file. The pages should be numbered consecutively, beginning with the first page of the blinded article file.

[3] Images: Submit good quality color images. **Each image should be less than 2 MB in size.** Size of the image can be reduced by decreasing the actual height and width of the images (keep up to 1600 x 1200 pixels or 5-6 inches). Images can be submitted as jpeg files. Do not zip the files. Legends for the figures/images should be included at the end of the article file.

[4] The contributors' / copyright transfer form (template provided below) has to be submitted in original with the signatures of all the contributors within two weeks of submission via courier, fax or email as a scanned image. Print ready hard copies of the images (one set) or digital images should be sent to the journal office at the time of submitting revised manuscript. High resolution images (up to 5 MB each) can be sent by email.

Contributors' form / copyright transfer form can be submitted online from the authors' area on https://review.jow.medknow.com/jasi.

Preparation of Manuscripts

Manuscripts must be prepared in accordance with "Uniform requirements for Manuscripts submitted to Biomedical Journals" developed by the International Committee of Medical Journal Editors (October 2008). The uniform requirements and specific requirement of Journal of the Anatomical Society of India are summarized below. Before submitting a manuscript, contributors are requested to check for the latest instructions available. Instructions are also available from the website of the journal (www.jasi.org.in) and from the manuscript submission site https://review.jow.medknow.com/jasi.

Journal of the Anatomical Society of India accepts manuscripts written in American English.

Copies of any permission(s)

It is the responsibility of authors/ contributors to obtain permissions for reproducing any copyrighted material. A copy of the permission obtained must accompany the manuscript. Copies of any and all published articles or other manuscripts in preparation or submitted elsewhere that are related to the manuscript must also accompany the manuscript.

Types of Manuscripts

Original articles:

These include randomized controlled trials, intervention studies, studies of screening and diagnostic test, outcome studies, cost effectiveness analyses, case-control series, and surveys with high response rate. The text of original articles amounting to up to 3000 words (excluding Abstract, references and Tables) should be divided into sections with the headings Abstract, Key-words, Introduction, Material and Methods, Results, Discussion and Conclusion, References, Tables and Figure legends.

An abstract should be in a structured format under following heads: **Introduction, Material and Methods, Results,** and **Discussion and Conclusion.**

Introduction: State the purpose and summarize the rationale for the study or observation.

Material and Methods: It should include and describe the following aspects:

Ethics: When reporting studies on human beings, indicate whether the procedures followed were in accordance with the ethical standards of the responsible committee on human experimentation (institutional or regional) and with the Helsinki Declaration of 1975, as revised in 2000 (available at http://www.wma.net/e/policy/17-c_e.html). For prospective studies involving human participants, authors are expected to mention about approval of (regional/ national/ institutional or independent Ethics Committee or Review Board, obtaining informed consent from adult research participants and obtaining assent for children aged over 7 years participating in the trial. The age beyond which assent would be required could vary as per regional and/ or national guidelines. Ensure confidentiality of subjects by desisting from mentioning participants' names, initials or hospital numbers, especially in illustrative material. When reporting experiments on animals, indicate whether the institution's or a national research council's guide for, or any national law on the care and use of laboratory animals was followed. Evidence for approval by a local Ethics Committee (for both human as well as animal studies) must be supplied by the authors on demand. Animal experimental procedures should be as humane as possible and the details of anesthetics and analgesics used should be clearly stated. The ethical standards of experiments must be in accordance with the guidelines provided by the CPCSEA and World Medical Association Declaration of Helsinki on Ethical Principles for Medical Research Involving Humans for studies involving experimental animals and human beings, respectively). The journal will not consider any paper which is ethically unacceptable. A statement on ethics committee permission and ethical practices must be included in all research articles under the 'Materials and Methods' section.

Study design:

Selection and Description of Participants: Describe your selection of the observational or experimental participants (patients or laboratory animals, including controls) clearly, including eligibility and exclusion criteria and a description of the source population. *Technical information*: Identify the methods, apparatus (give the manufacturer›s name and address in parentheses), and procedures in sufficient detail to allow other workers to reproduce the results. Give references to established methods, including statistical methods (see below); provide references and brief descriptions for methods that have been published but are not well known; describe new or substantially modified methods, give reasons for using them, and evaluate their limitations. Identify precisely all drugs and chemicals used, including generic name(s), dose(s), and route(s) of administration.

Reports of randomized clinical trials should present information on all major study elements, including the protocol, assignment of interventions (methods of randomization, concealment of allocation to treatment groups), and the method of masking (blinding), based on the CONSORT Statement (http://www.consort-statement.org).

Reporting Guidelines for Specific Study Designs

Initiative	Type of Study	Source
CONSORT	Randomized controlled trials	http://www.consort-statement.org
STARD	Studies of diagnostic accuracy	http://www.consort-statement.org/stardstatement.htm
QUOROM	Systematic reviews and meta-analyses	http://www.consort- statement.org/Initiatives/MOOSE/moose.pdf statement.org/Initiatives/MOOSE/moose.pdf
STROBE	Observational studies in epidemiology	http://www.strobe-statement.org
MOOSE	Meta-analyses of observational studies in epidemiology	http://www.consort- statement.org/Initiatives/MOOSE/moose.pdf

Statistics: Whenever possible quantify findings and present them with appropriate indicators of measurement error or uncertainty (such as confidence intervals). Authors should report losses to observation (such as, dropouts from a clinical trial). When data are summarized in the Results section, specify the statistical methods used to analyze them. Avoid non-technical uses of technical terms in statistics, such as 'random' (which implies a randomizing device), 'normal', 'significant', 'correlations', and 'sample'. Define statistical terms, abbreviations, and most symbols. Specify the computer software used. Use upper italics (*P* 0.048). For all *P* values include the exact value and not less than 0.05 or 0.001. Mean differences in continuous variables, proportions in categorical variables and relative risks including odds ratios and hazard ratios should be accompanied by their confidence intervals.

Results: Present your results in a logical sequence in the text, tables, and illustrations, giving the main or most important findings first. Do not repeat in the text all the data in the tables or illustrations; emphasize or summarize only important observations. Extra- or supplementary materials and technical detail can be placed in an appendix where it will be accessible but will not interrupt the flow of the text; alternatively, it can be published only in the electronic version of the journal.

When data are summarized in the Results section, give numeric results not only as derivatives (for example, percentages) but also as the absolute numbers from which the derivatives were calculated, and specify the statistical methods used to analyze them. Restrict tables and figures to those needed to explain the argument of the paper and to assess its support. Use graphs as an alternative to tables with many entries; do not duplicate data in graphs and tables. Where scientifically appropriate, analyses of the data by variables such as age and sex should be included.

Discussion: Include summary of *key findings* (primary outcome measures, secondary outcome measures, results as they relate to a prior hypothesis); *Strengths and limitations* of the study (study question, study design, data collection, analysis and interpretation); *Interpretation and implications* in the context of the totality of evidence (is there a systematic review to refer to, if not, could one be reasonably done here and now?, what this study adds to the available evidence, effects on patient care and health policy, possible mechanisms); *Controversies* raised by this study; and *Future research directions* (for this particular research collaboration, underlying mechanisms, clinical research).

Do not repeat in detail data or other material given in the Introduction or the Results section. In particular, contributors should avoid making statements on economic benefits and costs unless their manuscript includes economic data and analyses. Avoid claiming priority and alluding to work that has not been completed. New hypotheses may be stated if needed, however they should be clearly labeled as such. About 30 references can be included. These articles generally should not have more than six authors.

Review Articles:

These are comprehensive review articles on topics related to various fields of Anatomy. The entire manuscript should not exceed 7000 words with no more than 50 references and two authors. Following types of articles can be submitted under this category:

- Newer techniques of dissection and histology
- New methodology in Medical Education
- Review of a current concept

Please note that generally review articles are by invitation only. But unsolicited review articles will be considered for publication on merit basis.

Case reports:

New, interesting and rare cases can be reported. They should be unique, describing a great diagnostic or therapeutic challenge and providing a learning point for the readers. Cases with clinical significance or implications will be given priority. These communications could be of up to 1000 words (excluding Abstract and references) and should have the following headings: Abstract (unstructured), Key-words, Introduction, Case report, Discussion and Conclusion, Reference, Tables and Legends in that order.

The manuscript could be of up to 1000 words (excluding references and abstract) and could be supported with up to 10 references. Case Reports could be authored by up to four authors.

Letter to the Editor:

These should be short and decisive observations. They should preferably be related to articles previously published in the Journal or views expressed in the journal. They should not be preliminary observations that need a later

paper for validation. The letter could have up to 500 words and 5 references. It could be generally authored by not more than four authors.

Book Review: This consists of a critical appraisal of selected books on Anatomy. Potential authors or publishers may submit books, as well as a list of suggested reviewers, to the editorial office. The author/publisher has to pay INR 10,000 per book review.

Other:

Editorial, Guest Editorial, Commentary and Opinion are solicited by the editorial board.

References

References should be *numbered* consecutively in the order in which they are first mentioned in the text (not in alphabetic order). Identify references *in text*, tables, and legends by Arabic numerals in superscript with square bracket after the punctuation *marks. References cited only* in tables or figure legends should be numbered in accordance with the sequence established by the first identification in the text of the particular table or figure. Use the style of the examples below, which are based on the formats used by the NLM *in Index Medicus*. The titles of journals *should be abbreviated* according to the style used in Index Medicus. Use complete name of the journal for non-indexed journals. Avoid using abstracts as references. Information from manuscripts submitted but not accepted should be cited in the text as "unpublished observations" with written permission from the source. Avoid citing a "personal communication" unless it provides essential information not available from a public source, in which case the name of the person and date of communication should be cited in parentheses in the text. The commonly cited types of references are shown here, for other types of references such as newspaper items please refer to ICMJE Guidelines (http://www.icmje.org or http://www.nlm.nih.gov/bsd/uniform_requirements.html).

Articles in Journals

1. Standard journal article (for up to six authors): Parija S C, Ravinder PT, Shariff M. Detection of hydatid antigen in the fluid samples from hydatid cysts by co-agglutination. Trans. R.Soc. Trop. Med. Hyg.1996; 90:255–256.
2. Standard journal article (for more than six authors): List the first six contributors followed by *et al*.

Roddy P, Goiri J, Flevaud L, Palma PP, Morote S, Lima N. *et al*., Field Evaluation of a Rapid Immunochromatographic Assay for Detection of Trypanosoma cruzi Infection by Use of Whole Blood. J. Clin. Microbiol. 2008; 46: 2022-2027.

3. Volume with supplement: Otranto D, Capelli G, Genchi C: Changing distribution patterns of canine vector borne diseases in Italy: leishmaniosis vs. dirofilariosis. Parasites & Vectors 2009; Suppl 1:S2.

Books and Other Monographs

1. Personal author(s): Parija SC. Textbook of Medical Parasitology. 3rd ed. All India Publishers and Distributors. 2008.
2. Editor(s), compiler(s) as author: Garcia LS, Filarial Nematodes In: Garcia LS (editor) Diagnostic Medical Parasitology ASM press Washington DC 2007: pp 319-356.
3. Chapter in a book: Nesheim M C. Ascariasis and human nutrition. In Ascariasis and its prevention and control, D. W. T. Crompton, M. C. Nesbemi, and Z. S. Pawlowski (eds.). Taylor and Francis,London, U.K.1989, pp. 87–100.

Electronic Sources as reference

Journal article on the Internet: Parija SC, Khairnar K. Detection of excretory *Entamoeba histolytica* DNA in the urine, and detection of *E. histolytica* DNA and lectin antigen in the liver abscess pus for the diagnosis of amoebic liver abscess. *BMC Microbiology* 2007, **7**:41. doi:10.1186/1471-2180-7-41. http://www.biomedcentral.com/1471-2180/7/41

Tables

- Tables should be self-explanatory and should not duplicate textual material.
- Tables with more than 10 columns and 25 rows are not acceptable.
- Number tables, in Arabic numerals, consecutively in the order of their first citation in the text and supply a brief title for each.
- Place explanatory matter in footnotes, not in the heading.
- Explain in footnotes all non-standard abbreviations that are used in each table.
- Obtain permission for all fully borrowed, adapted, and modified tables and provide a credit line in the footnote.
- For footnotes use the following symbols, in this sequence: *, †, ‡, §, ‖,¶ , **, ††, ‡‡
- Tables with their legends should be provided at the end of the text after the references. The tables along with their number should be cited at the relevant place in the text

Illustrations (Figures)

- Upload the images in JPEG format. The file size should be within 1024 kb in size while uploading.
- Figures should be numbered consecutively according to the order in which they have been first cited in the text.
- Labels, numbers, and symbols should be clear and of uniform size. The lettering for figures should be large enough to be legible after reduction to fit the width of a printed column.
- Symbols, arrows, or letters used in photomicrographs

should contrast with the background and should be marked neatly with transfer type or by tissue overlay and not by pen.
- Titles and detailed explanations belong in the legends for illustrations not on the illustrations themselves.
- When graphs, scatter-grams or histograms are submitted the numerical data on which they are based should also be supplied.
- The photographs and figures should be trimmed to remove all the unwanted areas.
- If photographs of individuals are used, their pictures must be accompanied by written permission to use the photograph.
- If a figure has been published elsewhere, acknowledge the original source and submit written permission from the copyright holder to reproduce the material. A credit line should appear in the legend for such figures.
- Legends for illustrations: Type or print out legends (maximum 40 words, excluding the credit line) for illustrations using double spacing, with Arabic numerals corresponding to the illustrations. When symbols, arrows, numbers, or letters are used to identify parts of the illustrations, identify and explain each one in the legend. Explain the internal scale (magnification) and identify the method of staining in photomicrographs.
- Final figures for print production: Send sharp, glossy, un-mounted, color photographic prints, with height of 4 inches and width of 6 inches at the time of submitting the revised manuscript. Print outs of digital photographs are not acceptable. If digital images are the only source of images, ensure that the image has minimum resolution of 300 dpi or 1800 x 1600 pixels in TIFF format. Send the images on a CD. Each figure should have a label pasted (avoid use of liquid gum for pasting) on its back indicating the number of the figure, the running title, top of the figure and the legends of the figure. Do not write the contributor/s' name/s. Do not write on the back of figures, scratch, or mark them by using paper clips.
- The Journal reserves the right to crop, rotate, reduce, or enlarge the photographs to an acceptable size.

Protection of Patients' Rights to Privacy

Identifying information should not be published in written descriptions, photographs, sonograms, CT scans, etc., and pedigrees unless the information is essential for scientific purposes and the patient (or parent or guardian, wherever applicable) gives informed consent for publication. Authors should remove patients' names from figures unless they have obtained informed consent from the patients. The journal abides by ICMJE guidelines:

1. Authors, not the journals nor the publisher, need to obtain the patient consent form before the publication and have the form properly archived. The consent forms are not to be uploaded with the cover letter or sent through email to editorial or publisher offices.
2. If the manuscript contains patient images that preclude anonymity, or a description that has obvious indication to the identity of the patient, a statement about obtaining informed patient consent should be indicated in the manuscript.

Sending a revised manuscript

The revised version of the manuscript should be submitted online in a manner similar to that used for submission of the manuscript for the first time. However, there is no need to submit the "First Page" or "Covering Letter" file while submitting a revised version. When submitting a revised manuscript, contributors are requested to include, the 'referees' remarks along with point to point clarification at the beginning in the revised file itself. In addition, they are expected to mark the changes as underlined or colored text in the article.

Reprints and proofs

Journal provides no free printed reprints. Authors can purchase reprints, payment for which should be done at the time of submitting the proofs.

Publication schedule

The journal publishes articles on its website immediately on acceptance and follows a 'continuous publication' schedule. Articles are compiled in issues for 'print on demand' quarterly.

Copyrights

Checklist

Covering letter

- Signed by all contributors
- Previous publication / presentations mentioned
- Source of funding mentioned
- Conflicts of interest disclosed

Authors

- Last name and given name provided along with Middle name initials (where applicable)
- Author for correspondence, with e-mail address provided
- Number of contributors restricted as per the instructions
- Identity not revealed in paper except title page (e.g. name of the institute in Methods, citing previous study as 'our study', names on figure labels, name of institute in photographs, etc.)

Presentation and format

- Double spacing
- Margins 2.5 cm from all four sides
- Page numbers included at bottom
- Title page contains all the desired information
- Running title provided (not more than 50 characters)
- Abstract page contains the full title of the manuscript
- Abstract provided (structured abstract of 250 words for original articles, unstructured abstracts of about 150 words for all other manuscripts excluding letters to the Editor)
- Key words provided (three or more)
- Introduction of 75-100 words
- Headings in title case (not ALL CAPITALS)
- The references cited in the text should be after punctuation marks, in superscript with square bracket.
- References according to the journal's instructions, punctuation marks checked
- Send the article file without 'Track Changes'

Language and grammar

- Uniformly American English
- Write the full term for each abbreviation at its first use in the title, abstract, keywords and text separately unless it is a standard unit of measure. Numerals from 1 to 10 spelt out
- Numerals at the beginning of the sentence spelt out
- Check the manuscript for spelling, grammar and punctuation errors
- If a brand name is cited, supply the manufacturer's name and address (city and state/country).
- Species names should be in italics

Tables and figures

- No repetition of data in tables and graphs and in text
- Actual numbers from which graphs drawn, provided
- Figures necessary and of good quality (colour)
- Table and figure numbers in Arabic letters (not Roman)
- Labels pasted on back of the photographs (no names written)
- Figure legends provided (not more than 40 words)
- Patients' privacy maintained (if not permission taken)
- Credit note for borrowed figures/tables provided
- Write the full term for each abbreviation used in the table as a footnote

Journal of
The Anatomical Society of India

Salient Features:

- Publishes research articles related to all aspects of Anatomy and Allied medical/surgical sciences.
- Pre-Publication Peer Review and Post-Publication Peer Review
- Online Manuscript Submission System
- Selection of articles on the basis of MRS system
- Eminent academicians across the globe as the Editorial board members
- Electronic Table of Contents alerts
- Available in both online and print form.

The journal is registered with the following abstracting partners:
Baidu Scholar, CNKI (China National Knowledge Infrastructure), EBSCO Publishing's Electronic Databases, Ex Libris – Primo Central, Google Scholar, Hinari, Infotrieve, Netherlands ISSN center, ProQuest, TdNet, Wanfang Data

The journal is indexed with, or included in, the following:
SCOPUS, Science Citation Index Expanded, IndMed, MedInd, Scimago Journal Ranking, Emerging Sources Citation Index.

Impact Factor® as reported in the 2024 Journal Citation Reports® (Clarivate Analytics, 2025): 0.2

Editorial Office:
Dr. Vishram Singh, Editor-in-Chief, JASI
B5/3 Hahnemann Enclave, Plot No. 40, Sector 6,
Dwarka Phase – 2, New Delhi - 110 075, India.
Email: editorjasi@gmail.com
(O) | Website: www.asiindia.in

The journal is owned and run by The Anatomical Society of India